

**STUDIES ON SOME NONLINEAR OPTICAL PHENOMENA - OPTICAL PHASE  
CONJUGATION AND CONTINUOUS WAVE SECOND HARMONIC GENERATION**

**K. P. B. MOOSAD**

**THESIS SUBMITTED TO THE  
COCHIN UNIVERSITY OF SCIENCE AND TECHNOLOGY  
FOR THE AWARD OF THE DEGREE OF  
DOCTOR OF PHILOSOPHY**

**DEPARTMENT OF PHYSICS  
COCHIN UNIVERSITY OF SCIENCE AND TECHNOLOGY  
COCHIN - 682 022**

1988

DEDICATED TO

*Prof. Sathianandan*

## DECLARATION

I declare that the work presented in this thesis entitled "STUDIES ON SOME NONLINEAR OPTICAL PHENOMENA - OPTICAL PHASE CONJUGATION AND CONTINUOUS WAVE SECOND HARMONIC GENERATION" is based on the original research work done by me under the guidance of Dr V P N Nampoori, at the Department of Physics, Cochin University of Science and Technology, and has not been included in any other thesis submitted previously for the award of any degree.

Cochin 682 022

31 - 12 - 1988.



K P B MOOSAD

## CERTIFICATE

I certify that the work presented in this thesis entitled "STUDIES ON SOME NONLINEAR OPTICAL PHENOMENA - OPTICAL PHASE CONJUGATION AND CONTINUOUS WAVE SECOND HARMONIC GENERATION" is based on the bona fide research work done by Sri K P B Moosad, at the Department of Physics, Cochin University of Science and Technology, under my guidance, and has not been included in any other thesis submitted previously for the award of any degree.

Cochin 682 022

31 - 12 - 1988.



Dr V P N NAMPOORI  
Reader in Physics  
(Research Guide)

### *Acknowledgements*

*With a deep sense of gratitude, I acknowledge the helps rendered by several of my teachers, colleagues and friends, who have associated with me in various capacities, during the past few years of my research work at the Department of Physics, Cochin University of Science and Technology, Cochin 22, and later in compiling the results in the form of this thesis.*

*With no less regard to all the others, I would like to mention two names - Dr V P N Nampoori, who had been my mentor and the Council of Scientific and Industrial Research, Government of India, the benefactor.*

*X P B Meesad*

## CONTENTS

PREFACE

viii

### CHAPTER 1 INTRODUCTION

|      |   |    |
|------|---|----|
| 1.00 | General introduction to nonlinear optical phenomena         | 1  |
| 1.01 | An expression for the $r$ th order susceptibility tensor    | 8  |
| 1.02 | Effects due to the second order susceptibility.             |    |
|      | (i) The Pockel's effect                                     | 15 |
|      | (ii) Optical rectification                                  | 18 |
|      | (iii) Second Harmonic Generation                            | 19 |
|      | (iv) Mixing and parametric effects                          | 22 |
| 1.03 | Effects due to the third order susceptibility               |    |
|      | (i) The Kerr effect   | 26 |
|      | (ii) Third Harmonic Generation                              | 27 |
|      | (iii) Stimulated Raman Scattering and Two Photon Absorption | 30 |
|      | References  | 33 |

### CHAPTER 2 DEGENERATE FOUR WAVE MIXING AND OPTICAL PHASE CONJUGATION

|      |   |    |
|------|---|----|
| 2.00 | Degenerate Four Wave Mixing                         | 37 |
| 2.01 | Theory of DFWM and OPC in transparent media         | 38 |
| 2.02 | Theory of DFWM and OPC in absorbing media           | 45 |
| 2.03 | Saturable absorbers as candidates for low power OPC | 48 |
|      | References  | 49 |

CHAPTER 3 CHARACTERISATION OF A FEW SATURABLE ABSORBERS AS CANDIDATES FOR LOW POWER OPTICAL PHASE CONJUGATION

|       |  |    |
|-------|--|----|
| 3.00  | Materials for low power OPC                        |    |
| (i)   | Photorefractive crystals                           | 51 |
| (ii)  | Liquid crystals                                    | 53 |
| (iii) | Interfaces   | 53 |
| (iv)  | Saturable absorbers                                | 53 |
| 3.01  | Structure and details of the dyes and the matrices |    |
| (i)   | Eosin  | 55 |
| (ii)  | Erythrosin B                                       | 55 |
| (iii) | Rose Bengal  | 55 |
| (iv)  | Gelatin  | 55 |
| (v)   | Ployvinyl alcohol                                  | 55 |
| (vi)  | Boric acid glass                                   | 57 |
| 3.02  | Sample preparation                                 | 57 |
| 3.03  | Absorption spectra                                 | 58 |
| 3.04  | Saturation intensities                             | 61 |
| (i)   | A quick method of checking saturable absorption    | 62 |
| (ii)  | Actual measurements of the saturation intensities  | 66 |
| 3.05  | Triplet lifetimes                                  | 72 |
|       | References   | 77 |

CHAPTER 4 SECTION I LOW POWER OPTICAL PHASE CONJUGATION IN SOME SATURABLE ABSORBERS

|      |  |    |
|------|--|----|
| 4.10 | Low power OPC - earlier results in saturable absorbers | 87 |
| 4.11 | Samples and experimental set-up                        | 83 |

|  |  |     |
|--|--|-----|
| 4.12   | OPC Signals  | 86  |
| 4.13   | OPC reflectivity vs. intensity   | 87  |
| 4.14   | Relative efficiency of OPC in gelatin and PVA films                                | 91  |
| 4.15   | OPC reflectivity vs. absorption length   | 93  |
| 4.16   | OPC efficiency vs. wavelength  | 95  |
| 4.17   | Effect of vibrations   | 95  |
| 4.18   | Effect of photochemical damage   | 97  |
| SECTION II PHASE CONJUGATION OF A BROADBAND LASER  |  |     |
| 4.20   | OPC of broadband lasers  | 100 |
| 4.21   | Experimental details   | 101 |
| 4.22   | Results and discussions  | 103 |
|  | References   | 106 |
| CHAPTER 5 CONTINUOUS WAVE SECOND HARMONIC GENERATION IN A RING DYE LASER                                     |  |     |
| 5.00   | CW SHG   | 107 |
| 5.01   | Thin $\text{LiIO}_3$ crystals - cut details  | 109 |
| 5.02   | Experimental details   | 110 |
| 5.03   | Results and discussions  | 112 |
| 5.04   | An experiment using the second harmonic radiation - detection of hydroxyl radicals | 116 |
|  | References   | 119 |
| CHAPTER 6 CONCLUSIONS  |  |     |
|  | References   | 126 |
| APPENDIX I LUMINESCENCE SPECTRA OF THE DYES EOSIN, ERYTHROSIN B AND ROSE BENGAL DOPED IN DIFFERENT MATRICES. |  |     |
| I.01   | Introduction   | 128 |

|             |  |     |
|-------------|--|-----|
| I.02        | Experimental details   | 129 |
| I.03        | Results and discussions  | 130 |
|             | References   | 137 |
| APPENDIX II | OPTICAL PHASE CONJUGATION AS LABORATORY<br>EXPERIMENTS AT THE POSTGRADUATE LEVEL |     |
| II.01       | Introduction   | 138 |
| II.02       | Nonlinear medium   | 140 |
| II.03       | Experimental set-up  | 140 |
| II.04       | Results and discussions  | 145 |
|             | References   |     |

## PREFACE

Nonlinear optics has emerged as a new area of physics, following the development of various types of lasers. A number of advancements, both theoretical and experimental, have been made in the past two decades, by scientists all over the world. However, only few scientists have attempted to study the experimental aspects of nonlinear optical phenomena in Indian laboratories. This thesis is the report of an attempt made in this direction.

The thesis contains the details of the several investigations which the author has carried out in the past few years, on optical phase conjugation (OPC) and continuous wave (CW) second harmonic generation (SHG). OPC is a new branch of nonlinear optics, developed only in the past decade. The author has done a few experiments on low power OPC in dye molecules held in solid matrices, by making use of a degenerate four wave mixing (DFWM) scheme. These samples have been characterised by studies on their absorption-spectra, fluorescence spectra, triplet lifetimes and saturation intensities. Phase conjugation efficiencies with respect to the various parameters have been investigated. DFWM scheme was also employed in achieving phase conjugation of a broadband laser ( Nd:Glass ) using a dye solution as the nonlinear medium.

SHG is one of the most important of the several second order nonlinear optical effects, in view of its applications. Although SHG is common with pulsed lasers, it is not so in the case of CW lasers. The author has developed an indigenous system for SHG in a ring dye laser, making use of thin Lithium Iodate crystals. The tunable coherent ultraviolet beam thus obtained was successfully applied for spectroscopic investigations.

The thesis has been set in six chapters and two appendices. The FIRST CHAPTER is a general introduction to nonlinear optics. Various nonlinear optical effects due to the second and third order nonlinear susceptibilities are discussed. The derivation of an expression for nonlinear optical susceptibility is outlined.

CHAPTER TWO is an account of DFWM and OPC. The theories of DFWM in transparent and absorbing media are examined.

CHAPTER THREE contains the details of the experimental investigations made on a few low power saturable absorbers as candidates for low power OPC. The specific cases studied are the dyes eosin, erythrosin B and Rose Bengal, taken in thin films of gelatin, polyvinyl alcohol (PVA) and boric acid glass. The

properties of these systems in relation to their suitability for OPC are experimentally investigated, which include the absorption spectra, fluorescence spectra, triplet life times, and saturation intensities. The absorption spectra indicated that the boric acid glass samples do not absorb strongly at 514.5 nm wavelength while in the other two films it does, indicating that the boric acid glass samples cannot be used for working at the wavelength 514.5 nm of the argon ion laser. The time evolution of the fluorescence emission is shown to be a quick check for saturation in absorption in these films. However, the actual determination of the saturation intensities were done by plotting the transmission vs. incident intensity curves. It was found that the transmission increased indefinitely, suggesting that irreversible damage is occurring to the dye molecules. Saturation intensities were therefore measured by repeatedly plotting the transmission vs. incident intensity curves and making sure in each case that no irreversible changes had occurred. These measurements were supported by measurements of the triplet lifetimes also. A few studies of the fluorescence of these dyes in the above matrices, which, though interesting, are not directly related to the OPC studies, are described in the Appendix I.

SECTION I OF THE CHAPTER FOUR is the details of the studies of OPC in the above samples. Phase conjugation efficiencies versus the input powers, absorption lengths and wavelengths are studied and compared with the theoretical models discussed in the previous chapters. Of the three dyes used, erythrosin B showed the highest efficiency, both in gelatin and PVA films. Efficiencies were always greater in PVA films than in gelatin films. The best efficiency achieved was about  $10^{-5}$ , for erythrosin B in PVA film. Efficiency varied with the input power - peaked around the saturation intensity and then decreased. This was not only due the inherent behaviour of the interaction, but also due to the laser-induced damage of the dye molecules. This damage is found to occur very fast. Efficiency varies with the absorption length also. It was found that there exists an optimum for this. Another aspect affecting the efficiency is the "wash-out" effects due to vibration pick-ups. This also was found to be very severe.

In the SECTION II OF THE CHAPTER FOUR, OPC experiments using a Nd:Glass laser are described. An absorbing dye, Kodak 14015, dissolved in 1,2,dichloroethane is used as the nonlinear medium, in a simple DFWM scheme. There are only few reports of OPC via DFWM of broadband radiations. Actually, there are no reports at

all, where OPC of Nd:Glass laser has been achieved by a DFWM technique. The present investigations showed that it is possible to achieve this.

CHAPTER FIVE presents the details of the attempts made on developing an indigenous system for CW SHG, using Lithium Iodate crystals. Two types of crystals were used - "perpendicular-cut" and "Brewster-cut". The best output power obtained was about 1.85 milliwatts. Tunability of a few nanometers was possible. This beam was used in an experiment for detection of OH radicals in air contained in a multi-pass cell. The details of this experiment are also reported briefly in this chapter.

CHAPTER SIX is a summary of the main features of the work.

APPENDIX I presents the details of the studies on fluorescence spectra of the samples used for low power OPC. APPENDIX II is a pedagogical aspect of OPC. It is suggested that this method of obtaining an OPC beam is ideal for introducing OPC as laboratory topics in post-graduate courses. Details are discussed, alongwith suitable experimental evidences.

Most of the investigations presented in this thesis has been published/submitted for publication or presented in seminars/symposia, in the form of the following papers.

1. INVESTIGATIONS ON THIN FILM SATURABLE ABSORBERS SUITABLE FOR OPTICAL PHASE CONJUGATION, *Journal of Optics (India)*, Vol 17, 1988, pp.24-26
2. LOW POWER OPTICAL PHASE CONJUGATION IN SATURABLE ABSORBER FILMS, Proceedings of the First National Symposium on Lasers and Applications, IIT Kanpur, Dec 2-5,1987, p.44
3. OPTICAL PHASE CONJUGATION EFFICIENCY OF ERYTHROSIN B IN POLYVINYL ALCOHOL MATRIX, presented in the Workshop on Laser Spectroscopy and Laser Applications, Banaras Hindu University, Varanasi, Jan 15-20 1988.
4. SATURABLE ABSORBERS FOR LOW POWER OPTICAL PHASE CONJUGATION, *Pramana : Journal of Physics (India)*, Vol 31, 1988, pp.281-287
5. LOW POWER OPTICAL PHASE CONJUGATION IN DYES EMBEDDED IN POLYVINYL ALCOHOL FILMS, Communicated to *Applied Optics (U. S. A)*

6. OPTICAL PHASE CONJUGATION IN DYES EMBEDDED IN POLYMER FILMS, Communicated to *Optical Engineering* (U.S.A)
7. ON OPTICAL PHASE CONJUGATION USING EOSIN IN GELATIN FILMS, Communicated to *Journal of the Optical Society of America A* (U.S.A)
8. STUDIES ON OPTICAL PHASE CONJUGATION IN DYE FILMS, presented in the Young Physicists' colloquim at Saha Institute of Nuclear Physics, Calcutta, August 23-24, 1988 - to appear in *Physics Teacher* (India)
9. PHASE CONJUGATION OF Nd:GLASS LASER RADIATION VIA DEGENERATE FOUR WAVE MIXING IN AN ABSORBING DYE, Communicated to *Journal of Physics C : Applied Physics* (U.K)
10. INTRACAVITY SECOND HARMONIC GENERATION IN A RING DYE LASER USING THIN  $\text{LiIO}_3$  CRYSTALS, presented in the International Conference on Laser Applications in Spectroscopy and Optics (LASO 87), IIT Madras, Jan 2-5, 1987.
11. A MULTIPASS LONG-PATH CELL FOR ABSORPTION MEASUREMENTS, *Journal of Optics*(India), Vol.16, p.51, 1987.

12. LUMINESCENCE OF SOME ORGANIC DYES DOPED IN THIN FILMS OF GELATIN, POLYVINYL ALCOHOL AND BORIC ACID GLASS, presented in the symposium on CURRENT TRENDS IN PURE AND APPLIED PHYSICS, Department of Physics, Cochin University of Science and Technology, during October 24 - 25, 1988.
  
13. OPTICAL PHASE CONJUGATION FOR UNDERGRADUATES, *European Journal of Physics* (U.K.), (in press)

## CHAPTER 1

### INTRODUCTION

#### 1.00 General introduction to nonlinear optical phenomena :

The idea of nonlinearity in optics was first introduced in scientific literature by Nicholaas Bloembergen in early sixties of this century. The idea came essentially from a NMR analogy, in which case a radio frequency field at resonance tends to equalise the population of two spin levels, while a relaxation mechanism tries to maintain a population difference, corresponding to the Boltzmann distribution at the temperature of the other degrees of freedom in the sample [1]. It is a nonlinear phenomenon, as the magnitude of the susceptibility tends to decrease with increasing field amplitude. Nonlinear optical phenomena also result from a field dependent (optical) susceptibility. Development of various lasers during the latter part of the sixties caused a hectic search for nonlinear optical effects.

The interaction of optical radiation with matter is generally understood with the help of a linear harmonic oscillator model. But, whenever the driving force, viz. the electric field amplitude associated with the optical radiation is very high, the linear harmonic oscillator model obviously fail. The polarisation induced in the medium by the radiation field in

such cases contains higher order terms. A general expression for material polarisation due to an applied field  $E$ , therefore takes the form,

$$P_i = \chi_{ij} E_j + \chi_{ijk} E_{jk} + \chi_{ijkl} E_{jkl} \quad 1.01$$

rather than the usual linear response of the form,

$$P_i = \chi_{ij} E_j \quad 1.02$$

which is used alongwith the Maxwell's equations to obtain the usual wave equations for the propagation of electromagnetic waves through a medium. Although such nonlinear relationships in electromagnetic waves were known in the case of low frequencies (for example, audio and electrical engineers were familiar with the nonlinear relationship between magnetic induction in iron core solenoids in transformers, in the form  $B = \mu(HDH)$ , introducing such a relationship in the case of optical frequencies were thought of much later. The above expression for material polarisation considered alongwith the Maxwell's equations provide us with the laws of propagation of electromagnetic waves in the nonlinear medium and contain essentially all the subject matter of nonlinear optics.

The effects due to the higher order terms in the expression for polarisation manifest when field amplitudes become sufficiently high. A focussed laser beam can give field

amplitudes well above  $10^8$  Volts/cm, which is typically the electric field amplitudes inside atoms and molecules, responsible for binding of the valance electrons. Thus, when such a beam is incident on a medium these electrons are 'pulled out' and a plasma is formed. Obviously, effects due to the lowest order nonlinear terms manifest at much lower field strengths.

The complete nonlinear optical phenomena can be looked at as various frequency mixing (or wave mixing) processes. The lowest order nonlinear susceptibility  $\chi^{(2)}$  provide a coupling between three electromagnetic waves, each of which having its own frequency  $\omega_i$ , wave vector  $k_i$ , state of polarisation  $e_i$  and complex amplitude  $E_i = A_i \exp(i\phi_i)$ . In a similar manner  $\chi^{(3)}$  provide a coupling between four waves. A general formulation of three and four wave mixing was first developed by J.A. Armstrong *et al* [2], which has been modified by various authors in the later years.

Effects due to the second order nonlinear susceptibility appear as mixing processes involving three frequencies, in the form  $\omega_3 = \omega_1 \pm \omega_2$ . They take a variety of different forms. When there is only one frequency, the second order polarisation consists of a constant term and a term representing oscillations at double the incident frequency. The steady polarisation produces a steady electric field. Thus we get what is called the "optical rectification". Observation of such a rectification was first reported by Bass *et al.*[3] in the case of a pulsed ruby

laser radiation interacting with KDP and KD\*P crystals.

The polarisation at double the frequency radiates into the medium; thus we have the phenomena of second harmonic generation. This has been extensively studied by various workers, mainly because of its device application capabilities. Several reviews on this topic have been published by various authors [4]. The first experimental observation of SHG at optical frequencies was reported by Franken *et al* [5] in which a quartz crystal was used as the nonlinear medium. The conversion efficiency (ratio of the output power in the second harmonic to that in the fundamental) was very low - signal level was 'just detectable' only. Various materials have been tried out for achieving better efficiencies and at present, there are commercially available crystals which provide efficiencies in excess of 50 % [4].

When the incident optical field contains two different frequencies more interesting effects manifest. The simplest of them occurs when one of these frequencies is zero, i.e. when we allow a monochromatic wave of frequency  $\omega$  to interact with a nonlinear medium along with a steady electric field. The second order polarisation obviously will contain terms proportional to the products of the optical and the steady fields. One of them will be proportional to the optical field and its magnitude will be proportional to that of the steady field. This amounts to modifying the linear susceptibility tensor by a factor

proportional to the steady applied field. In other words, the refractive index at the optical frequency is modified by the value of the steady field. This is the linear electro-optic effect or Pockel's effect [6].

When the two frequencies involved are different, we get parametric mixing; generation of a new frequency  $\omega_i = \omega_p \pm \omega_s$ . When the incident field at frequency  $\omega_p$  (called the pump field) is strong and  $\omega_s$  is rather weak (called the signal field), the new field generated at  $\omega_i$  again interacts with that at  $\omega_p$  yielding a field at  $\omega_s = \omega_p - \omega_i$ . Production of this field at  $\omega_s$  will be proportional to the product of the signal field and the pump field intensities. The net effect is that this field at the frequency  $\omega_s$  is amplified at the expense of that at  $\omega_p$ . This is known as parametric amplification. This becomes particularly strong when the linear propagation constants  $k_s$ ,  $k_i$  and  $k_p$  at frequencies  $\omega_s$ ,  $\omega_i$  and  $\omega_p$  hold the "phase-matching" condition, viz.,

$$k_s + k_i = k_p \quad 1.03$$

The technique of parametric conversion of optical frequencies have been used by several workers to convert the 10.6  $\mu\text{m}$  radiation of  $\text{CO}_2$  lasers to the visible range, where efficient detectors are available [7].

Warner [8] has reviewed the state-of-art of parametric

conversion. It can be noted that parametric mixing can be used for frequency down-conversion also. This also has been reported by several authors, as reviewed by Byer *et al.* [9].

It can be seen that for materials with inversion symmetry, the second order nonlinear susceptibility tensor identically vanishes and then the lowest order nonlinearity will be the third order one. The variety of different phenomena that result out of this are together called Four Wave Mixing (FWM).

When a monochromatic wave interacts with a medium the immediate third order nonlinear phenomena to be manifested is the third harmonic generation (THG). Terhune and co-workers were the first to report the observation of THG [10].

A monochromatic field in the presence of another steady field can result what is called the quadratic electro-optic effect or Kerr effect, i.e. the refractive index of the material at the incident frequency will be modified by an amount proportional to the square of the steady field applied. This effect is frequently made use of in making electro-optic shutters for Q-switching and mode-locking [11].

When the frequencies involved are different, mixing schemes of the general form,  $\omega_4 = \omega_1 \pm \omega_2 \pm \omega_3$  take place. Though, in general, nonlinear optical phenomena due to the second and third order susceptibilities are classical in nature, some of the third

order phenomena are essentially quantal effects. For example, a weak signal wave at frequency  $\omega_s$  and an intense pump wave at  $\omega_p$  are allowed to interact in a medium, with  $\omega_s$  and  $\omega_p$  chosen in such a way that  $\omega_p + \omega_s = \omega_t$ , a transition frequency of the medium, then this resonant transition can actually take place, by the simultaneous absorption of two photons, one each from the pump and the signal waves. This is known as two photon absorption (TPA) and has been observed in several solids and liquids [12].

In the other case, viz., when  $\omega_p - \omega_s = \omega_t$ , the transition takes place by the simultaneous absorption of a pump photon and emission of a signal photon. This is known as stimulated Raman scattering (SRS) [13]. In ordinary Raman effect [14], a signal wave is absent, whereas in this case the presense of such a signal wave stimulates emission of the Stokes wave. Several organic liquids have shown this phenomena. Actually, SRS has been made use of by many workers to obtain laser emission at wavelengths slightly shifted from that of a standard laser [15].

Large volumes of research work have been done by scientists all over the world in understanding as well as making use of the various FWM processes in various media. Reviews have been appeared in the different categories of FWM, like tunable infrared generation, tunable vacuum ultra violet (VUV) generation etc. [16].

The most interesting third order nonlinear phenomenon is perhaps the optical phase conjugation (OPC). This happens when the nonlinear medium is subjected to three electromagnetic radiations of the same frequency, in such a way that two of them are intense and counter-propagating and the third one is rather weak and incident at a small angle to the other two. A new wave is then generated out of the nonlinear interaction (called degenerate four wave mixing (DFWM)) in the direction opposite to that of the weak probe beam. The spatial properties of this beam are very interesting - this will be a "phase-conjugate" or "time-reversed" replica of the probe beam. Under favourable conditions the newly generated wave can grow in intensity, at the expense of the pump beams. This is separately dealt with in chapter 2.

#### 1.01 An expression for the r th order susceptibility tensor :

To arrive at an expression for the r th order optical susceptibility, we follow the method adopted by Butcher [17]. To start with, the material polarisation is expanded in higher order terms as,

$$P(t) = P^0 + P^{(1)}(t) + P^{(2)}(t) + P^{(3)}(t) + \dots + P^{(r)}(t) + \dots \quad 1.04$$

where  $P^0$  is a steady polarisation independent of the applied field. The other terms represent the orders indicated, i.e the term  $P^{(2)}$  will be proportional to the square of the applied field,

$P^{(3)}$  to the cube of the applied field etc.

Taking the most general linear expression for  $P^{(4)}(t)$  in  $E(\omega)$ , we can write,

$$P^{(4)}(t) = \int_{-\infty}^{+\infty} \omega \, d\omega \, \chi^{(4)} \cdot E(\omega) \exp(-i\omega t) \quad 1.05$$

where  $\chi^{(4)}$  is the first order susceptibility tensor and  $E(\omega)$  is the Fourier transform of the field  $E(t)$ , given by

$$E(t) = \int_{-\infty}^{+\infty} d\omega \, E(\omega) \exp(-i\omega t) \quad 1.06$$

This expression  $P^{(4)}(t)$  can be generalised to any arbitrary order  $r$ , as

$$P^{(r)}(t) = \int_{-\infty}^{+\infty} d\omega_1 \dots \int_{-\infty}^{+\infty} d\omega_r \, \chi^{(r)} | E(\omega_1) E(\omega_2) \dots E(\omega_r) \exp(-it \sum_{m=1}^r \omega_m) \quad 1.07$$

where  $\chi^{(r)}(\omega_1 \dots \omega_r)$  is the  $r$ th order susceptibility tensor. The vertical line indicates that the last  $r$  suffixes on  $\chi^{(r)}$  are to be made equal to those on  $E(\omega_1), E(\omega_2), \dots, E(\omega_r)$  respectively, and summed over  $x, y$  and  $z$ . In suffix notation this reads,

$$P_{\mu}(t) = \int_{-\infty}^{+\infty} d\omega_1 \dots \int_{-\infty}^{+\infty} d\omega_r \chi_{\mu\alpha_1\alpha_2\dots\alpha_r}^{(r)}(\omega_1, \omega_2, \dots, \omega_r) \\ E_{\alpha_1\alpha_1}(\omega_1) E_{\alpha_2\alpha_2}(\omega_2) \dots E_{\alpha_r\alpha_r}(\omega_r) \exp(-it \sum_{m=1}^r \omega_m)$$

1.08

The integration paths are assumed to be parallel to the real axis in the upper half plane. The form of the above equation is such that  $\chi_{\mu\alpha_1\alpha_2\dots\alpha_r}^{(r)}(\omega_1, \dots, \omega_r)$  can always be chosen so as to be invariant under all permutations of the pairs  $\alpha_1\omega_1, \alpha_2\omega_2, \dots, \alpha_r\omega_r$ . This is due to the intrinsic permutation symmetry of the tensor elements.

Considering a volume  $V$  of the medium, which is small enough to neglect the variations of the field  $E(t)$  within it, and denoting the charge and position vector for each of the charged particle within it by  $q_j$  and  $r_j$  respectively, we can write, for the dipole moment  $R$  of the total charged particle system as,

$$R = \sum_j q_j r_j \quad 1.09$$

The macroscopic polarisation  $P(t)$  is then the expectation value of the dipole moment for unit volume. i.e.,

$$P(t) = V^{-1} \langle R \rangle = V^{-1} \text{Tr} \{ \rho(t) R \} \quad 1.10$$

where  $\rho(t)$  is the density operator of the charged particle

system. Energy of the dipole moment in an electric field  $E(t)$  is then,

$$H_1(t) = -R \cdot E(t) = -R_\alpha E_\alpha(t) \quad 1.11$$

Suffix  $\alpha$  denoting summation over  $x, y$  and  $z$ . This is the perturbation Hamiltonian of a charged particle system due to the presence of the electric field. Expanding the density operator in the usual perturbation series,

$$\rho(t) = \rho_0 + \rho_1(t) + \rho_2(t) + \dots + \rho_r(t) + \dots \quad 1.12$$

where  $\rho_0 = \xi \exp(-H_0/kT)$ , the normalised Boltzman factor,  $H_0$  being the Hamiltonian of the unperturbed system. The higher terms are given by,

$$\rho_r(t) = (i\hbar)^{-r} U_0(t) \int_{-\infty}^t dt_1 \int_{-\infty}^{t_1} dt_2 \dots \int_{-\infty}^{t_{r-1}} dt_r \left[ H_1'(t_1), [H_1'(t_2), \dots \dots [H_1'(t_r), \rho_0] \dots] \right] U_0(-t) \quad 1.13$$

$U_0$  being the wavefunction of the unperturbed system and  $H_1$  is the perturbation Hamiltonian [18].  $H_1'(t)$  is given by ,

$$H_1'(t) = U_0(-t) H_1(t) U_0(t) \quad 1.14$$

The expressions for the polarisation terms are then,

$$P^{(0)} = V^{-1} \text{Tr} \langle \rho_0 R \rangle \quad 1.15$$

$$P^{(r)} = V^{-1} \text{Tr} \langle \rho_r(t) R \rangle, \quad r \neq 0 \quad 1.16$$

Substituting for  $\rho_r(t)$  from 1.13 and simplifying, we arrive at,

$$\begin{aligned} \chi_{\mu\alpha_1\alpha_2\dots\alpha_r}^{(r)}(\omega_1, \omega_2, \dots, \omega_r) &= \frac{-1}{r!} S V^{-1} (-i\hbar)^r \int_{-\infty}^0 dt_1 \int_{-\infty}^{t_1} dt_2 \dots \\ &\dots \int_{-\infty}^{t_{r-1}} dt_r \left\{ \text{Tr} \left\{ \rho_0 \left[ \dots \left[ [R_\mu, R_{\alpha_1}^{(t_1)}], R_{\alpha_2}^{(t_2)} \right], \dots, R_{\alpha_r}^{(t_r)} \right] \right\} \right\} \\ &\qquad \qquad \qquad \exp \left( -i \sum_{m=1}^r \omega_m t_m \right) \end{aligned} \quad 1.17$$

where S indicates that the expression which follows it is to be summed over all the  $r!$  permutations of the pairs  $\alpha_1\omega_1, \alpha_2\omega_2, \dots, \alpha_r\omega_r$ .

If we assume that the system comprises of an assembly of identical molecules and making use of little more quantum mechanical ideas, we can arrive at the following expression for the linear susceptibility tensor,

$$\chi_{\mu\alpha}^{(1)}(\omega) = \frac{-n}{\hbar} \sum_{ab} \rho_{\alpha\alpha}^0 \left[ \frac{R_{ab}^{\mu} R_{ba}^{\alpha}}{\omega_{ab} + \omega} + \frac{R_{ab}^{\alpha} R_{ba}^{\mu}}{\omega_{ab} - \omega} \right] \quad 1.18$$

where  $n$  = number density of the particles and  $\rho_{\alpha\alpha}^0 = \xi \exp(-E_{\alpha}/kT)$  the unperturbed Boltzman factor.  $R_{\alpha}^{\mu}$  denotes the  $(ab)$ th matrix element of  $R^{\mu}$ .  $\omega_{ab}$  is the energy difference between the states  $a$  and  $b$ , divided by  $\hbar$ . In a similar manner, we get,

$$\chi_{\mu\alpha\beta}^{(2)}(\omega_1, \omega_2) = S \frac{n}{2\hbar^2} \sum_{abc} \rho_{\alpha\alpha}^0 \left[ \frac{R_{ab}^{\mu} R_{bc}^{\alpha} R_{ca}^{\beta}}{(\omega_{ab} + \omega_1 + \omega_2)(\omega_{ac} + \omega_2)} + \frac{R_{ab}^{\alpha} R_{bc}^{\mu} R_{ca}^{\beta}}{(\omega_{ab} - \omega_1)(\omega_{ac} + \omega_2)} + \frac{R_{ab}^{\alpha} R_{bc}^{\beta} R_{ca}^{\mu}}{(\omega_{ab} - \omega_2)(\omega_{ac} - \omega_1 - \omega_2)} \right] \quad 1.19$$

and so on.  $S$  denotes summation over the permutation of the pairs  $\mu\omega_0, \alpha\omega_1, \beta\omega_2$ . To simplify these expressions and get a more general expression for the  $r$ th order susceptibility we can make use of the overall permutation symmetry of the tensor elements. Then,

$$\chi_{\mu\alpha}^{(1)}(\omega) = \frac{-n}{\hbar} S_T \sum_{ab} \rho_{aa}^0 \left[ \frac{R_{ab}^\mu R_{ba}^\alpha}{\omega_{ab} + \omega} \right] \quad 1.21$$

where  $S_T$  is now the total symmetrisation operator, indicating summation of all the possible permutations of the pairs  $\mu\omega_0$  &  $\alpha\omega$ , where we have defined  $\omega_0 = -\omega$ . Similarly for the second order,

$$\chi_{\mu\alpha\beta}^{(2)}(\omega_1, \omega_2) = S_T \frac{n}{2\hbar^2} \sum_{abc} \rho_{aa}^0 \left[ \frac{R_{ab}^\mu R_{bc}^\alpha R_{ca}^\beta}{(\omega_{ab} + \omega_1 + \omega_3)(\omega_{ac} + \omega_2)} \right] \quad 1.22$$

and so on. Generalising this to any arbitrary order  $r$ , we get,

$$\chi_{\mu\alpha_1\alpha_2\dots\alpha_r}^{(r)}(\omega_1, \omega_2, \dots, \omega_r) = S_T \frac{(-1)^r n}{\hbar^r r!} \sum_{ab_1b_2b_3\dots b_r} \rho_{aa}^0 \left[ \frac{R_{ab_1}^\mu R_{b_1b_2}^{\alpha_1} R_{b_2b_3}^{\alpha_2} \dots R_{b_r b_a}^{\alpha_r}}{D(a, b_1, b_2, \dots, b_r; \omega_1, \omega_2, \dots, \omega_r)} \right] \quad 1.23$$

where,

$$\begin{aligned}
 D(a, b_1, b_2, \dots, b_r; \omega_1, \omega_2, \dots, \omega_r) &= \\
 & (\omega_{ab_1} + \omega_1 + \omega_2 + \dots + \omega_r) (\omega_{ab_2} + \omega_2 + \omega_3 + \dots + \omega_r) (\omega_{ab_3} + \omega_3 + \omega_4 + \dots + \omega_r) \dots \\
 & \dots \dots (\omega_{ab_{r-1}} + \omega_{r-1} + \omega_r) (\omega_{ab_r} + \omega_r) \qquad \qquad \qquad 1.24
 \end{aligned}$$

$S_T$  denoting summation over all the permutations of the pairs

$$\mu\omega_0, \alpha_1\omega_1, \alpha_2\omega_2, \dots, \alpha_r\omega_r \quad \text{where,} \quad \omega_0 = -(\omega_1 + \omega_2 + \omega_3 + \dots + \omega_r).$$

**1.02 Effects due to the second order susceptibility :**

(i) *The Pockel's Effect* : Pockels effect or the linear electro-optic effect has been known for many years. Twenty of the twentyone acentric point groups of the crystals exhibit this property with varying degrees [19]. When these crystals are subjected to a steady electric field, the optical refractive indices change. The magnitude of this change is specified by the electro-optic coefficient,  $Z_{\mu\alpha\beta}(\omega)$ , at the frequency  $\omega$ . This is a third rank tensor, defined by the equation,

$$\delta\epsilon_{\mu\alpha}^{-1}(\omega) = Z_{\mu\alpha\beta}(\omega) E_{0\beta} \qquad \qquad \qquad 1.25$$

where  $\delta\epsilon_{\mu\alpha}^{-1}(\omega)$  is the change of the inverse dielectric tensor at the frequency  $\omega$  produced by the steady field  $E_0$ .

If  $\epsilon$  and  $\epsilon^{-1}$  are the dielectric tensor in the absence of the field and its inverse, and  $\delta\epsilon$  and  $\delta\epsilon^{-1}$  are the changes produced by the field, then  $\delta\epsilon^{-1}$  is given by the equation 1.25. The total inverse dielectric tensor in the presence of the field is then  $\epsilon^{-1} + \delta\epsilon^{-1}$ . To the first order in  $\delta\epsilon^{-1}$ , inverse of  $(\epsilon^{-1} + \delta\epsilon^{-1})$  is  $\epsilon + \epsilon \cdot \delta\epsilon^{-1} \cdot \epsilon = \epsilon + \delta\epsilon$ . i.e.,

$$\delta\epsilon = \epsilon \cdot \delta\epsilon^{-1} \cdot \epsilon \quad 1.26$$

Making use of 1.23,

$$\delta\epsilon_{\mu\alpha}(\omega) = \epsilon_{\mu\mu}(\omega) \epsilon_{\alpha\alpha}(\omega) Z_{\mu\alpha\beta}(\omega) E_{\alpha\beta} \quad 1.27$$

$\beta$  to be summed over x, y and z. Considering an optical wave with electric field  $E \exp(-i\omega t) + C.C.$ , we can write,

$$P^{(1)}(t) = \chi^{(1)}(0) E_0 + \left[ \chi^{(1)}(\omega) \cdot E \exp(-i\omega t) + C.C. \right] \quad 1.28$$

and

$$P^{(2)}(t) = \chi^{(2)}(0,0) : E_0 E_0 + 2 \chi^{(2)}(\omega, -\omega) : E E^* \\ + \left[ 2\chi^{(2)}(\omega, 0) : E E_0 \exp(-i\omega t) + C.C. \right] \\ + \left[ \chi^{(2)}(\omega, \omega) : E E \exp(-2i\omega t) + C.C. \right] \quad 1.29$$

Combining these two, we get, in the suffix notation,

$$P_{\mu}(\omega, t) = \left[ \chi_{\mu\alpha}^{(1)}(\omega) + 2 \chi_{\mu\alpha\beta}^{(2)}(\omega, 0) E_{\alpha\beta} \right] E_{\alpha} \exp(-i\omega t) + \text{C.C.} \quad 1.30$$

from which it is immediately evident that the presence of the field  $E_0$  has changed the effective linear susceptibility by an amount  $2 \chi_{\mu\alpha\beta}^{(2)}(\omega, 0) E_{\alpha\beta}$ , and a change of

$$\delta\epsilon_{\mu\alpha}(\omega) = 8 \pi \chi_{\mu\alpha\beta}^{(2)}(\omega, 0) E_{\alpha\beta} \quad 1.31$$

in the effective dielectric constant.

The magnitude of this change is generally very small, since the nonvanishing components of  $\chi^{(2)}$  are generally of the order of  $10^{-8}$  e.s.u. However, since the optical wavelengths are so small, phase changes produced due to this change in the dielectric tensor, become appreciable within the length of a few centimetres itself. For example, in the case of a KDP crystal, a field of 10 kV/cm ( $\approx 30$  e.s.u.) cause a change of dielectric constant  $\delta\epsilon \approx 0.45 \times 10^{-4}$ . The consequent change of refractive index is  $\delta\eta \approx 1.5 \times 10^{-5}$ , which will produce a phase change of  $2\pi$  in transmission pathlength of  $l = \lambda/\delta\lambda \approx 3$  cm for a 500 nm radiation [17].

Electro-optic effect has been used for modulation of optical radiations. Both amplitude and phase modulations have been successfully achieved using different crystals [20].

(ii) *Optical rectification* : From equation 1.29, it can be seen that an optical field  $E \exp(i\omega t) + C.C.$  produces a steady component in the quadratic polarisation, which is given by,

$$P_o = 2\chi^{(2)}(\omega, -\omega) : E E^* \quad 1.32$$

This will induce a steady field  $E_o$ , determined by the electrostatic equations,

$$\nabla \cdot [\epsilon \cdot E_o + 4\pi P_o] = 0 \quad \text{and} \quad \nabla \times E_o = 0 \quad 1.33$$

and the boundary conditions pertinent to the particular experimental situation.  $\epsilon$  denotes the static dielectric tensor here.

The solutions of the equations 1.33 depend on the particular experimental conditions. For example, consider an idealised example of a parallel plate condenser filled with a nonlinear medium, say KDP, whose optic axis is perpendicular to the plates, and an optical radiation passing through it in the x-y plane. We ignore the nonlinearities in propagation. Also, it is assumed that the optical wave fills the nonlinear medium which does not touch the plates of the condenser. The equation for the optical wave can then be written as,

$$E = A a \exp \left[ i \frac{\omega}{c} \eta n \cdot r \right] \quad 1.34$$

Where  $A$ ,  $a$ ,  $\eta$  and  $n$  are respectively the amplitude, normalised polarisation vector, refractive index and direction of propagation. The steady term in the expression for polarisation can then be obtained by substituting 1.34 into 1.32 and 1.33. For a typical case with the nonvanishing component of  $\chi^{(2)}$  being equal to  $8.5 \times 10^{-8}$  e.s.u., and the parallel component of the dielectric constant  $\epsilon_{o\parallel} = 21.4$ , when a wave with a power density of 10 MW/sq.cm ( i.e.  $A = 150$  e.s.u. ) passes through the crystal at an angle of 45 degrees we get the z component of the rectified field  $E_{oz} = 0.5$  volts [17].

(iii) *Second Harmonic Generation (SHG)* : From equation 1.29, we see that the electric field  $E \exp(i\omega t) + C.C.$  produces a second harmonic term

$$P_2 = \chi^{(2)}(\omega, -\omega) : E E \quad 1.35$$

in the quadratic polarisation. This polarisation radiates into the medium, producing a second harmonic field  $E_2 \exp(-2i\omega t) + C.C.$  The equation which governs the growth of this  $E_2(t)$  can be obtained from the Maxwells equations. We have,

$$\nabla \times E(t) + \frac{1}{c} \frac{d}{dt} H(t) = 0 \quad 1.36$$

$$\text{and} \quad \nabla \times H(t) - \frac{1}{c} \frac{d}{dt} E(t) = \frac{4\pi}{c} \frac{d}{dt} P(t) \quad 1.37$$

and the resulting wave equation,

$$\nabla \times \nabla \times \mathbf{E}(t) + \frac{1}{c^2} \frac{d^2}{dt^2} \mathbf{E}(t) = \frac{-4\pi}{c^2} \frac{d^2}{dt^2} \mathbf{P}(t) \quad 1.38$$

Assuming solutions of the form,

$$\mathbf{E}(t) = \sum_f \mathbf{E}_f \exp(-i\omega_f t) \quad 1.39$$

$$\text{and } \mathbf{P}(t) = \sum_f \mathbf{P}_f \exp(-i\omega_f t) \quad 1.40$$

$$\text{we get, } \nabla \times \nabla \times \mathbf{E}_f - \frac{\omega_f^2}{c^2} \mathbf{E}_f = 4\pi \frac{\omega_f^2}{c^2} \mathbf{P}_f \quad 1.41$$

Now expressing the polarisation term in the form,

$$\mathbf{P}_f = \chi^{(1)}(\omega_f) \mathbf{E}_f + \mathbf{P}_f^{NL} \quad 1.42$$

where the latter term represents the contribution due to the nonlinear terms, 1.41 reduces to

$$\nabla \times \nabla \times \mathbf{E}_f - \frac{\omega_f^2}{c^2} \epsilon(\omega_f) \cdot \mathbf{E}_f = 4\pi \frac{\omega_f^2}{c^2} \mathbf{P}_f \quad 1.43$$

$$\text{where } \epsilon(\omega_f) = 1 + 4 \pi \chi^{(4)}(\omega_f) \quad 1.44$$

is the dielectric tensor at frequency  $\omega_f$ .

In the case of SHG, we have  $\omega_f = 2\omega$  ;  $P_f^{NL} = P_2$  and  $E_f = E_2$  ;  
then,

$$\nabla \times \nabla \times E_2 - \frac{4 \omega^2}{c^2} \epsilon(2\omega) \cdot E_2 = 16 \pi \frac{\omega^2}{c^2} P_2 \quad 1.45$$

Under the Slowly Varying Envelope (SVEA) [21] conditions, this equation can be shown to have a solution,

$$E_2 = \left[ A_2(\zeta) \mathbf{a}_2 + c_2(\zeta) \right] \exp(2i\omega\eta_2\zeta/c) \quad 1.46$$

where  $\zeta = \mathbf{n} \cdot \mathbf{r}$  ,  $\mathbf{a}_2$  is the normalised polarisation vector of the second harmonic wave,  $A_2(\zeta)$  is a slowly varying amplitude factor and  $c_2(\zeta)$  is a small and slowly varying correction term which arises from the components of  $P_2$  orthogonal to  $\mathbf{a}_2$ . This would lead us to a differential equation for  $A_2(\zeta)$ , in the form,

$$\frac{d}{d\zeta} A_2(\zeta) = \frac{i4\pi\omega}{c \eta_2} \frac{\mathbf{a}_2 \cdot P_2}{(\mathbf{n} \times \mathbf{a}_2)} \exp(-2i\omega\eta_2\zeta/c) \quad 1.47$$

from which,

$$A_2(\zeta) = \frac{i A}{L} \exp(i\Delta k \zeta/2) \frac{\sin(\Delta k \zeta/2)}{\Delta k/2} \quad 1.48$$

$$\text{where, } \Delta k = 2\omega (\eta - \eta_2) / c \quad 1.49$$

and

$$\frac{1}{L} = A \frac{4 \pi \omega}{c \eta_2} \frac{\chi^{(2)}(\omega, \omega) \cdot a_2 a a}{(n \times a_2)^2} \quad 1.50$$

Thus, we see that  $A_2(\zeta)$  oscillates sinusoidally when  $\Delta k \neq 0$ , but when  $\Delta k = 0$ , grows linearly with  $\zeta$  and  $|A_2(\zeta)| = A$ , when  $\zeta = L$ . Most of the optically transparent materials exhibit normal dispersion, i.e., increases with frequency. Thus the condition for perfect phase matching, i.e., for  $\eta_2 = \eta$ , so that  $\Delta k = 0$ , cannot be achieved when the second harmonic wave and the fundamental are of the same type. Giordmaine [22] and Maker et al [23] were the first to point out that the directional dependence of the extra-ordinary refractive indices in the case of uniaxial and biaxial crystals can be employed to balance out the effects of dispersion. In the later years, the field of SHG has grown to a vast extent. Several reviews have been published in this topic [4]. More of SHG is discussed in chapter 5.

(iv) *Mixing and parametric effects* : In the above sections we have considered the case of only one frequency. Mixing and

parametric effects result when there are more than one frequency, e.g., when there are two waves as  $E_1 \exp(-i\omega_1 t) + \text{C.C.}$  and  $E_2 \exp(-i\omega_2 t) + \text{C.C.}$ , where  $\omega_2 > \omega_1 > 0$ . Obviously, the quadratic polarisation contains a term of the form,

$$P_2 = 2\chi^{(2)}(\omega_2, \omega_1) : E_2 E_1^* \quad 1.51$$

The difference frequency  $\omega_2 - \omega_1 = \omega_3$ , generates a new field which varies as  $E_3 \exp(-i\omega_3 t) + \text{C.C.}$ . The equation which governs the growth of this field can be obtained by setting  $P_f^{\text{NL}} = P_2 = 2\chi^{(2)}(\omega_3, -\omega_1) : E_3 E_1^*$  in the equation 1.41. The equation then looks as,

$$\nabla \times \nabla \times E_2 - \frac{\omega_2^2}{c^2} \epsilon(\omega_2) \cdot E_2 = 4\pi \frac{\omega_2^2}{c^2} P_2 \quad 1.52$$

and differs from the case of SHG only by a change of  $2\omega$  to  $\omega_2$ . The solutions can be obtained in the SVEA, as in the case of SHG. Considering the case where  $E_1$  and  $E_2$  propagate in the same direction, we can write,

$$E_1 = A_1 a_1 \exp(i\omega_1 \eta_1 [n \cdot r]/c) \quad 1.53$$

$$E_2 = A_2 a_2 \exp(i\omega_2 \eta_2 [n \cdot r]/c) \quad 1.54$$

From 1.51, it follows that,

$$P_2 = 2A_2 A_1^* \chi^{(2)}(\omega_3, -\omega_1) : a_2 a_1 \exp \left[ i(\omega_3 \eta_3 - \omega_1 \eta_1)(n \cdot r)/c \right] \quad 1.55$$

When the phase matching condition,

$$\omega_2 \eta_2 = \omega_3 \eta_3 - \omega_1 \eta_1 \quad 1.56$$

is approximately satisfied, then we can write,

$$E_2 = \left[ A_2(\zeta) a_2 + c_2(\zeta) \right] \exp(i\omega_2 \eta_2 \zeta / c) \quad 1.57$$

and the differential equation for  $A_2(\zeta)$ ,

$$\frac{d}{d\zeta} A_2(\zeta) = \frac{14\pi\omega_2}{c \eta_2} \frac{\chi^{(2)}(\omega_3, \omega_1) : a_2 a_3 a_1}{(n \times a_2)^2} A_3 A_1^* \exp(i\Delta k \zeta) \quad 1.58$$

where,

$$\Delta k = ( \omega_3 \eta_3 - \omega_1 \eta_1 - \omega_2 \eta_2 ) / c \quad 1.59$$

This is the equation for the growth of the difference frequency field. The case of the sum frequency  $\omega_{2+} = \omega_3 - \omega_1$  also can be treated in a similar way and we would end up with the equation,

$$\frac{d}{d\zeta} A_{2+}(\zeta) = \frac{14\pi\omega_{2+}}{c \eta_{2+}} \frac{\chi^{(2)}(\omega_3, \omega_1) : a_{2+} a_3 a_1}{(n \times a_{2+})^2} A_3 A_1^* \exp(i\Delta k \zeta) \quad 1.60$$

$$\text{where } \Delta k = ( \omega_3 \eta_3 + \omega_1 \eta_1 - \omega_2 \eta_2 ) / c \quad 1.61$$

In actual practice, since it is not possible to minimise  $\Delta k$  in both 1.59 and 1.61 together, sum or difference frequency will be generated depending on, which of these conditions is more satisfied. Of these, the case of difference frequency generation is of particular interest, because of amplification and oscillation possibilities. This comes due to a term in the quadratic polarisation, of the form,

$$P_1 = 2\chi^{(2)}(\omega_3, -\omega_2) : E_3 E_2^* \quad 1.62$$

which represents an interaction between the newly generated field and the pump field  $E_3$ . This new polarisation radiates into the medium, generating a new field at  $\omega_1$ . As this process continues field at  $\omega_1$  grows, at the expense of that at  $\omega_3$ . Thus if we introduce an intense radiation at frequency  $\omega_3$  alongwith a weak one at  $\omega_1$  such that  $\omega_3 > \omega_1$ , the weak field gets amplified, provided we have chosen the phase-matching condition appropriately. This can go the extent that even without the presense of a weak radiation as such, a stray photon of the appropriate frequency may get amplified. If we place the crystal in a proper optical cavity, oscillations build up. This is called the Optical Parametric Oscillation (OPO). Experimental observations of this effect was first reported by Giordmaine and Miller [24]. A lot of work have been carried out in the later years. A review can be found in the reference [25].

### 1.03 Effects due to the third order susceptibility :

(i) *The Kerr Effect* : In media with inversion symmetry, the quadratic term in the polarisation vanishes and the lowest order nonlinear term in the total polarisation will be the cubic term given by

$$P^{(3)}(t) = \sum_{ijk} \chi^{(3)}(\omega_i, \omega_j, \omega_k) \vdots E_i E_j E_k \exp[-it(\omega_i + \omega_j + \omega_k)] \quad 1.63$$

The simplest phenomenon arising from this term is the Kerr effect. When a medium is subjected to a steady field and an optical wave with the electric field  $E \exp(-i\omega t) + C.C.$ , the above polarisation terms becomes  $3\chi^{(3)}(\omega, 0, 0) \vdots E_o E_o E_o$ . The total polarisation therefore becomes,

$$\begin{aligned} P_\mu &= \left[ \chi_{\mu\alpha}^{(1)}(\omega) E_\alpha \exp(-i\omega t) + C.C. \right] \\ &\quad + 3 \left[ \chi_{\mu\alpha\beta\gamma}^{(3)}(\omega, 0, 0) E_\alpha E_{o\beta} E_{o\gamma} \exp(-i\omega t) + C.C. \right] \\ &= \left[ \chi_{\mu\alpha}^{(1)}(\omega) + 3\chi_{\mu\alpha\beta\gamma}^{(3)}(\omega, 0, 0) E_{o\beta} E_{o\gamma} \right] E_\alpha \exp(-i\omega t) + C.C. \end{aligned}$$

1.64

That is, the steady field causes a change of  $3\chi_{\mu\alpha\beta\gamma}^{(3)}(\omega, 0, 0) E_{o\beta} E_{o\gamma}$  in the effective value of the linear susceptibility tensor at

frequency  $\omega$ . The change in the effective value of the dielectric tensor is

$$\delta \epsilon_{\mu\alpha}(\omega) = 12 \pi \chi_{\mu\alpha\beta\gamma}^{(3)}(\omega, 0, 0) E_{\alpha\beta} E_{\alpha\gamma} \quad 1.65$$

This is Kerr effect, which is specified by the tensor  $\chi_{\mu\alpha\beta\gamma}^{(3)}(\omega, 0, 0)$ .

The Kerr effect is employed in making Kerr cells which are electronically controllable optical gates. The nonlinear medium is generally an organic liquid like nitrobenzene. When no external field is applied, the liquid is optically isotropic. When a steady field of calculated value is applied, a preferred direction is introduced and the medium becomes uniaxial. The phase difference which occurs between the ordinary and the extraordinary waves as they propagate through the medium can be adjusted by varying the applied voltage so as to rotate the plane of polarisation of an incident beam by  $90^\circ$  or to convert the incident plane polarised beam into an elliptically or circularly polarised light. Nitrobenzene Kerr cells are used as Q-switches for Nd lasers [11].

(ii) *Third Harmonic Generation (THG)* : From equation 1.63, we can see that an optical electric field  $E \exp(-i\omega t) + C.C.$  produces a third harmonic term  $P_3 \exp(-i\omega t) + C.C.$  in the cubic polarisation, where,

$$P_3 = \chi^{(3)}(\omega, \omega, \omega) \vdots E E E \quad 1.66$$

As in the case of the second order nonlinearity, the growth of the induced third harmonic field  $E_3 \exp(-3i\omega t) + C.C.$  is governed by the equation,

$$\nabla \times \nabla \times E_3 - \frac{9 \omega^2}{c^2} \epsilon(3\omega) \cdot E = 36 \pi \frac{\omega}{c^2} P_3 \quad 1.67$$

This can be solved in a way similar to that of the case of SHG, i.e., ignoring the effects of nonlinearities on the propagation of the fundamental wave and writing,

$$E = A a \exp(i\omega \eta [n \cdot r]/c) \quad 1.68$$

Under properly phase-matched conditions (i.e.,  $\eta_3 \cong \eta$ ) the solution has the form,

$$E_3 = \left[ A_3(\zeta) a_3 + c_3(\zeta) \right] \exp(i3\omega \eta_3 \zeta/c) \quad 1.69.$$

where,  $\zeta = n \cdot r$ ,  $A_3(\zeta)$  is a slowly varying amplitude factor  $a_3$  is the normalised polarisation vector of the third harmonic wave and  $c_3(\zeta)$  is a small and slowly varying correction term. With a boundary condition  $A_3(0) = 0$ , this would lead to

$$A_3(\zeta) = \frac{i A}{L_3} \exp(i\Delta k \zeta/2) \frac{\sin(\Delta k \zeta/2)}{\Delta k/2} \quad 1.70$$

where,

$$\Delta k = 3\omega (\eta - \eta_s) / c \quad 1.71$$

and

$$\frac{1}{L_s} = A^2 \frac{6\pi\omega}{c\eta_s} \frac{\chi^{(3)}(\omega, \omega, \omega) \vdots a_s a_s a_s a_s}{(n \times a_s)} \quad 1.72$$

An estimate of THG in calcite [17] shows that this is an extremely weak effect. Terhune [10] has observed THG in calcite crystals under phase-matched conditions using 1 MW Q-switched ruby laser. In later years THG have been achieved with much more efficiencies [16] making use of the resonantly enhanced nonlinear susceptibilities. We have, from equation 1.23 and 1.24, the equation for the susceptibility responsible for THG as,

$$\chi_{\mu\alpha\beta\gamma}^{(3)}(-3\omega; \omega \omega \omega) = S \frac{-n}{6h^3} \sum_{ab_1 b_2 b_3} \rho_{00} \left[ \begin{aligned} & \frac{R_{ab_1}^{\mu} R_{b_1 b_2}^{\alpha} R_{b_2 b_3}^{\beta} R_{b_3 a}^{\gamma}}{(\omega_{ab_1} - 3\omega)(\omega_{ab_2} - 2\omega)(\omega_{ab_3} - \omega)} \\ & + \frac{R_{ab_1}^{\alpha} R_{b_1 b_2}^{\mu} R_{b_2 b_3}^{\beta} R_{b_3 a}^{\gamma}}{(\omega_{ab_1} + \omega)(\omega_{ab_2} - 2\omega)(\omega_{ab_3} - \omega)} + \frac{R_{ab_1}^{\alpha} R_{b_1 b_2}^{\beta} R_{b_2 b_3}^{\mu} R_{b_3 a}^{\gamma}}{(\omega_{ab_1} + \omega)(\omega_{ab_2} + 2\omega)(\omega_{ab_3} - \omega)} \\ & + \frac{R_{ab_1}^{\alpha} R_{b_1 b_2}^{\beta} R_{b_2 b_3}^{\gamma} R_{b_3 a_1}^{\mu}}{(\omega_{ab_1} + \omega)(\omega_{ab_2} + 2\omega)(\omega_{ab_3} + 3\omega)} \end{aligned} \right] \quad 1.73$$

It is obvious that the value of this susceptibility diverges around the frequencies corresponding to  $\omega$  or  $2\omega$ . In other words, this means that we can have a very large value for  $\chi^{(3)}$ , if we choose a nonlinear medium which has a real level corresponding to the optical frequency  $\omega$  or  $2\omega$ . In the former case it is called a one-photon resonance and in the latter, a two-photon resonance.

THG has been efficiently achieved in metal vapours and other gaseous media making use of the resonance enhancement. Several reviews have been appeared on this topic [16].

(iii) *Stimulated Raman Scattering and Two Photon Absorption :*

An intense laser beam at frequency  $\omega_p$  (p, for pump) and a weak one at  $\omega_s$  (s, for signal) together propagated through a nonlinear medium, show these two effects, depending on the resonance conditions. The signal beam is amplified at the expense of the pump if  $\omega_p - \omega_s = \omega_{to}$ , corresponds to an allowed transition in the medium. This is called Stimulated Raman Scattering. In the case of  $\omega_p + \omega_s = \omega'_{to}$ , corresponds to an allowed transition, both the beams get attenuated due to absorption. This is Two Photon Absorption. (It is assumed that  $\omega_p$  and  $\omega_s$  separately are not near to any allowed transitions in the medium).

Following the notations used in the previous sections, if we

consider a pump and signal beam amplitudes of the form,

$$E_p = A_p a_p \exp(i\omega_p \eta_p n.r/c) \quad \text{and} \quad E_s = A_s a_s \exp(i\omega_s \eta_s n.r/c)$$

1.74

we have a term in the cubic polarisation in the form,

$$\delta\chi^{(3)}(\omega_p, -\omega_p, \omega_s): E_p E_p^* E_s \exp(-i\omega t) + C.C. \quad 1.75$$

The total polarisation at  $\omega_s$  is then given by,

$$\begin{aligned} P_{\mu s}(t) &= [\chi_{\mu\gamma}^{(1)}(\omega_s) E_{s\gamma} \exp(-i\omega_s t) + C.C.] \\ &\quad + \delta [\chi_{\mu\alpha\beta\gamma}^{(3)}(\omega_p, -\omega_p, \omega_s) E_{p\alpha} E_{p\beta}^* E_{s\gamma} \exp(-i\omega_s t) + C.C.] \\ &= [\chi_{\mu\gamma}^{(1)}(\omega_s) + \delta |A_p|^2 \chi_{\mu\alpha\beta\gamma}^{(3)}(\omega_p, -\omega_p, \omega_s) a_{p\alpha} a_{p\beta}^*] E_{s\gamma} \exp(-i\omega_s t) + C.C. \end{aligned}$$

1.76

making use of 1.74.

Thus, the problem is equivalent to modifying the linear susceptibility by a factor of  $\delta |A_p|^2 \chi_{\mu\alpha\beta\gamma}^{(3)}(\omega_p, -\omega_p, \omega_s) a_{p\alpha} a_{p\beta}^*$ . The corresponding change in the dielectric tensor is then given by,

$$\delta\epsilon_{\mu\gamma}(\omega_s) = 24 \pi |A_p|^2 \chi_{\mu\alpha\beta\gamma}^{(3)}(\omega_p, -\omega_p, \omega_s) a_{p\alpha} a_{p\beta}^* \quad 1.77$$

and that in the refractive index is,

$$\delta\eta_s = |A_p f_{\beta\gamma} a_{p\gamma} a_{s\gamma}|^2 \left[ \frac{2\pi n}{\hbar^3 \eta_s (n \times a_s)^2} \right] \frac{(\omega_s - \omega_p - \omega_{ot}) - i\Gamma_{ot}}{(\omega_s - \omega_p - \omega_{ot})^2 - \Gamma_{ot}^2} \quad 1.78$$

where,

$$f_{\beta\gamma} = \sum_b \left[ \frac{R_{ob}^\beta R_{bt}^\gamma}{\omega_{ob} + \omega_p} + \frac{R_{ob}^\gamma R_{bt}^\beta}{\omega_{ob} - \omega_p} \right] \quad 1.79$$

$\Gamma_{ot}$  is a real and positive quantity which enters into the expression for susceptibility when we consider the interaction between the molecules (i.e., the effect of linewidth). A negative change in the imaginary part of the refractive index implies amplification. It can be shown that the signal wave at  $\omega_s$  is amplified at the expense of the pump wave at  $\omega_p$ .

TPA is a similar phenomenon. Proceeding exactly in the same lines, but for a resonance of the form  $\omega_p + \omega_s = \omega_{to}$ , one can see that change in the refractive index is positive, implying attenuation. Further analysis would show that both the waves are attenuated in this case. The absorbed energy is often emitted as fluorescence.

First experimental observation of SRS was reported by Woodbury and Ng [26]. A lot of theoretical and experimental

studies have been done thereafter. Reviews can be found in references [13,27]. TPA was first reported by Kaiser and Garrett [28]. Worlock [12] has reviewed the reported studies on TPA.

(iv) *Four Wave Mixing* : The phenomena described in the previous sub-sections are, in fact, only a few ones of the large number of the third order nonlinear optical phenomena, which are collectively called as Four Wave Mixing. A number of other phenomena also have been observed and subjected to theoretical and experimental investigations. In general, these are the effects due to various kinds of resonances (as indicated at the end of (ii) above) in the system. Such effects provide a method of probing into the energy level structures of the interacting species, and hence a whole area of spectroscopy has been developed upon the various third order nonlinear optical phenomena. Coherent Raman Spectroscopy (CRS), Coherent Stokes Raman Spectroscopy (CSRS), Coherent Antistokes Raman Spectroscopy (CARS), Raman Induced Kerr Effect Spectroscopy (RIKES) etc. are among these. A number of books have been published on these topics [16,20].

#### REFERENCES

- [1] N Bloembergen, 1981 Nobel lecture (Dec.8,1981), *Rev. Mod. Phys.*, 54, 685 (1982)
- [2] J A Armstrong, N Bloembergen, J Ducuing and P S Pershan, *Phy. Rev.*, 128, 606 (1962)

- [3] M Bass, P A Franken, J F Ward and G Weinreich, *Phy. Rev. Lett.*, 9, 466 (1962)
- [4] e.g., D A Kleinman, in "*Laser Handbook*", Vol.2, ed. F T Arecchi and E O Schulz-DeBois (North Holland, 1972), p.1229; D S Chemla, *Rep. Prog. Phys.*, 43, 1235 (1980); R S Adhav, "*Materials for Second Harmonic Generation*", *Laser Focus*, June 1983.
- [5] P A Franken, A E Hill, C W Peters and G Weinreich, *Phy. Rev. Lett.*, 7, 118 (1961)
- [6] P A Franken and J F Ward, *Rev. Mod. Phys.*, 35, 23 (1963)
- [7] G D Boyd, T J Bridges and E G Burkhardt, *IEEE J. Quantum Electron.*, QE 4, 515 (1968); W B Gaudrud and G D Boyd, *Opt. Commun.*, 1, 187 (1969); Y Klinger and F R Adams, *Proc. IEEE*, 57, 1797 (1969); J Warner, *Appl. Phys. Lett.*, 12, 222 (1968)
- [8] J Warner, in "*Quantum Electronics*", ed. H Rabin and C L Tang (Academic, 1975), pp.703-736
- [9] R L Byer, in "*Quantum Electronics*", ed. H Rabin and C L Tang (Academic, 1975), pp.558-694; R L Herbst, in "*Nonlinear Infrared Generation*", ed. Y R Shen (Springer-Verlag, 1977), pp.81-133
- [10] R W Terhune, P D Maker and G M Savage, *Appl. Phys. Lett.*, 2, 54 (1963)
- [11] W Koechner, in "*Solid State Laser Engineering*" (Springer-Verlag, 1976), pp.397-488
- [12] e.g., see J M Worlock, in "*Laser Handbook*", Vol.2, ed. F T Arecchi and E O Schulz-DoBois (North Holland, 1972), p.1323

- [13] N Bloembergen, *Am. J. Phys.*, 35, 989 (1967)
- [14] B P Straughan and S Walker (ed.), "*Spectroscopy*", Vol.2 (Chapman and Hall, 1976), pp.231-240
- [15] e.g., M Rokni and S Yatsiv, *Phys. Lett.*, 24 A, 277 (1967); M Rokni and S Yatsiv, *IEEE J. Quantum Electron.*, 3, 329 (1967)
- [16] e.g., D C Hanna, M A Yuratich and D Cotter, "*Nonlinear Optics of Free Atoms and Molecules*" (Springer-Verlag, 1976); W Jamroz and B P Stoicheff, *Prog. Opt.*, XX, ed. E Wolf (North Holland, 1976); J F Reintjes, "*Nonlinear Optical Parametric Processes in Liquids and Gases*" (Academic, 1984)
- [17] P N Butcher, "*Nonlinear Optical Phenomena*", Bulletin 200, Engg. Expt. Station, Ohio State University, 1965
- [18] L I Schiff, "*Quantum Mechanics*" (McGraw Hill, 1949)
- [19] S H Wemple, in "*Laser Handbook*", Vol 2, ed. F T Arecchi and E O Schulz-DoBois (North Holland, 1972), pp.975-994
- [20] A Yariv, C A Mead and J V Parker, *IEEE J. Quantum Electron.*, 2, 243 (1966); R M White and C E Enderby, *Proc. IEEE*, 51, 214 (1963); V J Fowler and J Schlaafer, *Proc. IEEE*, 54, 1437 (1966)
- [21] A Yariv and R A Fisher, in "*Optical Phase Conjugation*", ed. R A Fisher (Academic, 1983), p.7
- [22] J A Giordamine, *Phys. Rev. Lett.*, 8, 19 (1962)
- [23] P D Maker, R W Terhune, M Nisenoff and C M Savage, *Phys. Rev. Lett.*, 8, 21 (1962)
- [24] J A Giordmaine and R C Miller, *Phys. Rev. Lett.*, 14, 973 (1965)

- [25] F Zernike and J E Midwinter, "*Applied Nonlinear Optics*" (John Wiley, 1973); R G Smith, in "*Laser Handbook*", Vol 2 ed. F T Arecchi and E O Schulz-DoBois (North Holland, 1972), p.837
- [26] E J Woodbury and W K Ng, *Proc. IRE*, 50, 2367 (1962)
- [27] Y R Shen and N Bloembergen, *Phy. Rev.*, 137, A 1787 (1965); W Kaiser and M Maier, in "*Laser Handbook*", Vol 2, ed. F T Arecchi and E O Schulz-DoBois (North Holland, 1972), pp.419-472; C S Wang, in "*Quantum Electronics*", ed. H Rabin and R L Tang (Academic, 1975)
- [28] W Kaiser and C G B Garrett, *Phy. Rev. Lett.*, 7, 229 (1961)
- [29] e.g., V S Letokhov and V P Chebotayev, "*Nonlinear Laser Spectroscopy*" (Springer-Verlag, 1977); M S Feld and V S Letokhov (ed.), "*Coherent Nonlinear Optics*" (Springer-Verlag, 1980); A B Harvey (ed.), "*Chemical Applications of Nonlinear Raman Spectroscopy*" (Academic, 1981); M D Levenson, "*Introduction to Nonlinear Laser Spectroscopy*" (Academic, 1982).

## CHAPTER 2

### DEGENERATE FOUR WAVE MIXING AND OPTICAL PHASE CONJUGATION

#### 2.00 Degenerate Four Wave Mixing :

Four wave Mixing is the general term used to denote all the phenomena arising from the third order nonlinear optical susceptibility. When all the frequencies involved are identical, it is the case of a Degenerate Four Wave Mixing (DFWM). From equation 1.63, the polarisation induced in the medium from such an interaction will be of the form,

$$P^{(3)}(t) = 6 \chi^{(3)}(-\omega; \omega, \omega, -\omega) \vdots E_1 E_2 E_3^* \exp(-i\omega t) \quad 2.01$$

If  $E_1 \approx \exp(-ik_1 \cdot r)$ ,  $E_2 \approx \exp(-ik_2 \cdot r)$  and  $E_3 \approx \exp(-ik_3 \cdot r)$  then,  $P^{(3)} \approx \exp(-ik_4 \cdot r)$ , where  $k_4 = k_1 + k_2 + k_3$ .

For a condition,  $k_2 = -k_1$ , we have  $k_4 = -k_3$  and then,  $P^{(3)} \approx \exp(ik_3 \cdot r)$ . This polarisation radiates into the medium, which is obviously the complex conjugate of the wave 3. Phase matching conditions is automatically satisfied for any value of  $k_3$ . Thus, the arrangement of counterpropagating waves 1 and 2 leads to the generation of a "phase conjugate" wave of the third wave 3. Since phase-matching is inherently satisfied for all values of  $k_3$  it follows that all the plane wave components of a wave 3 undergo conjugation and hence phase conjugation of any arbitrary wavefronts can be achieved. This is equivalent to the generation of a time-reversed replica of the

object wave and means that, for example, phase aberrations produced in an object beam as it passes through an imperfect medium can be removed by generating reversed image wave and passing this back through the aberrating medium. The various possible applications that stem from this basic property have aroused much interest in DFWM and other similar interactions and as a result Optical Phase Conjugation (OPC) has now developed into a separate branch of nonlinear optics. From the 1983 issues, the Physics Abstracts and Classification System (PACS) contains a separate sub-head for OPC - 42.65 F.

## 2.01 Theory of DFWM and OPC in transparent media :

Though the idea of backward-wave generation was marginally touched upon by a few earlier authors [1-6], mostly in connection with studies of holographic storage properties in various media [2-6], exact ideas of OPC as a third order nonlinear phenomenon were conceived after the experimental results reported by a few Soviet scientists [7,8]. Zel'dovich *et al* [8] are perhaps the first authors to present a theory to account the ability of a nonlinear interaction to achieve phase conjugation ( wavefront reversal, as the Soviet authors always call it). During mid-seventies, Amnon Yariv [9-11] showed that many other nonlinear phenomena can also yield complex conjugate fields. Hellwarth [12] was the first to suggest the use of a DFWM interaction for OPC, in consideration to the fact that the phase matching condition is always satisfied in this. Later, Yariv and Pepper [13], presented a theory for phase conjugation and

amplified reflection in the case of DFWM. In the following, their theory is briefly outlined.

The beam geometry for the interaction is as shown in the figure 2.01. We have three waves as,

$$E_{\alpha}(r,t) = \frac{1}{2} A_{\alpha}(r) \exp [-i(\omega t - k_{\alpha} \cdot r)] + C.C. \quad 2.02$$

where  $\alpha$  stands for 1, 2 (denoting the counterpropagating intense pump beams) and p (denoting the third weak beam, the probe beam). Considering the third order polarisation term as in equation 2.01, one can see that there will a new field radiated, which has the form,

$$E_c(r,t) = \frac{1}{2} A_c(r) \exp [-i(\omega t - k_c \cdot r)] + C.C. \quad 2.03$$

Taking the amplitudes only,

$$E_{\alpha}(r,t) = \frac{1}{2} A_{\alpha}(r) \exp [-i(\omega t - k_{\alpha} \cdot r)] + C.C. \quad 2.04$$

where  $\alpha$  now stands for 1,2,p and c. The evolution of the conjugate field  $E_c(r,t)$  can be analysed in the usual way, i.e., by making use of the wave equation,

$$\nabla \times \nabla \times E_c - \frac{\epsilon}{c^2} \frac{\partial^2 E_c}{\partial t^2} = - \frac{4 \pi}{c^2} \frac{\partial^2}{\partial t^2} P^{NL} \quad 2.05$$

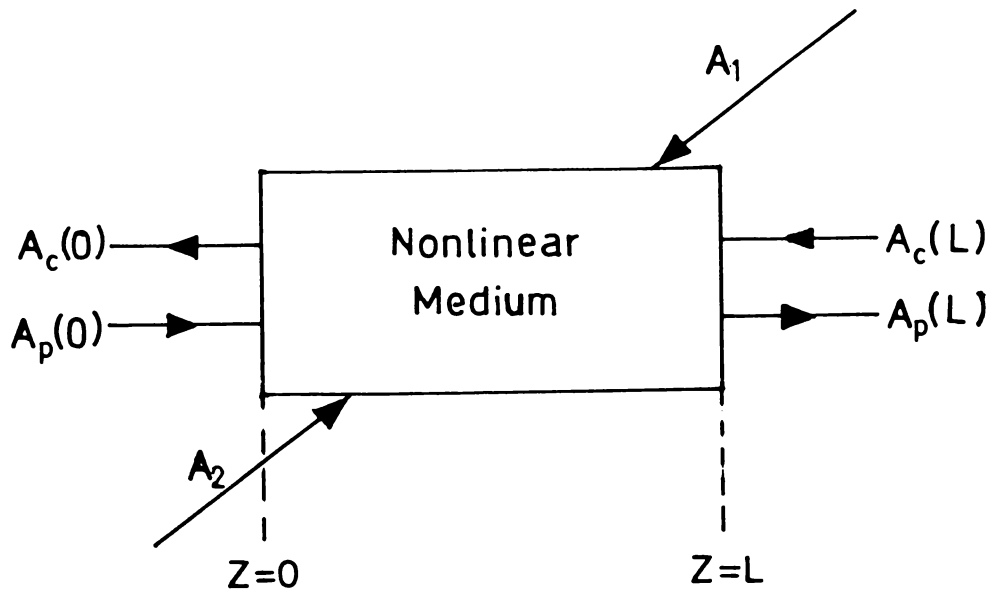


Figure 2.01 The basic geometry of phase conjugation by DFWM.  $A_1$  and  $A_2$  are the nondepleted pump beam amplitudes.  $A_p$  and  $A_c$  are the corresponding probe and conjugate beam amplitudes.

where  $P^{NL}$  is the polarisation as given by equation 2.01. The effect on  $E_p(r,t)$  due to the presence of the new field  $E_c(r,t)$  is described by a similar equation, i.e.,

$$\nabla \times \nabla \times E_p - \frac{\epsilon}{c^2} \frac{\partial^2 E_p}{\partial t^2} = - \frac{4\pi}{c^2} \frac{\partial^2}{\partial t^2} P^{NL} \quad 2.06$$

where  $P^{NL} \approx \chi^{(3)}(-\omega; \omega, -\omega, \omega) : A_1 A_2 A_c^* \exp[-i(\omega t - k \cdot r)]$ .

On solving these equations we end up with the following equations for the amplitudes.

$$\begin{aligned} \frac{dA_p}{dz} &= -i \frac{2p\omega}{c\eta} \chi A_1 A_2 A_c^* \exp[-i(k_1 + k_2 + k_3 + k_4) \cdot r] \\ &= -i \chi^* A_c^* \end{aligned} \quad 2.07a$$

$$\frac{dA_c}{dz} = i \chi^* A_p^* \quad 2.07b$$

In arriving at these equations the fact that  $k_1 + k_2 = 0$  and  $k_p + k_c = 0$  has been used. Z direction is taken as that of  $k_4$ . Also the counterpropagating strong beams are assumed to be of equal intensities and undepleted during the interaction. Further, the SVEA, as,

$$\left| \frac{d^2 A_\alpha}{dz^2} \right| \ll \left| k_\alpha \frac{d A_\alpha}{dz} \right| \quad 2.08$$

also has been used.

These equations have been first derived by Yariv and Pepper [13] and independently by Bloom and Bjorklund [14]. If we now specify the complex amplitudes  $A_c(L)$  and  $A_p(0)$  of the two weak waves at the planes  $z = L$  and  $z = 0$ , the solutions to these equations have the following form.

$$A_p(z) = -i \frac{k \sin(kz)}{\alpha \cos(kL)} A_c^*(L) + \frac{\cos[k(z-L)]}{\cos(kL)} A_p(0) \quad 2.09a$$

$$A_c(z) = i \frac{\alpha^* \sin[k(z-L)]}{k \cos(kL)} A_p(0) + \frac{\cos(kz)}{\cos(kL)} A_c(L) \quad 2.09b$$

where  $k$  stands for  $|\alpha|$ .

In a practical case, where  $A_p(0)$  is finite and  $A_c(L) = 0$ , the amplitude of the conjugate wave at  $z = 0$ , is given by,

$$A_c(0) = -i [\alpha^* \tan(kL) / kL] A_p(0) \quad 2.10a$$

and the probe wave at  $z = L$ ,

$$A_p(L) = A_p(0) / \cos(kL) \quad 2.10b$$

The most interesting feature of these equations is that for a regime  $\pi/4 < kL < 3\pi/4$ , the amplitude squares (power) of the

beams) has a form as shown in figure 2.02 (a). Considering the interacting medium as a reflector, the reflected output ( $P_{c,out}$ ) far exceeds the input ( $P_{p,in}$ ). Thus the interaction is capable of forming an "amplifying phase conjugate reflector". At the transmission end also the output ( $P_{p,out}$ ) exceeds the input, suggesting that the interaction also forms a "coherent transmission amplifier".

When  $kL = \pi/2$ , we have  $A_c(0) / A_p(0) = \infty$ , and  $A_p(L) / A_p(0) = \infty$ , which correspond to oscillation. i.e., there is a finite output even if there is no input. Thus, at this particular condition, DFWM interaction is capable of oscillation without feed-back. The field distribution in this case will be as shown in the figure 2.02 (b)

Amplified reflection and oscillation using DFWM in a transparent medium was first reported by Pepper *et al* [16]. Later, use of this as a laser reflector ( now known as a Phase Conjugate Mirror - PCM ) has been analysed and experimentally demonstrated by AuYeung *et al* [17]. Vast amount of research work followed this and numerous interesting results have been reported on lasers employing PCMs. Reviews of this can be found in reference [18].

As evident from the above results, a Phase Conjugate (PC) reflectivity can be now defined for the DFWM interaction, as

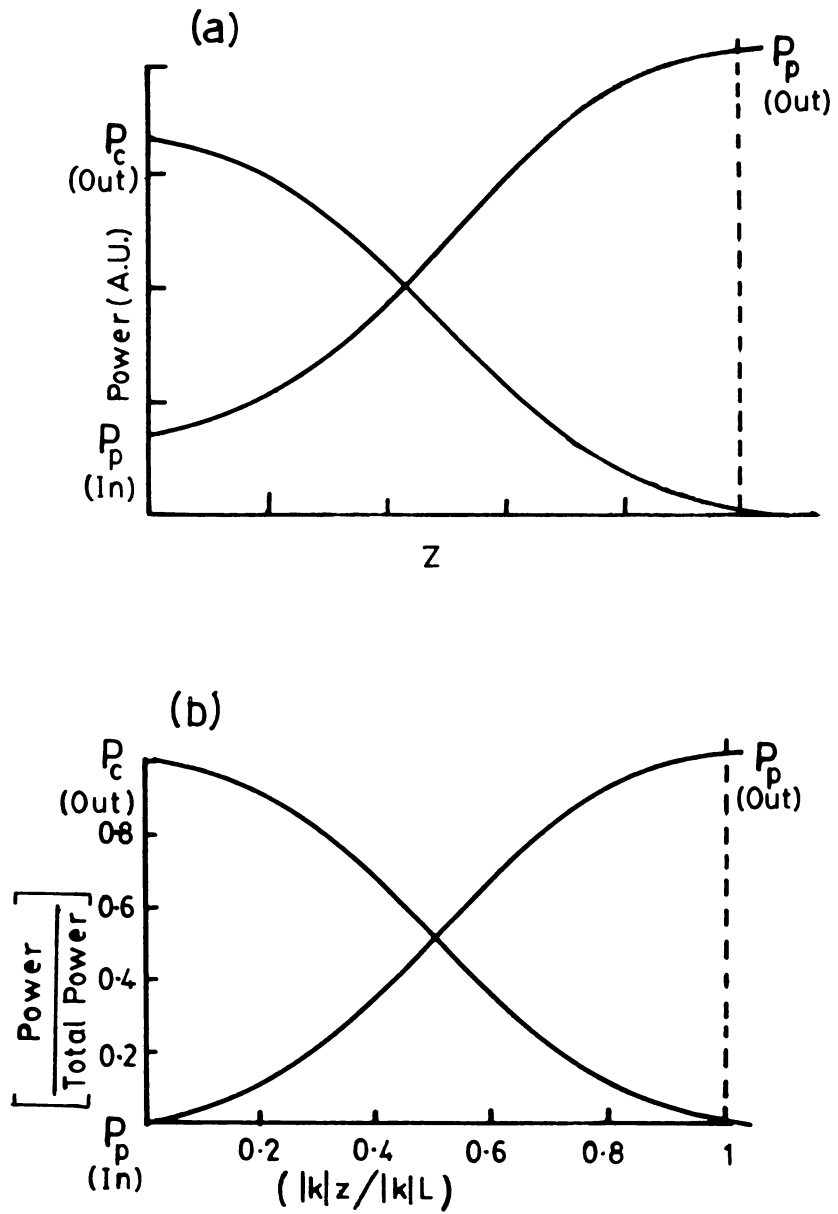


Figure 2.02 (a) Amplification by DFWM - a typical case with  $\pi/4 \leq |k|L \leq 3\pi/4$  (after ref. [15]). (b) Amplification and oscillation by DFWM - a typical case with  $|k|L \approx \pi/2$  (after ref. [13]).

$$R = \left| \frac{A_c(O)}{A_p(O)} \right|^2 = \tan^2(kL) \quad 2.11a$$

and a transmission coefficient as,

$$T = \left| \frac{A_p(O)}{A_c(O)} \right|^3 = \sec^2(kL) \quad 2.11b$$

Of these two quantities, the former one is often used as a characteristic value to be specified for the materials used for OPC. By symmetry considerations any optical material has a nonvanishing third order susceptibility and therefore can be used for generating a PC beam. But since the value of the third order susceptibility is extremely small, very large fields are necessary to induce a detectable level of power into the PC beam. For example in the case of Carbon di Sulphide liquid, the nonvanishing component of the third order susceptibility has a value of  $2.73 \times 10^{-19}$  e.s.u.. Using this and taking the amplitudes  $A_1 = A_2 = (8\pi I / c\eta)^{1/2}$ , one can make an estimate[19] of the value of  $k$ , so as to obtain a detectable power in the PC beam, as,  $k = 0.21 I \text{ MW/cm}^2/\text{meter}$ , at  $\lambda = 1 \mu\text{m}$  and  $\eta = 1.62$  (for  $\text{CS}_2$ ). Thus several megawatts of power is needed for achieving this.

## 2.02 Theory of DFWM and OPC in absorbing media :

A possible way of obtaining OPC at low power levels is to use resonance enhancement of the susceptibility as indicated at

the end of chapter 1. Abrams and Lind [20] have analysed the case of an absorbing medium, as a candidate for OPC. They have assumed a two-level model and have obtained a relation for the third order susceptibility in the form,

$$\chi(E) = - \frac{2 \alpha_0}{k} \frac{(i + \delta)}{(1 + \delta^2 + |E/E_s|^2)} \quad 2.12$$

where  $\delta = (\omega - \omega_0) T_2$  is the normalised detuning from the line centre  $\omega_0$ .  $T_2$  is the transverse relaxation time [21].  $|E_s|^2$  corresponds to the line centre saturation intensity.  $\alpha_0$  is the line centre small-signal-field attenuation coefficient, with  $k =$  magnitude of the wavenumber at frequency  $\omega$ . Using this relation for  $\chi(E)$  and considering the total field in the form  $E = E_0 + \Delta E$  where  $\Delta E$  is due to the weak probe and conjugate beams and  $E_0$  is that due to the strong counterpropagating beams, and then expanding  $E$  to the first order in  $\Delta E$ , they have obtained the equations for the amplitudes as,

$$\frac{dA_3}{dz} = \alpha A_3 + i \kappa^* A_4^* \quad 2.13a$$

$$\frac{dA_4}{dz} = -\alpha^* A_4 + i \kappa A_3 \quad 2.13b$$

where  $\alpha$  and the coupling coefficient  $\kappa$  are given by,

$$\alpha = \alpha_0 \frac{(1 + i\delta)}{(1 + \delta^2)} \frac{1 + 2I/I_s}{(1 + 4I/I_s)^{3/2}} = \alpha_R - i\alpha_I \quad 2.14$$

$$\alpha^* = i\alpha_0 \frac{(1 - i\delta)}{(1 + \delta^2)} \frac{2I/I_s}{(1 + 4I/I_s)^{3/2}} \quad 2.15$$

where  $I_s$  stands for the corresponding intensities;  $I = I_1 = I_2$ .  $I_s$  denotes the saturation intensity. Defining a new parameter,

$$\omega = (\kappa^2 - \alpha_R^2)^{1/2}, \quad 2.16$$

the equation for  $A_3$  and  $A_4$  are given as,

$$A_3(z) = \frac{A_3(L)[\omega \cos(\omega z) + \alpha_R \sin(\omega z)] \exp(-i\alpha_I(z-L)) + i\alpha^* A_4^*(0) \exp(-i\alpha_I z) \sin(\omega(z-L))}{\omega \cos(\omega L) + \alpha_R \sin(\omega L)} \quad 2.17a$$

and

$$A_4^*(z) = \frac{i\alpha A_3(L) \sin(\omega z) \exp(-i\alpha_R z) + A_4^*(0)[\omega \cos(\omega(z-L)) - \alpha_R \sin(\omega(z-L))] \exp(-i\alpha_R z)}{\omega \cos(\omega L) + \alpha_R \sin(\omega L)} \quad 2.17b$$

The reflection coefficient is then

$$R = \frac{|A_9(\omega)|^2}{|A_4(\omega)|^2} = \frac{|\kappa \sin(\omega L)|^2}{|\omega \cos(\omega L) + \alpha_R \sin(\omega L)|^2} \quad 2.18$$

### 2.03 Saturable absorbers as candidates for low power OPC :

A close examination of the above relation for the PC reflectivity tells us that its dependence on the power of the beams is through the ratio  $I/I_s$ , rather than the absolute values of the intensities. Since reflectivity depends on the ratio  $I/I_s$  it immediately follows that OPC can be achieved at low power levels if we use some medium which has a low value for the saturation intensity  $I_s$ . It can be further noticed that the reflectivities peak around  $I = I_s$ , and for increased reflectivity one can use large values of  $\alpha_0 L$ .

Hercher [22] has analysed the behaviour of a saturable absorber, in an idealised three level model, making use of rate equations. For the case of an optical excitation from the ground level 1 to an upper level 2, followed by a fast transition from level 2 to an intermediate level 3, it has been shown that the saturation intensity  $I_s$  is given as

$$I_s = \hbar\omega / \sigma\tau, \quad 2.19$$

where  $\sigma$  is the ground state absorption cross-section and  $\tau$  is the lifetime associated with the level 3.

Thus a low saturation intensity would mean a large value for the lifetime for the level 3 and a fast 1 to 2 transition. A possible candidate for this, is organic dyes doped in solid matrices. This is considered in detail in the next chapter.

## REFERENCES

- [1] H J Gerritson, *Appl. Phys. Lett.*, **10**, 237 (1967)
- [2] J P Woerdman, *Opt. Commun.*, **2**, 212 (1971)
- [3] D L Staebler and A J Amodei, *J. Appl. Phys.*, **43**, 1042 (1972)
- [4] H Kogelnik, *Bell Syst. Tech. J.*, **44**, 2451 (1965)
- [5] H Kogelnik and K S Pennington, *J. Opt. Soc. Am.*, **58**, 273 (1968)
- [6] W Lukosz, *J. Opt. Soc. Am.*, **58**, 1084 (1968)
- [7] B I Stepanov, E V Evakin and R S Rubanov, *Sov. Phys. Tech. Phys. Dokl.*, **16**, 1 (1971)
- [8] B Ya Zel'dovich, V I Popovichev, V V Ragulskii and F S Faisullov, *Sov. Phys. JETP Lett.*, **16**, 435 (1972)
- [9] A Yariv, *Appl. Phys. Lett.*, **28**, 88 (1976)
- [10] A Yariv, *J. Opt. Soc. Am.*, **66**, 301 (1976)
- [11] A Yariv, *Opt. Commun.*, **21**, 49 (1977)
- [12] R W Hellwarth, *J. Opt. Soc. Am.*, **67**, 1 (1977)
- [13] A Yariv and D M Pepper, *Opt. Lett.*, **1**, 16 (1977)
- [14] D M Bloom and G C Bjorklund, *Appl. Phys. Lett.*, **31**, 592 (1977)
- [15] D M Pepper, *Opt. Engg.*, **21**, 156 (1982)
- [16] D M Pepper, D Fekete and A Yariv, *Appl. Phys. Lett.*, **33**, 41 (1978)

- [17] J AuYeung, D Fekete, D M Pepper, A Yariv and R K Jain, *Opt. Lett.*, **4**, 42 (1979)
- [18] A E Siegman, P A Belanger and A Hardy, in "*Optical Phase Conjugation*", ed. R A Fisher (Academic, 1983), p.466
- [19] D M Pepper and A Yariv, in "*Optical Phase Conjugation*", ed. R A Fisher (Academic, 1983), p.39
- [20] R L Abrams and R C Lind, **2**, 94 (1978) and **3**, 205 (1978)
- [21] A Yariv, in "*Quantum Electronics*" (Wiley, 1975), pp.149-158
- [22] M Hercher, *Appl. Opt.*, **6**, 947 (1967)

## CHAPTER 3

### CHARACTERISATION OF A FEW SATURABLE ABSORBERS AS CANDIDATES FOR LOW POWER OPTICAL PHASE CONJUGATION.

#### 3.00 Materials for low power OPC :

Ever since the first experimental observation of optical wavefront reversal was reported by the Soviets [1], scientists are engaged in identifying and characterising suitable materials for optical phase conjugation (OPC). Being a third order nonlinear optical phenomenon, OPC was earlier expected only for the case of high power pulsed lasers [2]. However, it was later found that phenomena like photorefractive effect and saturable absorption enhance the effective third order optical susceptibility considerably, making it possible to achieve OPC using low power lasers as well [3,4]. Among the materials which are successfully used now-a-days for low power OPC are (i) photorefractive crystals, (ii) liquid crystals, (iii) interfaces and (iv) saturable absorbers.

(i) *Photorefractive crystals* : Photorefractive effect [5] is the name given to the effect due to the existence of charges in a crystalline medium, while irradiation with laser beams. The origin of these charges are uncertain, but in many cases, it is assumed to be arising from some low-lying impurity or defect states in the crystals. The effect was first observed as a nuisance, causing degradation of the crystals used for Second

Harmonic Generation [6,7]. It was later made use of in the storage of holographic images in crystals [8]. This was suggestive of a possible computer storage application and therefore was followed by hectic research activity in this area. Early reviews in this area [9-11] highlights this aspect of photorefractive effect.

Migration of charges, which can cause formation of grating structures following the intensity pattern of the light beam, is the basic idea of the storage application possibility of photorefractive effect. The same can be applied in the case of a degenerate four wave mixing scheme using low power laser beams to achieve OPC. In the first reports of OPC using photorefractive effect, crystals of Bismuth Silicon Oxide ( $\text{Bi}_{12}\text{SiO}_{20}$  or simply BSO), Lithium Niobate ( $\text{LiNbO}_3$ ) and Lithium Tantalum Oxide ( $\text{LiTaO}_3$ ) have been used [3,12]. Several other crystals have been thereafter used successfully for generation of Phase Conjugate beams in the low power regime. Review are found in the references [13-16]. In most of the cases, a few milliwatts of laser power is sufficient to achieve OPC and reflectivities in excess of 100 % were obtained. The most striking demonstration of low power OPC using photorefractive crystals is perhaps the one in [17], wherein lasing has been achieved on reflection on a kitchen spatula, making use of an OPC mirror formed by a Barium Titanate ( $\text{BaTiO}_3$ ) crystal. General Electric Company has recently announced the development of an image processing system which exploits the photorefractive effect in a BSO crystal, via a real-time holographic process [18].

(ii) *Liquid crystals* : The high sensitivity of the orientational effects in liquid crystals have been recently found to be an excellent method for the generation of phase conjugate beams of low power. An early discussion of this is found in [19]. The first experimental observation was then reported in [20]. Light beams of a few microwatts are necessary to generate PC beams in these materials. A few other authors have also reported studies on OPC using liquid crystals [21-24].

(iii) *Interfaces* Low power OPC has also been achieved by modulation of a reflecting surface. This was first suggested by Zel'dovich *et al* [25]. In the first reported experiment of this kind [26], this was done by a surface destruction and hence involved the use of high power levels. Later Golubustov *et al* [27] have successfully obtained PC of a low power He-Ne laser, by the modulation of the reflecting surface formed by an epoxy resin. Philipetskii *et al* [28] have reviewed this method of obtaining a PC beam. A few other works also have been reported in the later years [29].

(iv) *Saturable absorbers* : As indicated in chapter 2, saturable absorbers can be used for obtaining low power OPC. Metal vapours and gases have been used in this way for achieving OPC of CW dye lasers [4,30,31].

Organic dyes doped in solid matrices form another excellent media for low power OPC. Active search for nonlinear organic

materials, especially in the form of thin films have been made in the past few years. Kowel *et al* [32] have reviewed this. The interest in thin film samples is mainly due to their attractive device possibilities. Nonlinear optical effects always demand phase-matching conditions, which are often very stringent and cumbersome to maintain. The use of thin films facilitate easy alignments and avoids depth-of-focus problems. However, only a few reports have been appeared on low power OPC using thin films of organic dyes kept in some solid matrices. The pioneering work in this area was reported by Silberberg and Bar-Joseph [33,34], who have used the dyes, eosin and erythrosin, doped in gelatin films. The experiments were done using an argon ion laser working at 514.5 nm line with a few tens of milliwatts power. They have achieved a reflectivity of the order of  $10^{-4}$ . Fujiwara and Nakagawa [35,36] have reported the use of fluorescein and eosin in gelatin films. In the work reported by Kramer *et al* [37,38] fluorescein dye was used in boric acid glass films, which showed a reflectivity of about 0.6 % as compared to that of  $10^{-4}$ , in the case of eosin in gelatin films [34]. Jingjiang *et al* [39] have described the use of dichromated gelatin for OPC.

In what follows, a detailed account of the characterisation of a few saturable absorber samples, prepared by incorporating dyes into solid matrices, as candidates for low power OPC are given.

### 3.01 Structure and details of the dyes and the matrices :

The dyes used are eosin, erythrosin B and Rose Bengal. All these belong to the Xanthene family of dyes and are water-soluble.

(i) *Eosin* : The structure of this dye is given in figure 3.01 (a). It has a formula weight of 624.8.

(ii) *Erythrosin B* : All the bromine atoms in eosin is replaced by iodine atoms in this case (as shown in figure 3.01 (b)). Formula weight is 879.87.

(iii) *Rose Bengal* Structure of Rose Bengal significantly differs from that of eosin and erythrosin. It has more atoms attached to the main core. The structure is shown in figure 3.01 (c). Formula weight is 1017.65

The matrices used are gelatin, polyvinyl alcohol (PVA) and boric acid glass. The first two are water soluble polymers.

(iv) *Gelatin* : Gelatin is a polymeric material derived from animal skins and bones [40]. It is soluble in water, but not in any organic solvents. In the following experiments gelatin samples used are of food-grade.

(v) *Polyvinyl alcohol (PVA)* : PVA is a water-soluble polymer

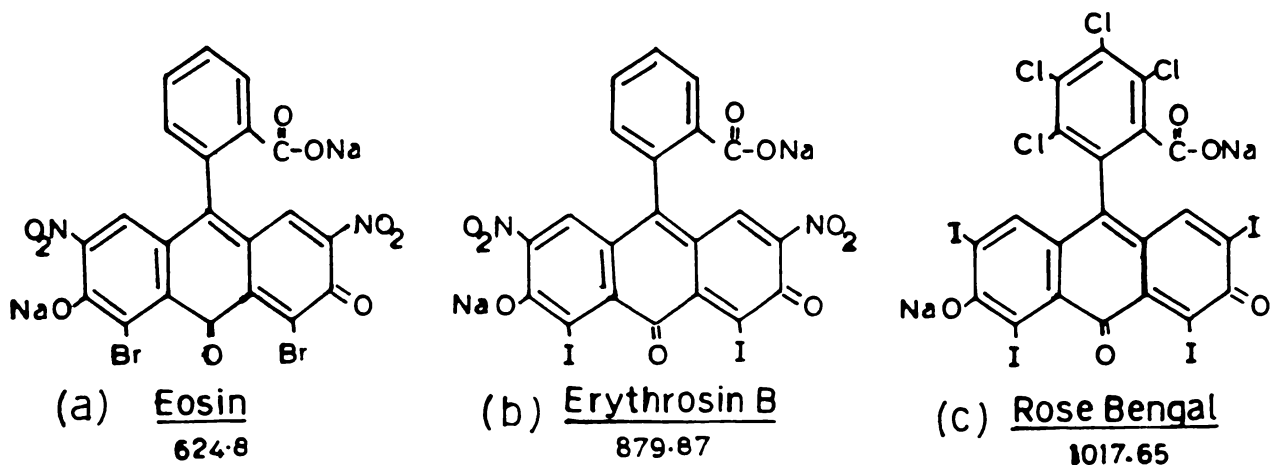


Figure 3.01 Structures of (a) eosin, (b) erythrosin B and (c) Rose Bengal molecules. Numbers denote the corresponding formula weights.

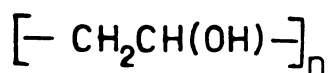
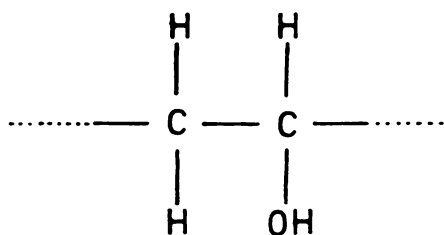


Figure 3.02 Structure of the polymeric chain of PVA.

having the structure shown in figure 3.02. On dissolving in water it forms a viscous fluid, which on drying, forms thin films. A commercial grade product is used in the following experiments.

(vi) *Boric acid glass (BAG)* : This is a glassy material formed by melting ortho boric acid -  $H_3BO_3 \cdot 6H_2O$ .

### 3.02 Sample preparation :

Methods for incorporating dyes into polymer matrices have been known for quite some time, in connection with flash photolysis studies [40] and electrophoretic studies [41]. For OPC also the previous workers have resorted to these methods. The method involves dissolving the polymer and the dye in a common solvent and then allow the solvent to evaporate. In the present case both the dye and polymer are water soluble. Equal grammoles of the dyes are dissolved in dilute solutions of the polymers in warm distilled water. For most of the experiments, 2 gms of of the polymer was dissolved in 20 ml of distilled water at about 50 °C. The resulting solution is dropped over glass-slides and allowed to dry overnight. The thickness of the films depend on the concentration of the polymer. A few tens of microns is the typical thickness of the films subjected to the investigations. Only rough estimates of the thickness have been made, since the thickness as such does not appear in the calculations. The filmsformed in polyvinyl alcohol show better uniformity and surface quality than the gelatin films.

Various methods of doping boric acid glass with organic dyes are described in literature [42-44]. The dye and boric acid powder is melted together in a crucible, dropped onto pre-heated glass slides, covered with another glass slide, pressed and allowed to cool. It is observed that among these dyes, eosin is the one that goes most readily into the BAG matrix and Rose Bengal is the most difficult one. While melting the samples temperatures have to be carefully monitored : otherwise the dyes get charred. Although one would be tempted to attempt a BAG matrix sample of these dyes, in view of the increased OPC reflectivity reported in the case of fluorescein in a BAG matrix [37], it becomes immediately evident that these dyes, in general, does not provide nice films in BAG as in the case of fluorescein. Furthermore, as described below, the absorption spectra also change considerably.

### 3.03 Absorption spectra :

As shown in the figure 3.03 absorption spectra of all these dyes are peaked around 520 nm, while in dilute water solutions and would seem to be suitable for working at 514.5 nm line of the argon ion laser. But on doping in various host matrices, the absorption spectra show deviations. In figures 3.04 (a) to (c), absorption spectra of these dyes when doped in low concentrations in the matrices of gelatin, PVA and BAG matrices are shown. As is evident, the BAG samples do not show much absorption at 514.5 nm and as such are not suitable for working at this wavelength.

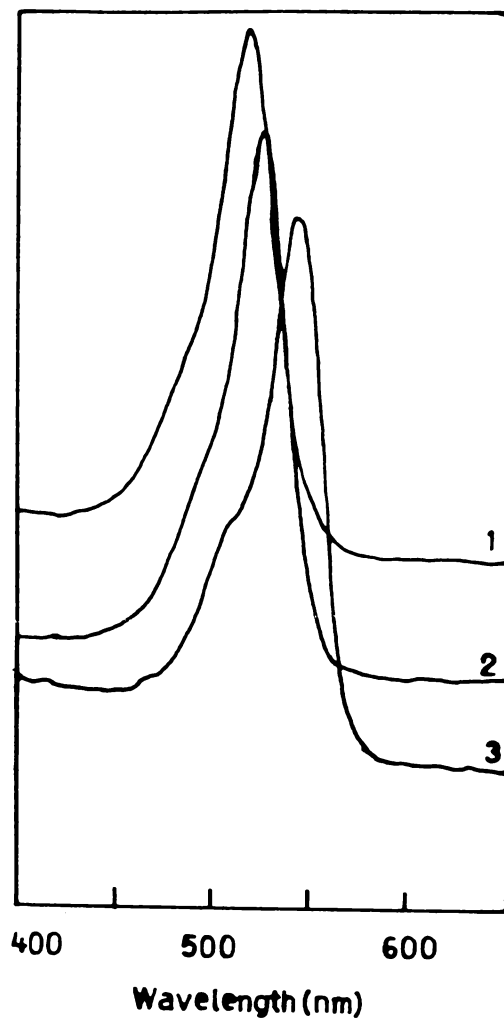


Figure 3.03 Absorption spectra of dilute water solutions of (1) eosin, (2) erythrosin B and (3) Rose Bengal. (Scales are different on the vertical axis).

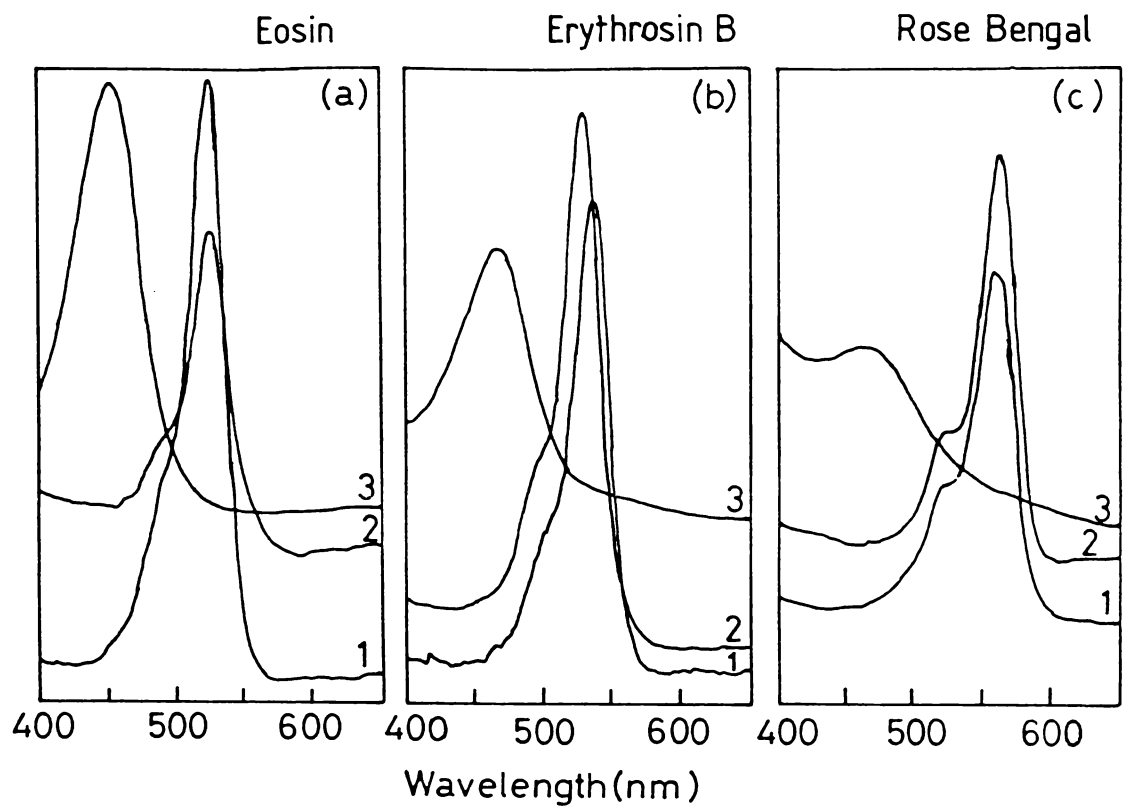


Figure 3.04 Absorption spectra of (a) eosin, (b) erythrosin B and (c) Rose Bengal in matrices of (1) gelatin, (2) PVA and (3) BAG. (Scales are different on the vertical axes).

All these absorption spectra are recorded using a Hitachi model 330 UV-VIS-NIR Spectrophotometer.

### 3.04 Saturation intensities :

For achieving OPC of low power laser beams, the saturation intensities of these samples have to be small. Few reports of the measurements of saturation intensities in the low power regimes have appeared in literature. Saturable absorption is more known in connection with Q-switching and mode-locking of high power pulsed lasers [44] and hence measurements of saturation intensities have been mostly reported in the case of samples with high saturation intensities. Penzkofer [45] has recently reported measurements of saturation intensities of Rhodamine 6G solutions using a mode-locked Nd:glass laser. The method is a direct method ; the transmission percentages at different incident intensities are measured and plotted. In connection with OPC, Moses and Wu [46] have measured the saturation intensities of the dye BDN, which also is at large intensities. Silberberg and Bar-Joseph [33] have reported direct measurements of the saturation intensities of eosin and erythrosin, doped in gelatin films. In the present investigations, a new method of quickly checking the samples for saturable absorption is attempted. Actual measurements are, however, done by the direct method itself.

(i) *A quick method of checking saturable absorption* : The method involves the observation of the temporal pattern of the fluorescence emission from these samples. As indicated in chapter 2, the mechanism of saturable absorption in these samples involves a "bottle-necking" at the triplet levels. Molecules, on optical absorption, are excited to the singlet levels, wherefrom they undergo intersystem crossing to the triplet levels [47]. If there is a large cross-section for this cross-over, molecules get trapped in the triplet levels, resulting in a decrease in the number of molecules available for absorption. This would reflect in fluorescence emission also. Fluorescence intensity would fall from an initial peak, the rate of fall being related to the triplet lifetime and saturation intensity. Obviously this peaking behaviour manifests only when the incident intensity is in excess of the saturation intensity at the wavelength of operation.

Such an initial peaking behaviour is known in literature, in the analysis of the fluorescence emission from magnetic ions in crystals. Bartolo [48] has analysed such a system under transient excitation. He has shown that the fluorescence emission from these systems for a time  $t$ , such that  $0 \leq t \leq \tau$ ,  $\tau$  being the duration of the excitation, follows the relation,

$$I_F(t) = A + B \exp(s_1 t) + C \exp(s_2 t) \quad 3.01$$

where  $A$ ,  $B$ ,  $C$ ,  $s_1$  and  $s_2$  are functions of the various lifetimes involved, which are given as,

$$s_{1,2} = \frac{1}{2} \left[ -(p_1 + p_2 + p_3 + 2w) \pm \left( (p_1 + p_2 - p_3 + 2w)^2 - 4wp_2 \right)^{1/2} \right]$$

3.02

where,

$$A = w N_0 p_3 / s_1 s_2 \tag{3.03}$$

$$B = w N_0 (s_1 + p_3) / s_1 (s_1 - s_2) \tag{3.04}$$

$$\text{and } C = w N_0 (s_2 + p_3) / s_2 (s_2 - s_1) \tag{3.05}$$

where  $p_1$ ,  $p_2$  and  $p_3$  are the rates of the fluorescence emission, intersystem crossing and phosphorescence emission (as indicated in the figure 3.05) respectively.  $w$  is the rate of excitation and  $N_0$  is the ground state number density.

In systems which are expected to behave as saturable absorbers at low intensities,  $p_2$  and  $p_3$  have to be sufficiently high.  $p_1$  is generally of the order of  $10^8 \text{ sec}^{-1}$ . For a case with  $p_2 = 10^7 \text{ sec}^{-1}$  and  $p_3 = 2 \times 10^4 \text{ sec}^{-1}$ , with an excitation rate  $w = 10^4 \text{ sec}^{-1}$ , the fluorescence intensity for a time duration of 5 ms would look like the one shown in figure 3.06 (a). Figure 3.06 (b) show the variation of this with the excitation rate  $w$ .

The experimental set-up required for observing this is shown

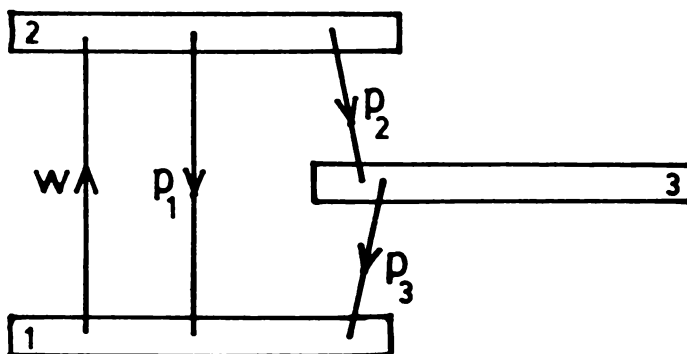


Figure 3.05 Simplified energy level diagram for a dye molecule. 1 - ground levels, 2 - singlet levels and 3 - triplet levels.  $w$  - rate of excitation,  $p_1$  - rate of fluorescence,  $p_2$  - rate of intersystem crossing and  $p_3$  - rate of phosphorescence.

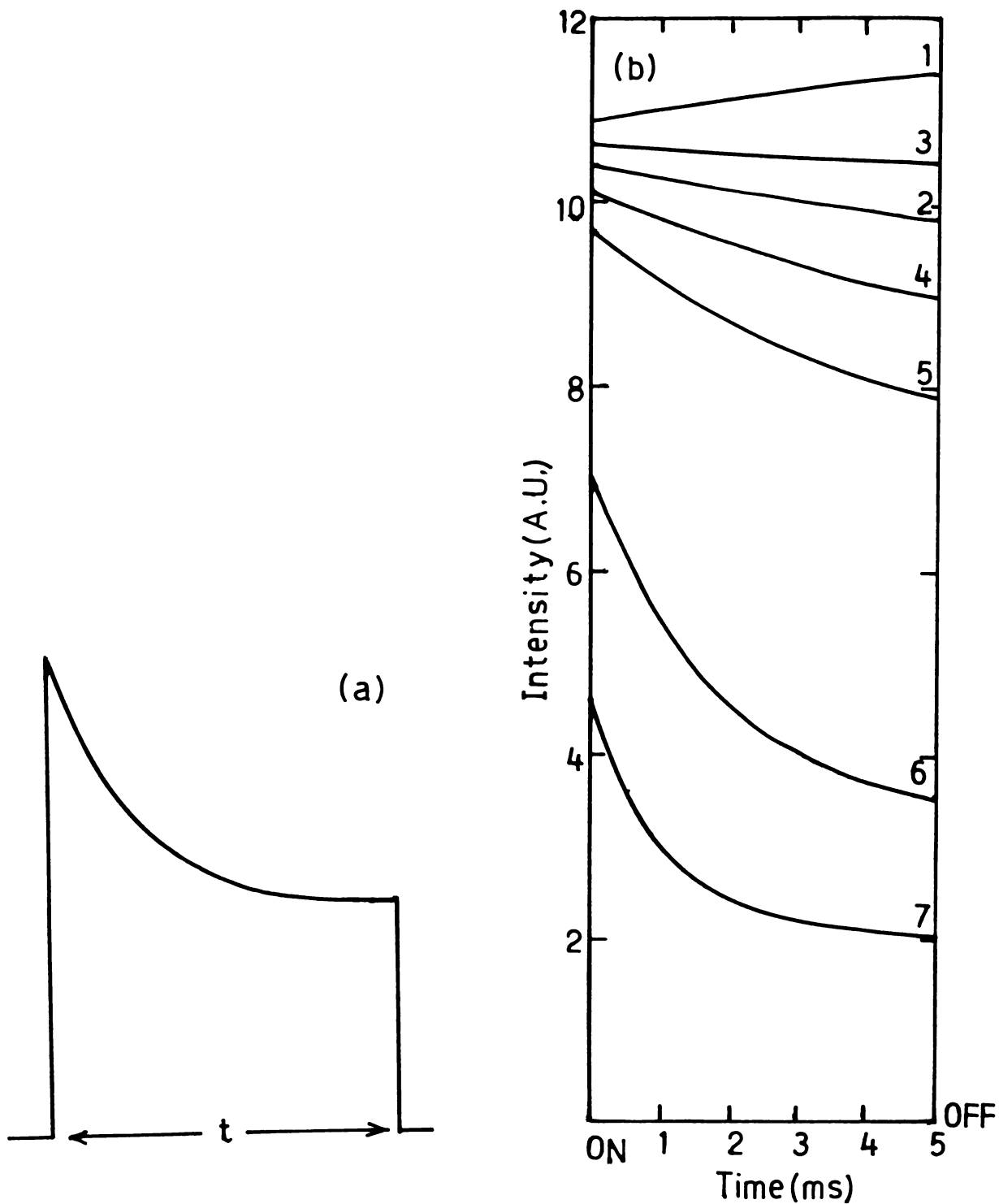


Figure 3.06 (a) Calculated fluorescence emission from a sample with  $p_1 = 10^8$ ,  $p_2 = 10^7$ ,  $p_3 = 2 \times 10^4$  and  $w = 10^4$ , for a time  $t = 5$  ms. (b) Variation of emission with change in excitation rate -  $w = (1) 10^2$ , (2)  $1.5 \times 10^2$ , (3)  $2 \times 10^2$ , (4)  $2.5 \times 10^2$ , (5)  $3 \times 10^2$ , (6)  $5 \times 10^3$  and (7)  $10^4$

in the figure 3.07. The laser-induced fluorescence emission is collected and fed to an oscilloscope via a monochromator-PMT combination, tuned to the peak of the spectrum (The luminescence spectra of these samples are discussed in the Appendix I). The exciting beam is chopped using a mechanical chopper and the fluorescence pattern is recorded in the oscilloscope. Initially, when the power of the laser is small, there is no initial peaking behaviour, as seen in the figure 3.08 (a). As the intensity increases the peak appears. This is shown in the figures 3.08 (b) to (d), in the case of an eosin-doped gelatin film. The obvious inference is that the film behaves as a saturable absorber at 514.5 nm wavelength at these power levels. In the figures 3.09 (a) and (b) the cases of erythrosin B and Rose Bengal are shown. Figure 3.10 shows the case of Rhodamine 6G -doped gelatin film, recorded for an incident power of about 500 mW, which, as expected does not show the peaking behaviour.

(ii) *Actual measurements of the saturation intensities* : Though the above observations provide a rough estimate of the saturation intensities, it do not give the exact values. This has been, therefore, done in the direct method by observing the transmitted and incident intensities. If  $\Delta I$  is the change in the transmitted intensity, the intensity corresponding to a change of  $\Delta I/2$  is the saturation intensity [49]. Figure 3.11 shows the plot of the transmitted intensity vs. incident intensity for the three dyes, doped in gelatin films. The saturation intensities are found to be  $0.06 \text{ Watts/cm}^2$ ,  $0.26 \text{ W/cm}^2$  and  $0.65 \text{ W/cm}^2$  respectively for eosin, erythrosin B and Rose

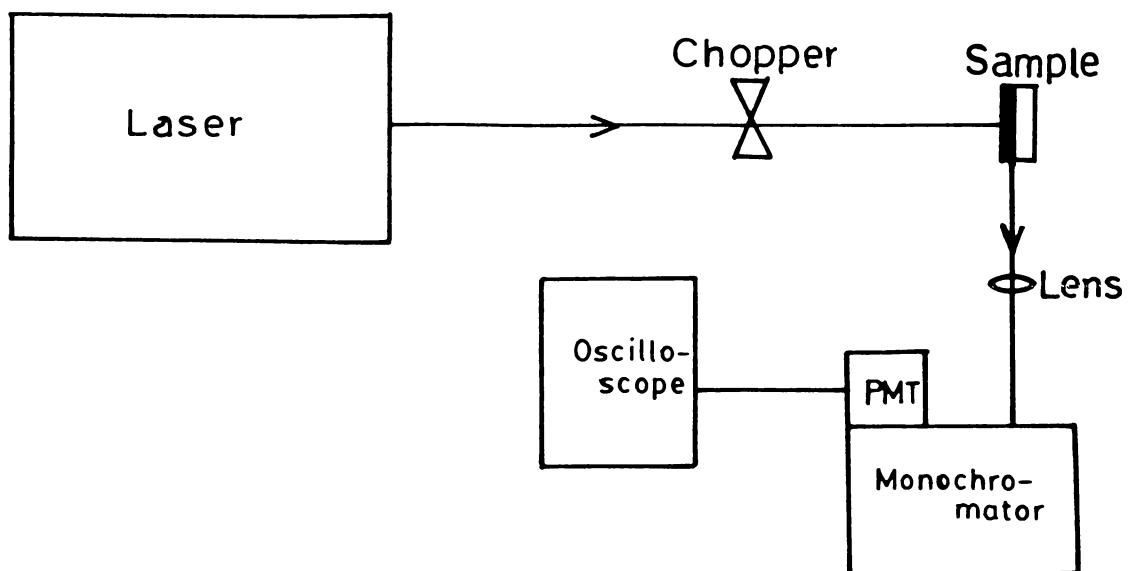


Figure 3.07 Set-up for recording the fluorescence emission patterns.

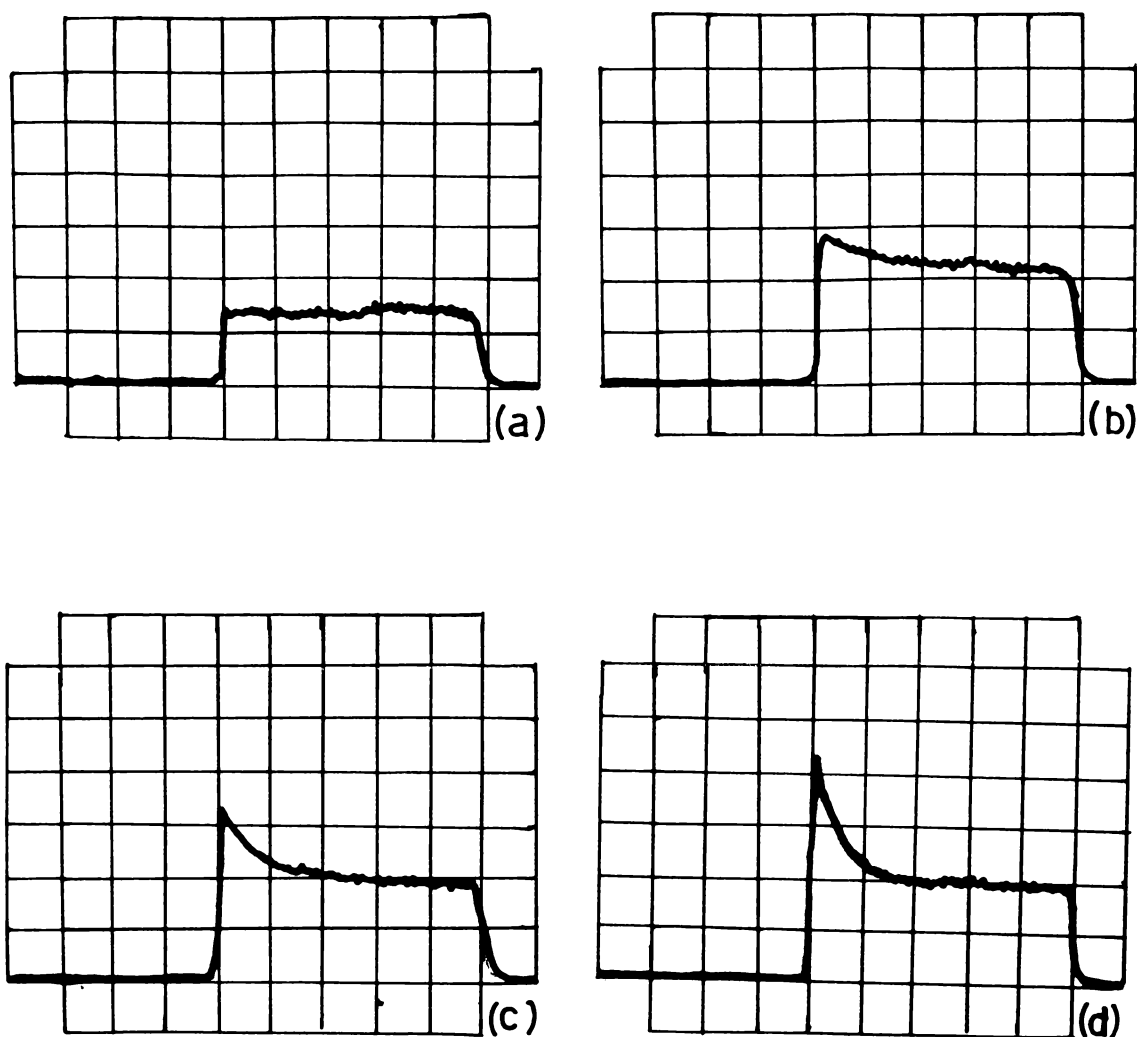


Figure 3.08 Oscillograms of the fluorescence emission patterns from eosin doped in gelatin films at different excitation rates - (a) at laser power about 10 mW, (b) power increased to about 50 mW, (c) power increased to about 80 mW and (d) power increased to about 250 mW. Sweep speed = 1 ms/div.

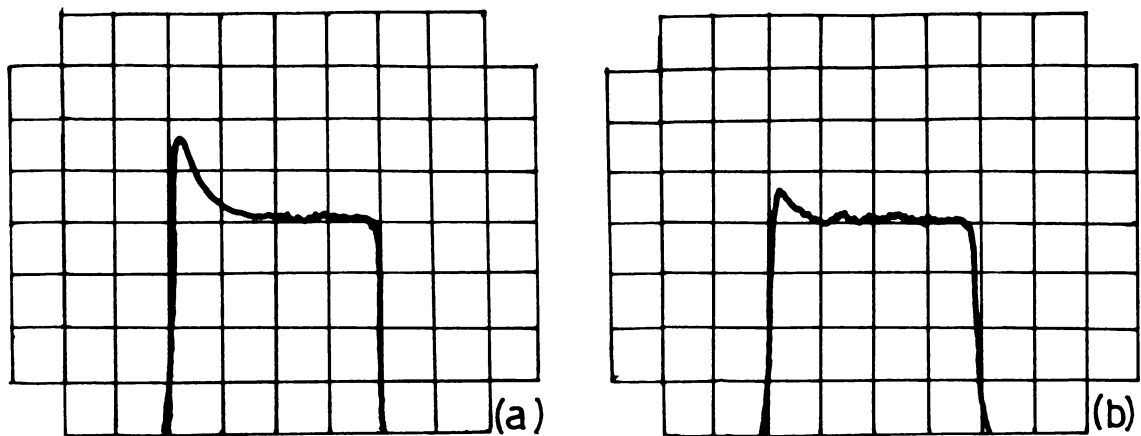


Figure 3.09 Oscillograms of the fluorescence emission patterns from (a) erythrosin B and (b) Rose Bengal doped in gelatin films, at a laser power of about 250 mW. Sweep speed = 1 ms/div.

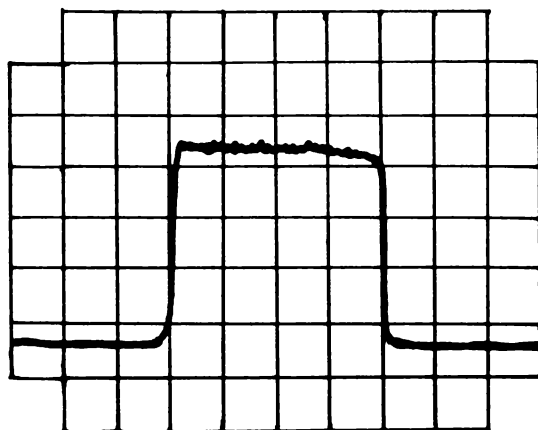


Figure 3.10 Oscillogram of the fluorescence emission pattern from Rhodamine 6G doped in gelatin film, at a laser power of about 500 mW. Sweep speed = 1 ms/div.

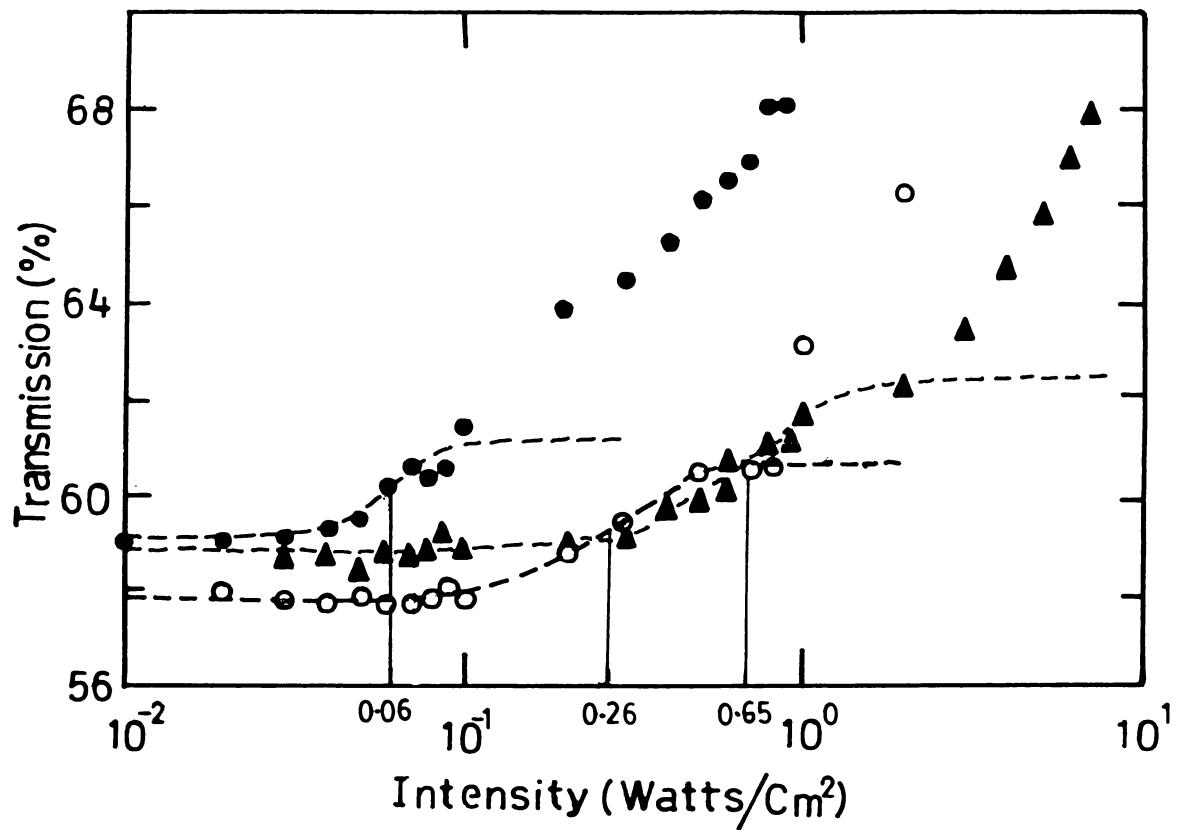


Figure 3.11 Transmission vs. incident intensity plots for the films used in the experiments. ● - eosin, ○ - erythrosin B, and ▲ - Rose Bengal. The saturation intensities are found to be 0.06, 0.26 and 0.65 Watts/cm<sup>2</sup> respectively.

Bengal, doped in gelatin films.

While attempting to plot these curves, it was noticed that the dyes easily undergo photo-bleaching, on continuous exposure to the laser beams. This happens much more quickly when the intensity is high. The plots given in the figure 3.11 are typical of a number of plots drawn, each time taking care to assure that the films are not undergoing permanent damage. For this, the following procedure is adopted - from each point of observation, the values of the previous point is re-checked and confirmed. An attempt is made to characterise these films by assigning a "damage threshold" value - the intensity at which the retracibility of the transmission curve is lost. For eosin films, this is found to be as low as  $0.1 \text{ W/cm}^2$ , for erythrosin B,  $1 \text{ W/cm}^2$  and for Rose Bengal,  $3 \text{ W/cm}^2$ . These are measured for exposure times of about 10 seconds.

The measured values of the saturation intensities of eosin and erythrosin show significant deviations from the values reported in literature, which are  $0.6 \text{ W/cm}^2$  and  $1.8 \text{ W/cm}^2$  respectively [33]. It is known that the properties of dyes doped in solid matrices are critically dependent on the exact structure and texture of the host matrices and results obtained in such systems often show large variations [50]. It is believed that the variation in the values of the saturation intensities in the case of eosin and erythrosin are caused by the difference in the texture of the gelatin samples used. To confirm this, estimates of the triplet lifetimes have been done.

### 3.05 Triplet lifetimes :

Triplet lifetimes of these dyes have been measured in the past by flash photolysis method. Forster and Dudley [51] have reported measurements of meanlife of the phosphorescence of eosin and erythrosin in a rigid glass matrix at 77°K. They have obtained the values as 9.4 mS and 0.63 mS respectively. Buettner [40], by flash photolysis method, have measured these and have obtained the values as 4.2 mS, 0.63 mS and 0.32 mS respectively for eosin, erythrosin and Rose Bengal, doped in gelatin films. The difference in the two values is attributed to the difference in the rigidity of the matrices. The decrease in the lifetimes in the three cases is consistent with the "heavy-atom effect"; i.e., it decreases in the order of the increasing atomic weight of the substituent atoms.

Referring again to the analysis made by Bartolo [48] and the figure 3.05, it can be seen that for these species, when  $p_1 + p_2 \gg p_3$ , the decay of luminescence emission after removing the exciting source, follows an exponential pattern, with  $p_3$  as the exponential constant. Thus by observing the decay of the luminescence emission after blocking the exciting beam (i.e., the phosphorescence emission) and plotting an intensity vs. time curve, one can calculate the triplet lifetime. This has been done for these dyes doped in gelatin and PVA films. The experimental set-up for these observations are the same as in figure 3.07. The monochromator is tuned to the red-end of the

luminescence spectra (discussed in Appendix I). This is for collecting an increased component of phosphorescence emission, which will be of larger wavelength than those due to fluorescence and delayed fluorescence. The exciting beam is chopped and the pattern of the decay of the phosphorescence is recorded in an oscilloscope. These are shown in the figures 3.12 (a) to (c) and 3.13 (a) to (c). The patterns turn out to be the same in either of the cases, indicating that the lifetimes are equal in both the cases.

Figures 14 (a) and (b) show the  $\log(\text{intensity})$  vs. time plots obtained from the decay traces in figure 3.12. From the slope of the graphs, the lifetimes of the three dyes in the gelatin matrix is calculated to be 8.83 mS, 0.95 mS and 0.51 mS respectively. The plots in the case of PVA matrices gave the same values.

The deviation of these values from the reported values [40] is also believed to be due to the difference in the quality of the gelatin used. In the reference cited, an Eastman grade purified calfskin gelatin was used, whereas in the present studies, a commercial food-grade product was used. The nature of the deviations shown in the case of the saturation intensities and the triplet lifetimes are consistent. In the case of the lifetimes, the decrease of the values is in consistence with the heavy-atom effect also.

Referring to the equation 2.19, one finds that the effect of

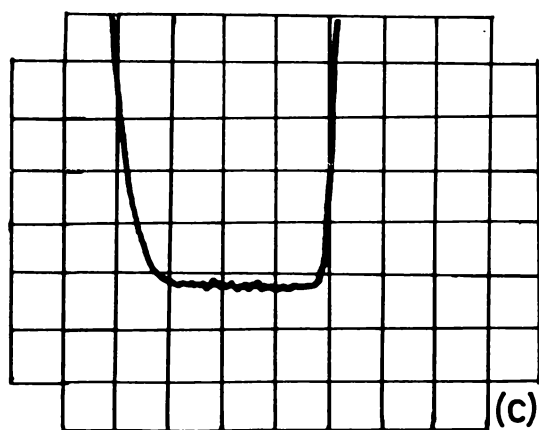
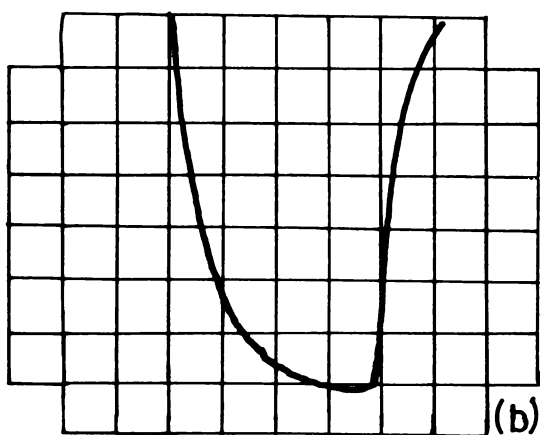
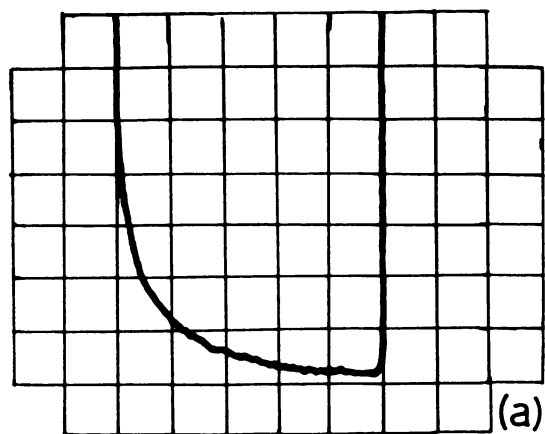


Figure 3.12 Oscillograms of the phosphorescence decay of (a) eosin, (b) erythrosin B and (c) Rose Bengal, doped in gelatin films. Sweep speed = 5 ms/div. for the former and 1 ms/div. for the other two.

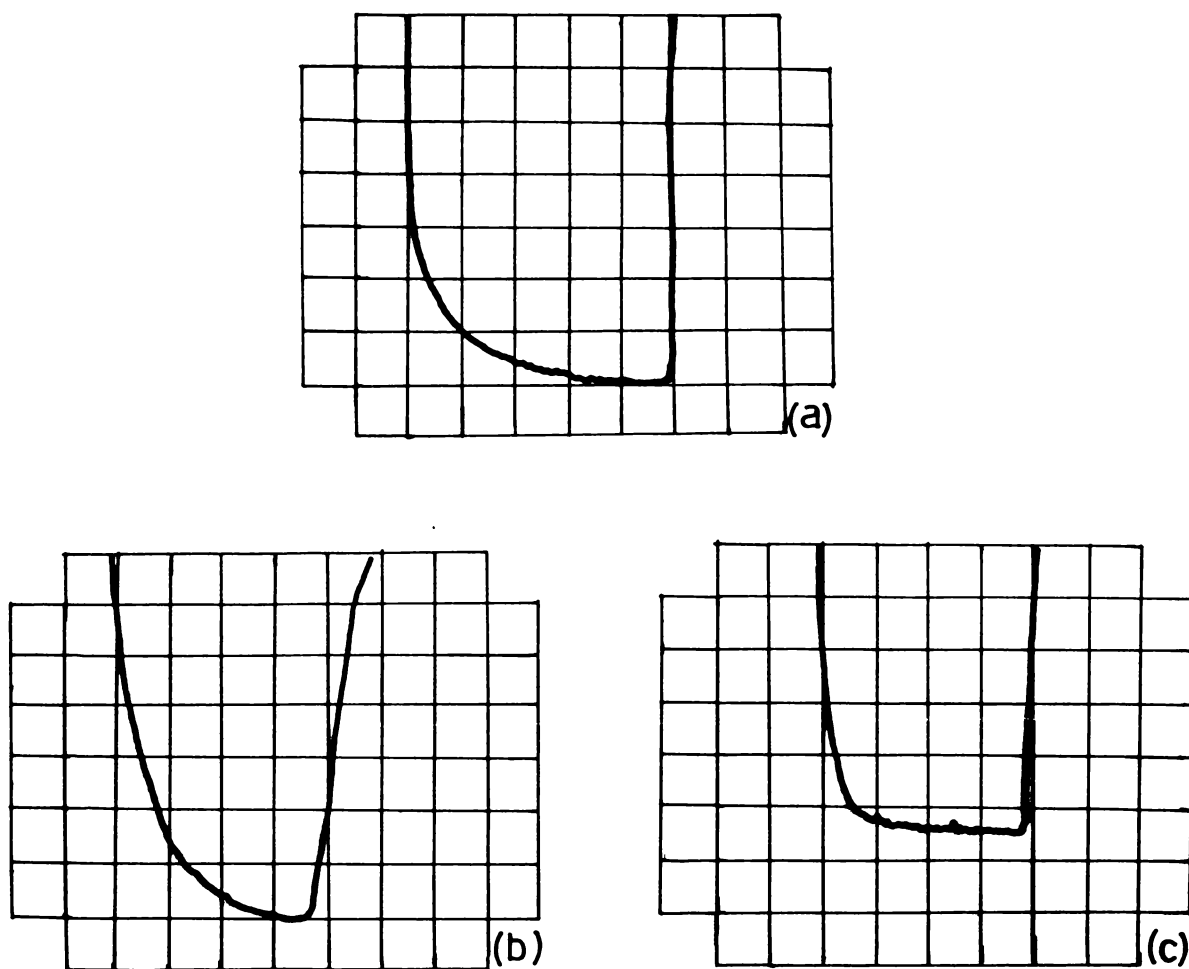


Figure 3.13 Oscillograms of the phosphorescence decay of (a) eosin, (b) erythrosin B and (c) Rose Bengal, doped in PVA films. Sweep speed = 5 ms/div. for the former and 1 ms/div. for the other two.

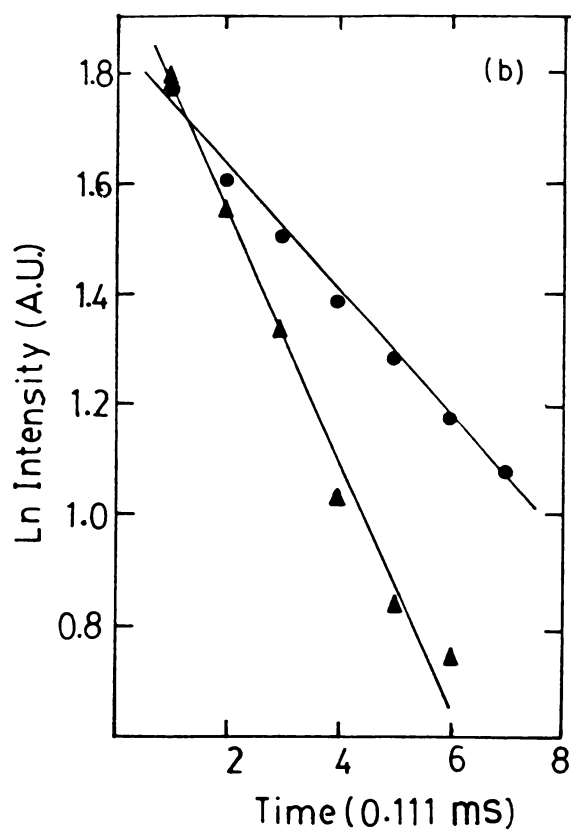
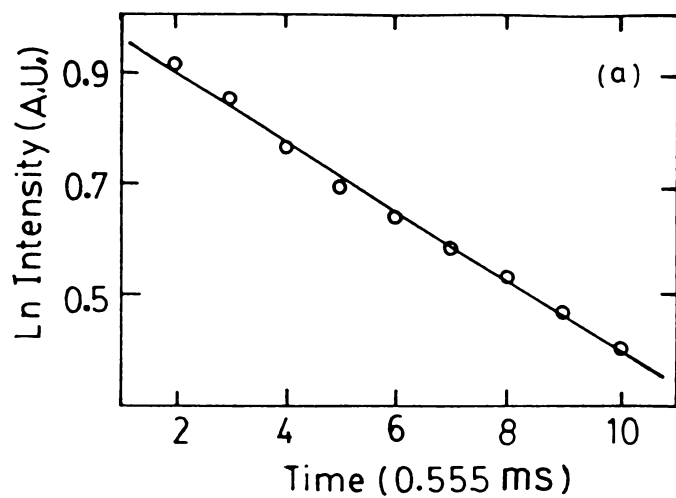


Figure 3.14 Logarithm (intensity) vs. time plots for (a) eosin in gelatin film [decay curve shown in figure 3.12 (a)] and (b) erythrosin B(●) & Rose Bengal (▲) [decay curves shown figures 3.12 (b) & (c)].

matrices in the saturation intensities of the dyes comes through the triplet lifetime and the ground state absorption cross-section. Since the absorption spectra of these dye do not differ much in gelatin and PVA matrices and their triplet lifetimes are the same it is assumed that the saturation intensities of these dyes have the same values, both in gelatin and PVA matrices. The effect of concentration on the triplet lifetimes is also found to be not very significant, for the range of concentrations used in the experiments. This was done by recording the decay traces for the different concentrations and plotting the log(intensity) vs. time plots in each case.

#### REFERENCES

- [1] B I Stepanov, E V Evakin and A S Rubanov, *Sov. Phys. Tech. Phys. Dokl.*, **16**, 265 (1971)
- [2] A Yariv and D M Pepper, *Opt. Lett.*, **1**, 16 (1977)
- [3] J P Huigard, J P Herrian, R Rivet and P Günter, *Opt. Lett.*, **5**, 102 (1980)
- [4] P F Liao, D M Bloom and N P Economou, *Appl. Phys. Lett.*, **32**, 813 (1978)
- [5] A Ashkin, G D Boyde, J M Dzidzic, R G Smith, A A Ballman, H J Levenstein and K Nassan, *Appl. Phys. Lett.*, **9**, 72 (1966)
- [6] F S Chen, *Appl. Phys.*, **38**, 3418 (1967)
- [7] F S Chen, J T La Macchia and D B Fraser, *Appl. Phys. Lett.*, **13**, 223 (1968)
- [8] D Von der Linde and A M Glass, *Appl. Phys.*, **8**, 85 (1975)

- [9] D M Kim, T A Rabson, R R Shah and F K Tittel, *Opt. Engg.*, **16**, 189 (1977)
- [10] A M Glass, *Opt. Engg.*, **17**, 470 (1978)
- [11] N Kukhtarev and S Odulov, *Opt. commun.*, **32**, 183 (1980)
- [12] M Cronin Goloumb, B Fischer, J O White and A Yariv, *J. Opt. Soc. Am.*, **12**, 1564 (1981)
- [13] R Fisher (ed.), "*Optical Phase Conjugation*" (Academic, 1983)
- [14] M C Gower, *Nature*, **316**, 12 (1985)
- [15] J P Huiguard, H Rajbenbach, Ph. Refregier and L Solymar, *Opt. Engg.*, **24**, 586 (1985)
- [16] Cover feature of *Laser Focus*, Dec. 1981.
- [17] "Techbrief", No. 1101/1, released by Hirst Research Centre (GEC), Middlesex, England
- [18] B Ya Zel'dovich and N V Tabiryian, *Sov. J. Quantum Electron.*, **11**, 257 (1981)
- [19] O V Garibyan, I N Kompanets, A V Parfyononov, N F Pilipetskii, V V Shkunov, A N Sudarkin, A N Sukhov, N V Tabiryian, A A Vasihev and B Ya Zel'dovich, *Opt. Commun.*, **38**, 67 (1981)
- [20] I C Khoo, *Appl. Phys. Lett.*, **47**, 908 (1985)
- [21] I C Khoo, *Opt. Engg.*, **24**, 579 (1985)
- [22] I C Khoo and R Normandin, *IEEE J. Quantum Electron.*, **QE 21**, 329 (1985)
- [23] F Simoni and R Bartolino, *Opt. Commun.*, **53**, 210 (1985)
- [24] B Ya Zel'dovich, N F Pilipetskii, A n Sudarkin and V V Shuknov, *Sov. Phys. Dokl.*, **25**, 377 (1980)
- [25] O L Kukilov, N F Pilipetskii, A N Sudarkin and V V Shuknov, *Sov. Phys. JETP Lett.*, **31**, 345 (1980)

- [26] A A Golubustov, N F Pilipetskii, A N Sudarkin and V V Shuknov, *Sov. J. Quantum Electron.*, **11**, 218 (1981)
- [27] N F Pilipetskii, V V Shuknov, A N Sudarkin and B Ya Zel'dovich, in "*Optical Phase Conjugation*", ed. R A Fisher (Academic, 1983) p.445-462
- [28] M Neito, *Opt. Acta*, **32**, 881 (1985)
- [29] Y Prior and E Yarkoni, *Phy. Rev. A*, **28**, 3689 (1983)
- [30] R K Raj, Q F Gao, D Bloch and M Ducloy, *Opt. Commun.*, **51**, 117 (1984)
- [31] S T Kowel, Liangxiu Ye, Yixiang Zhang and L M Hayden, *Opt. Engg.*, **26**, 607 (1987)
- [32] Y Silberberg and I Bar-Joseph, *IEEE J. Quantum Electron.*, **QE 17**, 1967 (1981)
- [33] Y Silberberg and I Bar-Joseph, *Opt. Commun.*, **39**, 265 (1981)
- [34] H Fujiwara and K Nakagawa, *Opt. Commun.*, **55**, 386 (1985)
- [35] H Fujiwara and K Nakagawa, *J. Opt. Soc. Am. A*, **4**, 121 (1987)
- [36] M A Kramer, W R Tompkin, J Krasinski and R W Boyd, *J. Lumin.*, **31/32**, 789 (1984)
- [37] M A Kramer, W R Tompkin and R W Boyd, *Phy. Rev. A*, **34**, 2026 (1986)
- [38] Z Jingjiang, W Shuying and Bao Cailong, *Opt. Engg.*, **25**, 677 (1986)
- [39] <sup>40</sup> e.g., see "*The Merck Index*" (Merck and Co., Rahway, USA 1976), 9th edition, p. 564, Index # 4217
- [40] A V Buettner, *J. Phys. Chem.*, **68**, 3253 (1964)
- [41] E E Havinga and P Van Pelt, in "*Electro-optics and Dielectrics of Macromolecules and Colloids*", ed. B R Jennings (Plenum, New York 1979), p.89

- [42] M Kasha, *J. Opt. Soc. Am.*, **38**, 1068 (1948)
- [43] T A Shankoff, *Appl. Optics.*, **8**, 2282 (1969)
- [44] O Svelto, "*Principles of Lasers*" (Plenum, 1976)
- [45] A Penzkofer, *Appl. Phys. B*, **40**, 85 (1986)
- [46] E I Moses and F Y Wu, *Opt. Lett.*, **5**, 65 (1980)
- [47] e.g., see K H Drexhage, in "*Dye Lasers*", ed. F P Schäfer (Springer-Verlag, 1977)
- [48] B D Bartolo, in "*Optical Interactions in Solids*" (Wiley, 1967), p.441
- [49] M Hercher, *Appl. Optics*, **6**, 947 (1967)
- [50] e.g. see C A Parker, in "*The Triplet State*", ed. A B Zahlan (Cambridge University, 1967), p.372
- [51] L S Forster and D Dudley, *J. Phys. Chem.*, **66**, 838 (1962)

## CHAPTER 4

### SECTION I

#### LOW POWER OPTICAL PHASE CONJUGATION IN SOME SATURABLE ABSORBERS

##### 4.10 Low power OPC - earlier results in saturable absorbers :

As indicated in the previous chapters, low power OPC in saturable absorbers have described by a few authors [1-5]. In the pioneering work by Silberberg and Bar-Joseph [1], gelatin films doped with eosin and erythrosin dyes were used as the samples. In contrast to an earlier work of this kind, where a ruby crystal was used as a nonlinear medium [6], OPC was found to be achievable at power density levels as low as  $1 \text{ Watt/cm}^2$ , and available from unfocussed beams of an argon ion laser. They have noticed that although OPC using saturable absorbers are inherently less efficient than using photorefractive crystals, some characteristics of this method prove advantageous especially in the field of image processing. The thin film form is particularly suitable for image processing applications. Working with thin films also reduce the constraints of an exact Bragg condition and by reducing the film thickness it can be carried to the limit of thin holograms which are more suitable for image processing applications. With these objectives they have studied OPC in these films and their results showed that a reflectivity of the order of  $10^{-4}$  is achievable in the case of eosin dye doped in gelatin films, whereas in the case of erythrosin dye it is a little less. They have neither studied the variation of the efficiency of OPC with the thickness of the

films nor have specified the value of the absorption length ( $\alpha_0 L$ ) at which they have made their measurements. But in view of the fact that these samples are studied with an aim of going down to the limit of thin holograms, such a study is of much importance. These authors have also shown that the variation of the reflectivity is in accordance with the theory of Abrams and Lind [7] even at an intensity ten times the saturation intensity. They have presented striking photographs of the aberration correction property of these films. In a subsequent publication [2], these authors have reported some studies on the transient effects in the DFWM interaction in these samples. They have shown by theoretical considerations that there exists an initial peak in the phase conjugate reflectivity for these samples. Experimental investigations using eosin dye in gelatin films with an absorption length  $\alpha_0 L = 0.3$ , have shown these effects [2]. The transient peak appeared at intensities higher than half of the saturation intensity. Because of this transient nature, the measurements of OPC efficiency in the case of DFWM with pulsed pump beams may show significant deviations from the theoretical estimates using a steady-state theory such as the one proposed by Abrams and Lind [7]. These become evident if one measures the integrated reflectivities in the case of pump pulses of different durations. This also was shown in their work.

Fujiwara and Nakagawa [5] have later showed the existence of these transient peaks much more explicitly, using chopped light beams as (i) pump and (ii) probe beams. In the former case the transients were indeed observable whereas in the latter

they were not.

Fujiwara and Nakagawa have observed OPC and holographic storage in gelatin films doped with fluorescein dye [4]. They have observed that a small component of the phase conjugate beam is still visible, on blocking one of the pump beams. They have argued that this is due to a holographic process which contribute to the mechanism of OPC. They have even separated the two components and have studied how each of this decays in time.

Kramer *et al* [3], have studied the polarisation dependence of saturable absorption in the case of boric acid films doped with fluorescein dye. The reflectivity obtained was as high as 0.66 %, in the case of a sample with absorption length  $\alpha_0 L = 0.66$  at a pump intensity of 200 Watts/cm<sup>2</sup>, which is ten times the saturation intensity in this case.

Present investigations cover three dyes, eosin, erythrosin B and Rose Bengal, doped in two different matrices viz. gelatin and polyvinyl alcohol. These samples were characterised as described in chapter 3. The results obtained in the following OPC experiments show deviations from that obtained by the previous authors.

#### 4.11 Samples and experimental set-up :

The films required for these studies were prepared as described in the previous chapter. PVA films showed higher

surface quality but the film edges showed some swellings.

The experimental set-up is as shown in figure 4.01. Spectra-Physics Model 171 Argon ion laser was used as the source, without introducing the intracavity etalon. The beam is split into two, making use of a beam-splitter ( $BS_1$ ). Using two mirrors ( $M_1$  and  $M_2$ ) these two are made to counter-propagate. A second beam-splitter ( $BS_2$ ) is used to provide the weak probe beam and a third one ( $BS_3$ ) to direct this to the sample (S). The pathlengths of all these beams are adjusted to be the same. The beam splitters  $BS_2$  and  $BS_3$  are plane glass plates, whereas  $BS_1$  is a partially coated glass plate. The mirrors are also aluminium coated glass plates. In most of our experiments the two pump beams were not of the same intensity - they differed by about 10 %. The intensity of the probe beam was less than 10 % of the pump beams. A few apertures (A) are used to avoid the scattered noise. Beyond the sample, the probe beam is stopped using a beam stopper (BST).

To locate the direction of the phase conjugate beam, the probe beam was retro-reflected using a mirror. On removing this mirror and using an erythrosin film as the sample, the phase conjugate beam spot was clearly visible on a screen kept beyond the beam-splitter  $BS_3$ .

To confirm that this is actually the phase conjugate beam, the following tests were done. (i) It did not diverge much, on going away from the beam-splitter  $BS_3$ . (ii) It disappeared on

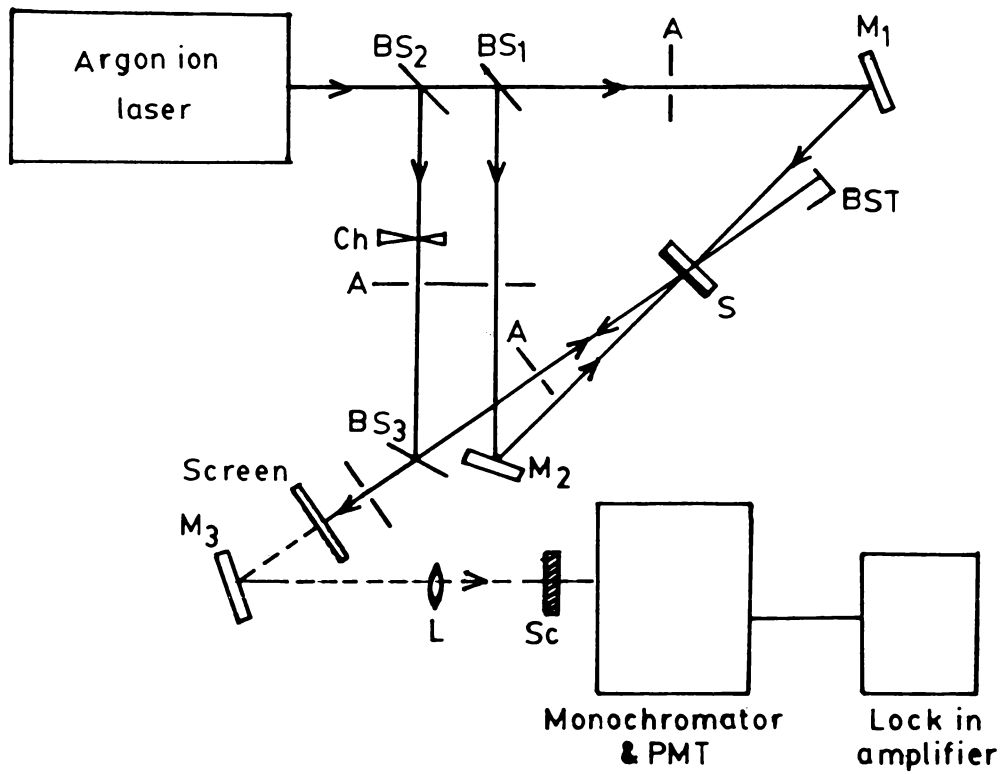


Figure 4.01 Set-up for recording the OPC signals.  
 BS - Beam splitters, M - Mirrors, L - Lens  
 A - Aperatures, BST - Beam stopper,  
 S - Sample, Sc - Scatterer, Ch - Chopper.

blocking any of the three interacting beams. (iii) Such a signal is not observed using a sample of Rhodamine 6G dye (iv) It showed the aberration-correction property as follows - a cylindrical lens was used to focus the probe beam to the interaction region. But the phase conjugate beam imaged on the screen remained as before. For want of sufficient intensity and due to the scattered noise, it was not possible for us to take a photograph of the aberrated and the corrected beam-spots.

On using a photodetector at the place of the screen, it was observed that the signal was fluctuating. Therefore, to make measurements of the PC beam intensity, a lock-in detection was made. For this, the probe beam was chopped using a mechanical chopper (EG&G PARC Model 192) and the chopped signal was processed using a lock-in amplifier (EG&G PARC Model 124 A). To avoid the contributions due to the fluorescence of the dye, the PC beam was detected through a monochromator (Jarell Ash 0.5 Meter) tuned to 514.5 nm wavelength, which was used for the experiments. The detector was a PMT (Hamamatsu 9683 KQB), attached to the monochromator. Since plane glass plates were used as beam splitters, ghost images were formed and both the probe and the phase conjugate beams showed interference fringes across. Therefore, for detection the phase conjugate beam was focussed onto a scatterer and the scattered intensity was monitored.

#### 4.12 OPC signals :

The OPC signals thus recorded from the different samples

are shown in figure 4.02 (a) and (b). These are recorded from films made using equal grammoles of the dyes and were having absorption lengths ( $\alpha_0 L$ ) of 1.13, 2.19 and 0.59 respectively for eosin, erythroin B and Rose Bengal, at the wavelength of 514.5 nm. It can be noticed that erythrosin samples shows higher signal strengths.

#### 4.13 OPC reflectivity vs. intensity :

A relative measure of the OPC reflectivity can be had by dividing the OPC signal strengths by the corresponding probe laser powers. An absolute measurement of the reflectivity is not possible in the present set-up.

As mentioned in chapter 2, the OPC reflectivity for saturable absorber samples have been theoretically estimated by Abrams and Lind [7] and a relation for the reflectivity in terms of absorption lengths and intensities has been given. Silberberg and Bar-Joseph have modified this relation to suit the dye samples and for differing pump beam intensities [1]. The modified relation looks as,

$$R = \frac{|k|^2}{|\alpha + \omega \cos(\omega L)|^2} \quad 4.01$$

where

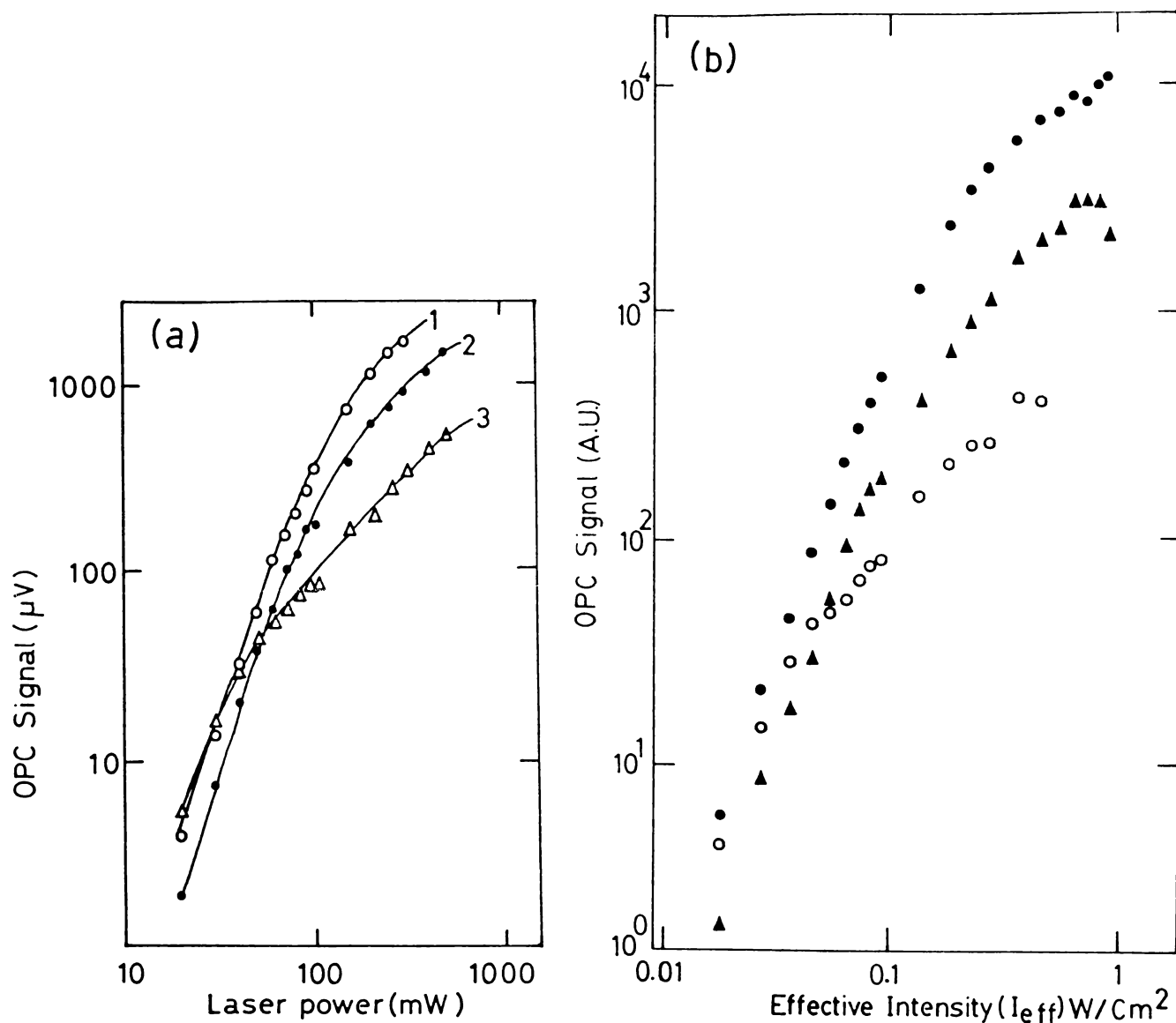


Figure 4.02 OPC signals vs. laser power. (a) Signals (from the lock-in amplifier) vs. power of the laser - cases of (1) erythrosin B, (2) Rose Bengal and (3) eosin, doped in PVA films. (b) The signal strength vs. effective intensity at the interaction region - cases of (●) erythrosin B, (▲) Rose Bengal and (○) eosin, doped in gelatin films.

$$\alpha = \frac{1 + (I_{\text{eff}}/I_s)}{(1 + 2(I_{\text{eff}}/I_s) + (I_{\text{diff}}/I_s)^2)^{3/2}}, \quad 4.02$$

$$k = -2i \frac{(I_1 I_2)^{1/2}/I_s}{(1 + 2(I_{\text{eff}}/I_s) + (I_{\text{diff}}/I_s)^2)^{3/2}} \quad 4.03$$

and

$$\omega = (|k|^2 - \alpha^2)^{1/2} \quad 4.04$$

$I_{\text{eff}}$  stands for the effective intensity at the interaction region which is  $(I_1 + I_2)$ , (assuming  $I_s$  to be small enough to be neglected) and  $I_{\text{diff}}$  stands for the difference in the intensities of the two pump beams.  $I_s$  is the saturation intensity.

In figure 4.03, reflectivity curves calculated as per the above relation are shown. The  $\alpha_0 L$  values are 1.13, 2.19 and 0.59 respectively for eosin, erythrosin B and Rose Bengal and the saturation intensities 0.06 Watts/cm<sup>2</sup>, 0.26 W/cm<sup>2</sup> and 0.65 W/cm<sup>2</sup> (from chapter 3). Along with these curves we have plotted the normalised signal strengths (to the probe beam intensity). Since it is not possible to draw any quantitative comparisons we have compared the shape of the curves only. The experimental points are scaled to suit the theoretical curves. It has been observed that in all the three cases, the variation of OPC reflectivity with power is mostly in accordance with the above

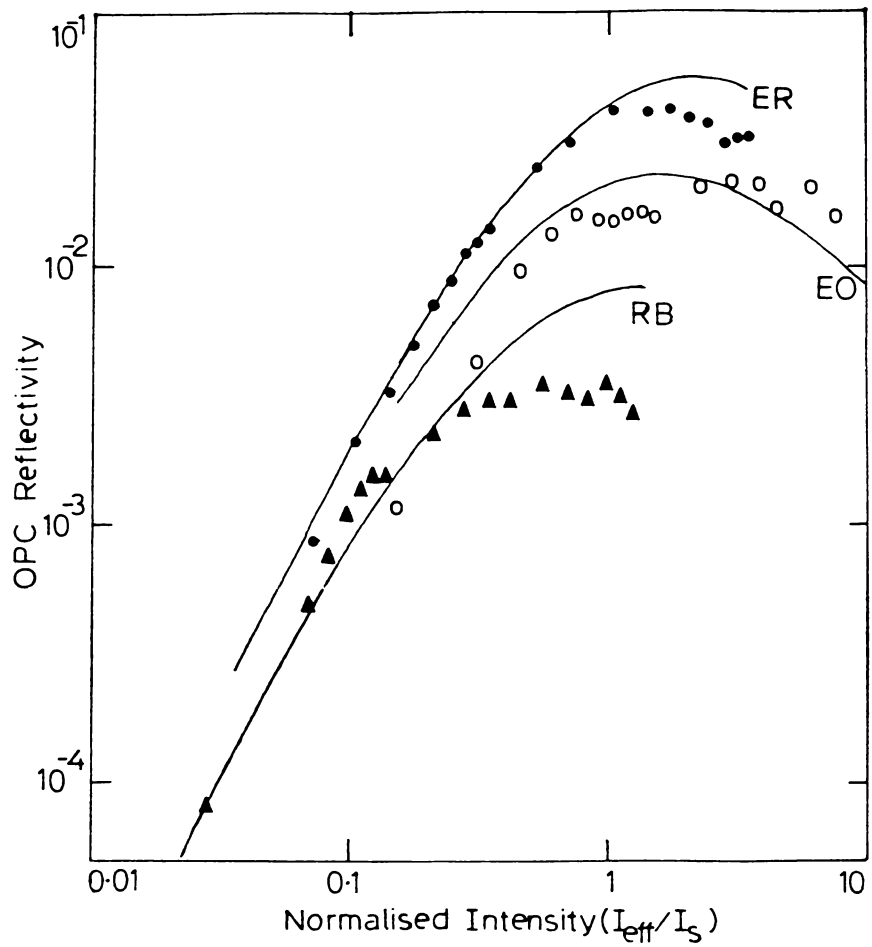


Figure 4.03 OPC reflectivity vs. normalised intensity - cases of (●) erythrosin B, (○) eosin and (▲) Rose Bengal, doped in gelatin films, as compared to the corresponding theoretical curves (ER, EO and RB respectively). Scale on the horizontal axis applied to the theoretical curves only.

theory. The reflectivity increases upto a point of  $I_{\text{off}} \approx I_s$  and then falls. When intensity increases beyond the saturation intensity the observed reflectivity falls much faster than the theoretical one. This might be due to some photochemical changes in the dye molecules. According to the theory, the maximum OPC reflectivity at any intensity for these samples should increase in the order of Rose Bengal, eosin and erythrosin B, for the range of intensities used in the experiment. But in the present experiments signals from eosin were stronger than that from Rose Bengal only at very small intensities (see figure 4.02). When intensity was increased signals from eosin films remained the weakest. We attribute this to photochemical damage of the dye molecules. Since saturation intensity of eosin much smaller than that of the other two, it may be much more susceptible to photochemical damage at the level of intensities used here.

#### **4.14 Relative efficiency of OPC in gelatin and PVA films :**

OPC using dyes doped in PVA films have been first reported in literature as a result of the present investigations [8]. All the three dyes mentioned above showed increased OPC efficiency in PVA films compared to gelatin films of equal absorption lengths. In figure 4.04, we have plotted the OPC signals from erythrosin B doped in gelatin and PVA films. In both the cases the films had an initial transmission of 4.7 %. At the maximum OPC signal strength an attempt was made to measure the absolute power in the phase conjugate beam, making use of a powermeter (EG&G Gamma Scientific Model 460 Laser Powermeter).

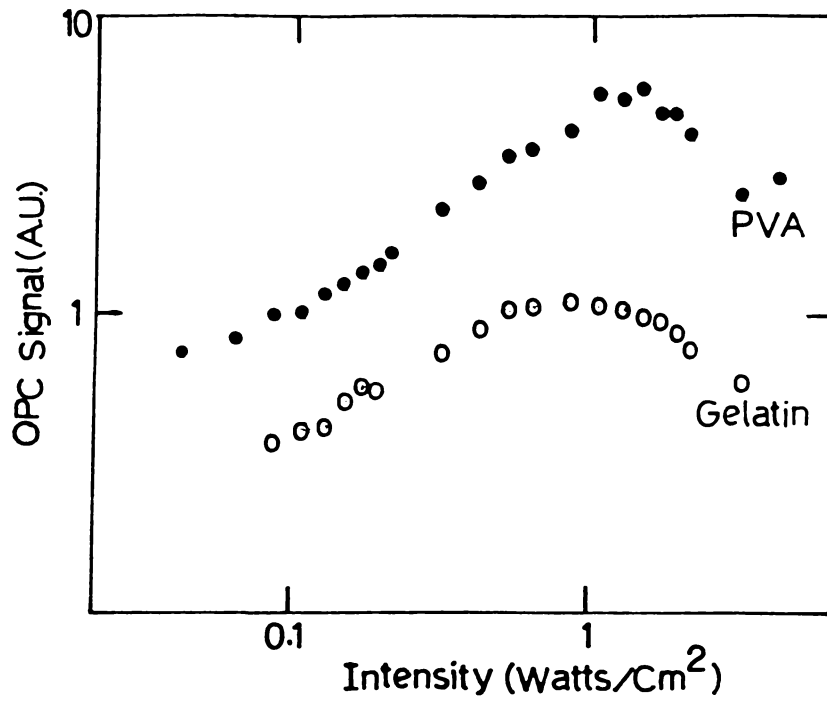


Figure 4.04 Relative OPC signals (normalised to the probe beam intensity) from (●) PVA and (○) gelatin matrices - case of erythrosin B

The measured power in the phase conjugate beam, after accounting for the loss at the beam-splitter BS<sub>9</sub>, was  $3.3 \times 10^{-7}$  Watts. The probe beam power was about  $10^{-2}$  Watts. This implies a reflectivity of  $10^{-5}$ . In the case of gelatin it is a little less. The difference may be attributed to the surface quality of the two films.

#### 4.15 OPC reflectivity vs. absorption length :

The theory of Abrams and Lind [7] was formulated for non-depleted pump beams. They have plotted the reflectivity curves for a number of absorption lengths, upto a value of 14. But in the case of the present samples, this value is too large for the non-depleted pump beam approximation to hold good. In the present investigations a study of the variation of the OPC efficiency with absorption length has been made, using a number of samples with different values of  $\alpha_0 L$ . These were made from solutions with different concentrations of the dye. Because of the increased signal strength erythrosin B was chosen for this study.

In figure 4.05 (a) we have plotted the OPC reflectivity vs. normalised intensity for a number of absorption lengths. In figure 4.05 (b) the corresponding theoretical curves are given. It is seen that for low values of  $\alpha_0 L$  there is fair agreement between theory and experiment, which increases as  $\alpha_0 L$  increases. The best agreement is obtained at a value of  $\alpha_0 L = 1.9$ . On still increasing this value, agreement worsens and for  $\alpha_0 L = 6.67$

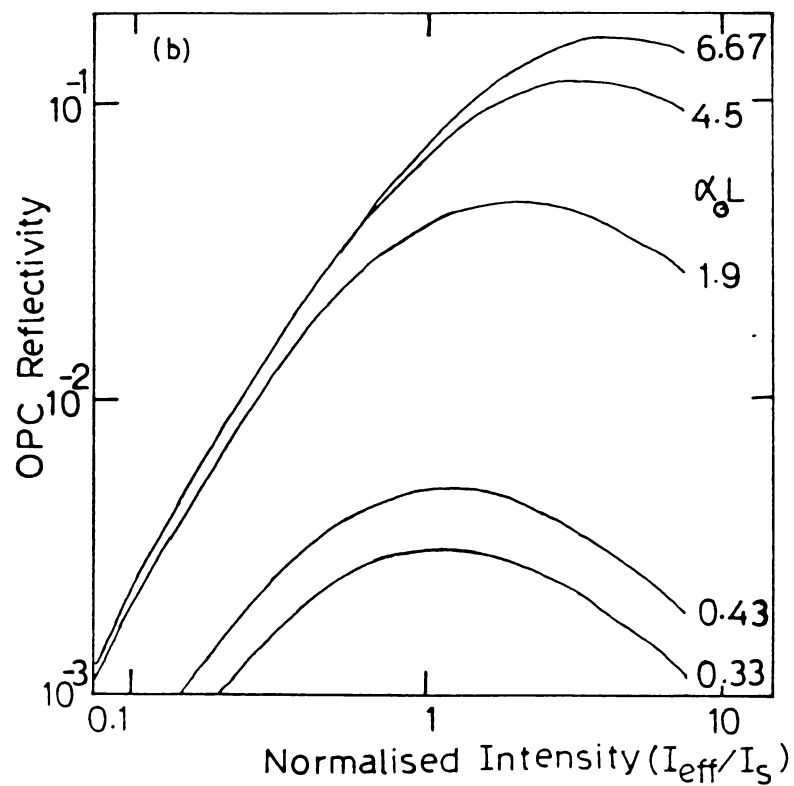
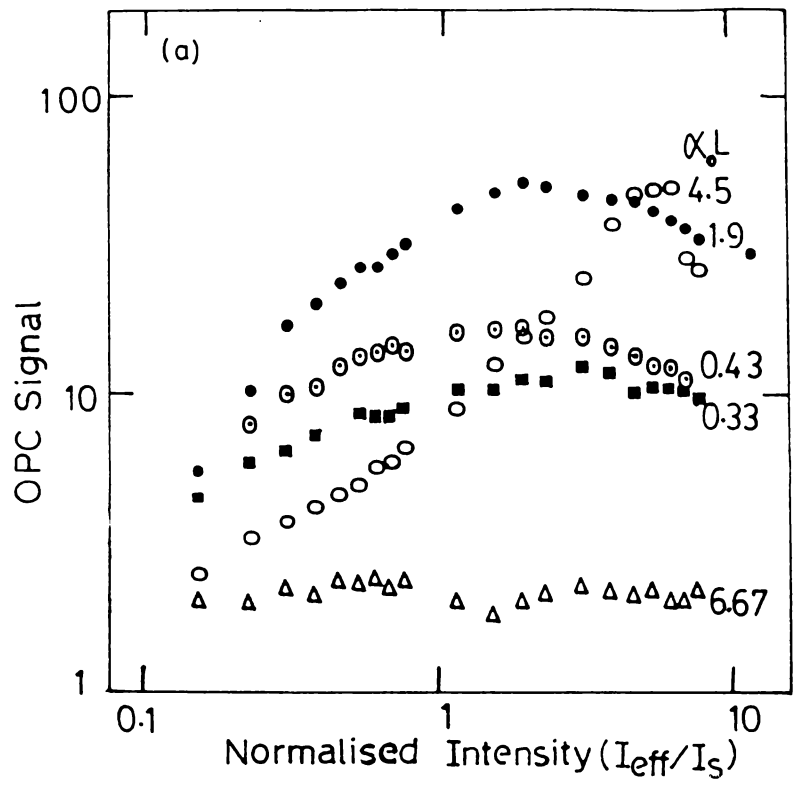


Figure 4.05 (a) OPC signal strengths (normalised to the probe beam intensity) vs. normalised intensity for various absorption lengths - case of erythrosin B doped in PVA film. (b) The corresponding theoretical curves.

the curve is flat, indicating that there is no phase conjugation at all.

#### 4.16 OPC efficiency vs. wavelength :

The effect of wavelength appears in the relation for OPC reflectivity through the absorption coefficient  $\alpha_0$ . The dependence of wavelength can be expected to roughly follow the absorption spectrum. The different lines of the argon ion laser has been used to investigate this. In figures 4.06 (a) and (b) we have plotted the relative efficiencies of OPC in the cases of erythrosin B in PVA and gelatin matrices. The dependence on wavelength in both the cases seem to be identical.

#### 4.17 Effect of vibrations :

Though one would tend to expect an instantaneous response from a saturable absorber, in the present cases, since the saturation is effected by "bottle-necking" at the triplet levels, which takes place in a time scale of milliseconds, there is a finite rise-time for the OPC signals to form. Wash-out effects due to mechanical vibrations therefore become detrimental. The earlier authors have overlooked this factor while emphasizing the application possibilities of the thin film phase conjugators. In our studies, we have found these effects to be very severe. In fact, because of the very high sensitivity of interaction to vibrations it was not possible for us to investigate the transient effects. Figure 4.07 (a) shows the temporal profile

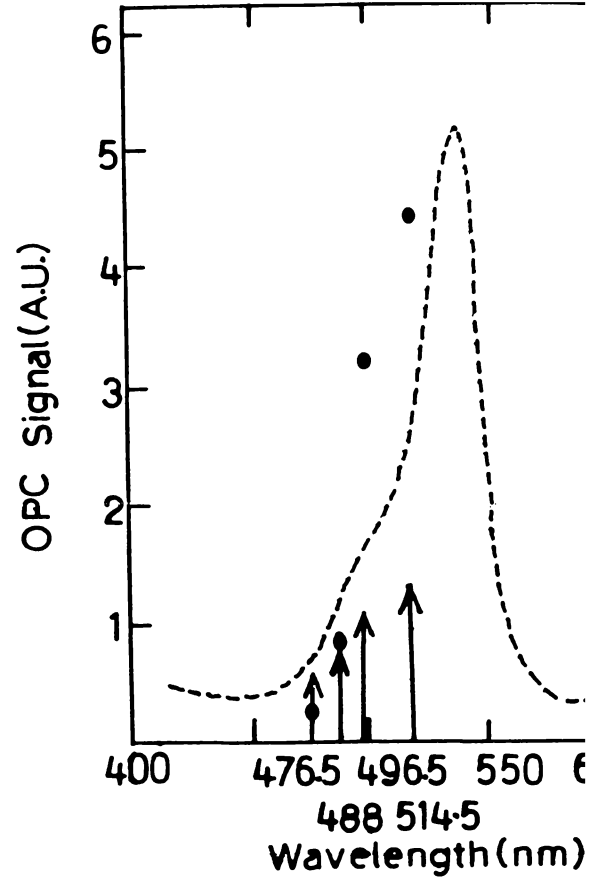
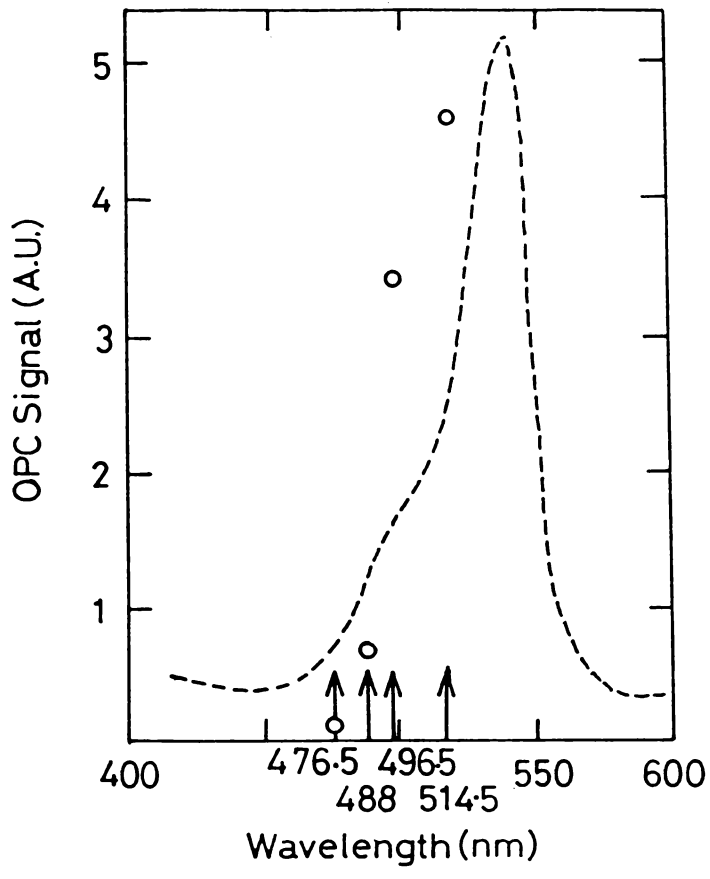


Figure 4.06 Relative OPC signal strengths at the different argon ion laser wavelengths, plotted in the background of the absorption spectra (broken lines) - case of erythrosin B in (a) PVA film and (b) gelatin film.

of the OPC signal with which we were working. The experimental set-up was laid over an ordinary stone-top table. In an attempt to use indigenous vibration isolation techniques (thermocool, rubberised coir etc.) we have ended up with a profile as shown in figure 4.07 (b). The periodic fluctuations in this case was later found to be occurring due the vibrations picked up from a motor which was working near-by (a microphone picked up the same vibrations from the floor, when the motor was working and it disappeared when the motor switched off). In our set-up, it was not possible to remove the motor and therefore it was not possible to obtain a fluctuation-free OPC signal.

#### 4.18 Effect of photochemical damage :

This is another point which has been overlooked by the previous authors. These systems do not behave completely as saturable absorbers. There is always a good amount of unsaturable component for absorption and this, alongwith various nonradiative processes contribute to the damage of the dye molecules. On attempting to measure the saturation intensities (chapter 3) we have observed that this damage poses a severe problem. Figures 4.08 (a) and (b), show this effect in the case of an erythrosin B and Rose Bengal samples, at various incident intensities. As the intensity increases the signal decays very faster. A working level of intensities which allows reasonably good signals can however be fixed. On comparing the damage effect on the three dyes, we have seen that Rose Bengal is the most damage-resistant whereas eosin is the least.

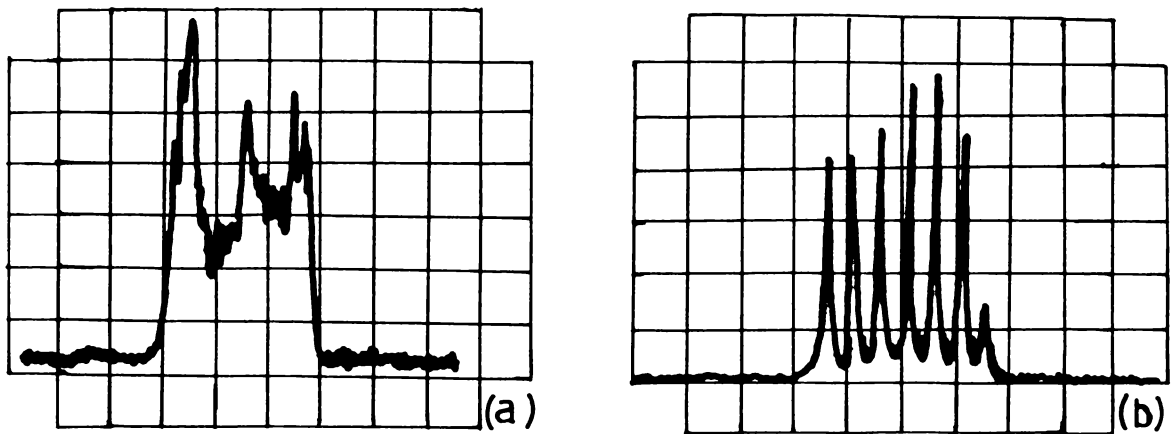


Figure 4.07 Oscillograms of the temporal profiles of the phase conjugate beam. Laser source and optical set-up kept on ordinary table tops (a) without any vibrational isolation devices and (b) with indigenous vibration isolation devices. Sweep speed in the former is 5 ms/div. which is reduced 20 ms/div. in the latter for showing the periodic change.

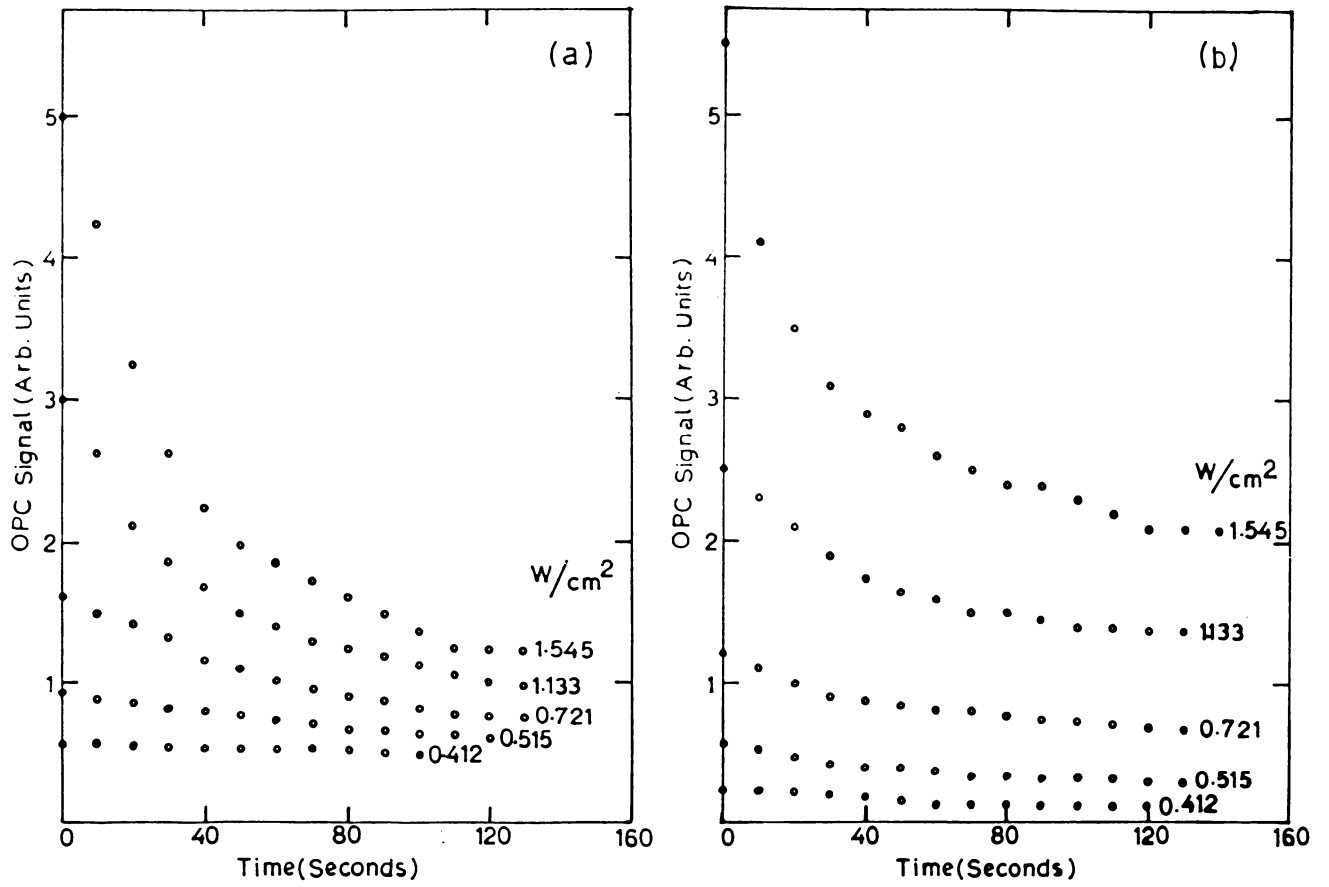


Figure 4.08 Decay of the OPC signals with time - cases of (a) erythrosin B and (b) Rose bengal doped in PVA films.

## CHAPTER 4

### SECTION II

#### PHASE CONJUGATION OF A BROADBAND LASER

##### 4.20 OPC of broadband lasers :

Although DFWM has been widely studied as a method for producing phase conjugate (PC) wavefronts, only a few reports have been appeared in literature on attempts to obtain PC beams from broadband lasers. Theoretical considerations show that [9] small bandwidths are almost essential for the production of PC beams. Analysis of the broadband effects in DFWM in absorbing media has been recently reported by Alber *et al* [10]. They have concluded that for pump beams below the saturation intensity the PC reflectivity generated by broadband lasers is reduced compared to monochromatic case. This is in contrast to an earlier result by Saxena and Agarwal [11] that the statistical fluctuations of a chaotic field enhances the PC reflectivity over the corresponding monochromatic case.

In the present investigations, phase conjugate signals have been detected via DFWM of a Nd:glass laser in Kodak 14015 dye, dissolved in 1,2, dichloroethane.

The bandwidth of a Nd:glass laser is typically 22 to 29 nm [12] and is therefore suitable for experimental investigations on the broadband effects in DFWM. But there are not many reports

of OPC experiments using Nd:glass lasers. Attempts on using simple mechanisms like DFWM in an absorbing dye have not been so far appeared in literature. Phase conjugation of Nd:glass laser is particularly of interest in applications like target-tracking in laser fusion [13]. Investigations in this area may, therefore, fall into the category of classified research and escape normal reporting. Therefore it was interesting to look for a PC beam of the Nd:glass laser emission. The experiment was very difficult to carry out mainly due to the limitations of the source laser used and we had to be contented with the detection of a PC signal, at the end of a number of efforts. The experiment was conducted in the following manner.

#### 4.21 Experimental details :

The laser source used was a single-shot Nd:glass laser, which was fabricated in our laboratory [14]. It can deliver about 1 - 2 J in the free-running mode and about 100 mJ (in about 20 ns pulses) when Q-switched with Kodak 14015 dye solution. The experimental set-up is shown in figure 4.09. The retro-reflecting mirror (M) was a gold-coated plane glass plate which was kept at about a metre from the output mirror of the laser. The beam-splitters (BS) were uncoated glass plates. The probe beam was incident at the sample at about 20 degrees to the pump beam. The nonlinear medium (S) was Kodak 14015 dye, dissolved in 1,2-dichloroethane. The solution was taken in a thin cell, of about 100  $\mu\text{m}$  thickness, formed by cementing two glass plates together. This was kept close to the mirror. The

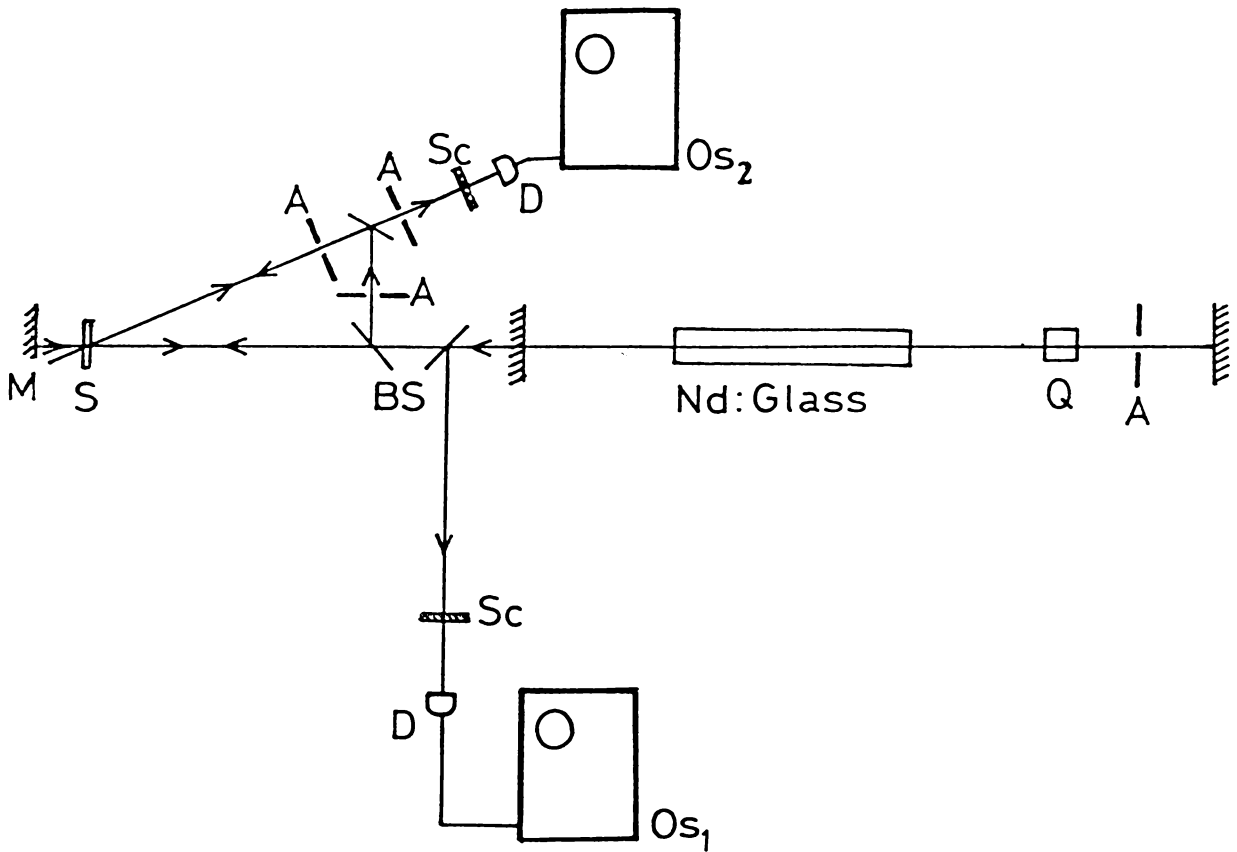


Figure 4.09 Set-up for the phase conjugation of Nd:glass laser. M - Mirror, BS - Beam splitters, S - Sample, Q - Q-switch, A - Apertures, Sc - Scatterers, D - Photo-diodes, Os<sub>1</sub> & Os<sub>2</sub> - Oscilloscopes (the former for reference and the latter for signal detection).

optical set-up was aligned with the help of a He-Ne laser. The direction of the PC beam was located by retro-reflecting the probe beam. Detection was done by two PIN photodiodes (HP 4207), one for monitoring the laser intensity and the other for detecting the signal in the phase conjugate direction [15]. To eliminate noise due to the stray off-axis radiations from the laser cavity a number of apertures (A) were used.

#### 4.22 Results and discussions :

On carefully aligning the system it was possible to detect very weak signals in the PC direction when the laser was operated in the free-running mode, with a total pulse energy of about 1 J, spread in a number of microsecond pulses, lasting for about half a millisecond. When the laser was Q-switched using a dye Q-switch, the signals became appreciable. For taking some measurements, so as to confirm the nonlinear nature of these signals, we operated the laser in a multiple Q-switched mode (figure 4.10). The total pulse energy was a few tens of millijoules in this case. The signal and the reference beams were simultaneously detected and stored in two storage oscilloscopes (Tektronix 466 and Philips PM 3219). Both of these exhibited the same temporal profile, as shown in figure 4.10, but with differing heights of the peaks. The heights of the corresponding peaks are compared to establish the nonlinear nature of the signal [15]. A typical plot is given in figure 4.11. In order to confirm that these signals actually originated from a four wave interaction in the dye, the pump beam

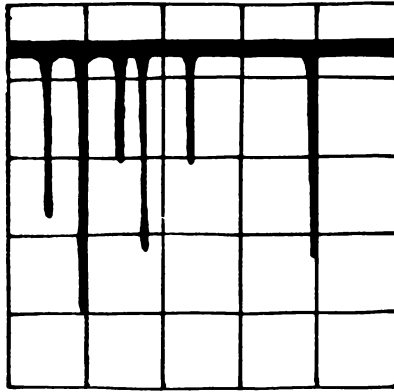


Figure 4.10 A part of the oscillogram of the multiple Q-switched output of the Nd:glass laser used in the experiment. Sweep speed =  $50 \mu\text{s}/\text{div}$ .

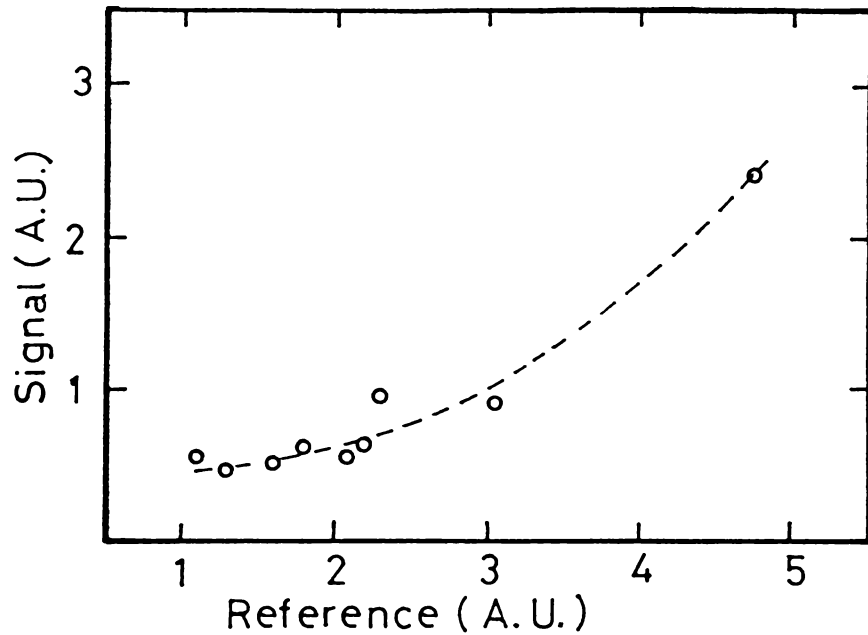


Figure 4.11 A typical plot of the heights of the peaks recorded in the signal and the reference channels. Scales on the axes are divisions on the oscilloscope screen.

was blocked. There was no signal then. Also on replacing the dye cell with a similar cell containing solvent, no signal was observed.

Thus these investigations have shown that it is possible to obtain a phase conjugate beam of a Nd:glass laser using a DFWM scheme in an absorbing dye. We have also attempted an intra-cavity configuration, which will be of greater interest for target-tracking applications. But excessive noise due to the off-axis radiations from the cavity, it was difficult to isolate the signal. The problem appeared when it was attempted to use the dye solution in a thick cell instead of a thin cell. It was not possible (due to equipment constraints) to make precise measurements and therefore rough estimates of the power levels were made as mentioned above (making use of a Scientech Model 362 Laser Power/Energymeter separately).

A detailed investigation covering the quantitative aspects of the efficiency, fidelity of phase conjugation etc. is necessary to evolve a complete picture. The physical mechanism of the development of the PC beam also has not been conclusively determined, but it is believed to be saturable absorption, in line with the earlier work of Moses and Wu [16], who have used the same dye, in a toluene solution, for phase conjugation of a Nd:YAG laser radiation. In the very low concentrations of the dye used in the present case, intensities must be far exceeding the saturation intensity and therefore a pure saturable absorption cannot contribute much to phase conjugation. Some

other mechanisms like thermal non-linearity also may be contributing to some extent.

## REFERENCES

- [1] Y Silberberg and I Bar-Joseph, *Opt. Commun.*, 39, 295 (1981)
- [2] Y Silberberg and I Bar-Joseph, *IEEE J. Quantum Electron.*, QE 17, 1967 (1981)
- [3] M A Kramer, W R Tompkin, J Krasinski and R W Boyd, *J. Lumin.*, 31/32, 789 (1984); M A Kramer, W R Tompkin and R W Boyd, *Phy. Rev. A*, 34, 2026 (1986)
- [4] H Fujiwara and K Nakagawa, *Opt. Commun.*, 55, 386 (1985)
- [5] H Fujiwara and K Nakagawa, *J. Opt. Soc. Am. B*, 4, 121 (1987)
- [6] P F Liao and D M Bloom, *Opt. Lett.*, 3, 3 (1978)
- [7] R L Abrams and R C Lind, *Opt. Lett.*, 2, 94 (1978) and 3, 205 (1978)
- [8] K P B Moosad and V P N Nampoore, *Pramana*, 31, 281 (1985)
- [9] e.g., see D M Pepper and A Yariv, in "Optical Phase Conjugation", ed. R A Fisher (Academic, 1983), p.61
- [10] G Alber, J Cooper and P Ewart, *Phy. Rev. A*, 31, 2344 (1984)
- [11] R Saxena and G S Agarwal, *Opt. Lett.*, 8, 566 (1983)
- [12] W Koechner, in "Solid State Laser Engineering" (Springer-Verlag, 1976), p.62
- [13] C R Giulaino, *Physics Today*, 34, 27 (1981)
- [14] N Subhash and K Sathianandan, *IEEE J. Quantum Electron.*, 20, 11 (1984)
- [15] I S Ruddock and G S Scott, *Eur. J. Phys.*, 4, 45 (1983)
- [16] E I Moses and F Y Wu, *Opt. Lett.*, 5, 64 (1980)

## CHAPTER 5

### CONTINUOUS WAVE SECOND HARMONIC GENERATION IN A RING DYE LASER

#### 5.00 Second Harmonic Generation of CW lasers :

Research in Second Harmonic Generation has developed to the extent that the few percentages of efficiency of conversion into the Second Harmonic which was obtained in the early days now has become in excess of 50 % [1]. Because of the nonlinear character, this has been generally become successful in the case of pulsed lasers. Phase matching is obtained in two ways, viz. angle tuning and temperature tuning. In the former one a suitable angle of incidence is chosen (with respect to the crystal axis) so that the phase matching condition is satisfied for the ordinary and the extraordinary rays. In the latter case, the temperature dependent refractive index is made use of [2,3].

The most popularly used crystals include Lithium Niobate ( $\text{LiNbO}_3$ ), Ammonium Dihydrogen Phosphate (ADP), Potassium Dihydrogen Phosphate (KDP), deuterated Potassium Dihydrogen Phosphate ( $\text{KD}^*\text{P}$ ) etc.[4]. A number of organic crystals also have been attempted these days [5].

Although continuous wave, tunable UV radiation of narrow linewidth find several applications in high resolution spectroscopy, attempts to generate this have been of limited success. Intra-cavity SHG of dye lasers have been described by a few authors for this purpose [6]. SHG is more known in the

case of pulsed lasers and only very few attempts on CW SHG have been successful . In the case of intracavity configuration, since high power densities are available, there are more chances for success. All the above authors have used temperature tuning (for phase matching) in different crystals, kept in the intracavity space. Varying the temperature provided the necessary tuning of wavelength. These techniques are costly and cumbersome. A temperature stability of the order of 0.03 °C across a crystal length of 20 mm is the typical requirement in such systems, which is obviously very expensive. Also due to the thermal degradation of the crystals tuning range is often limited. In the case of a ring cavity, introduction of such thick elements necessitates the use of extra optics for compensating the beam walk-off problems, which will further complicate the alignments.

The use of thin crystals as an alternative was suggested and demonstrated by Majewski [7], in the case of a stabilised ring dye laser (Spectra Physics 380 D). Output powers upto 15 mW with linewidth 180 - 500 kHz in the range of 293 - 330 nm were obtained using a 1 mm thick crystal of Lithium Iodate. Majewski has used a highly sophisticated laser and had re-positioned some of the intra-cavity elements of the ring laser. Also he had to introduce an extra element into the cavity. Altogether it was a laser technologist's job rather than that of a normal laser user.

In the present work, we have used a 0.7 mm thick Lithium Iodate ( $\text{LiIO}_3$ ) crystal for the intra-cavity frequency doubling of

a commercial ring dye laser (Spectra-Physics 380 A), which is much simpler than the one used by Majewski. Also we have not made much modifications to the laser. We have carried out experiments with two crystals, one "perpendicular-cut" and the other "Brewster-cut". Our results indicated that this technique offers advantages of extended tuning range, ease of operation and low cost as compared to the use of temperature tuned crystal for intracavity SHG. In the following sub-sections the details of these experiments are given.

#### 5.01 Thin $\text{LiIO}_3$ crystals - Cut details :

The intracavity phase matching conditions for angle tuning are different from single pass extracavity SHG. Since SHG power is proportional to the square of the crystal thickness (chapter 1) usage of thick crystals can, in principle, improve efficiency. But insertion of a plane parallel crystal in the path of the beam inside the cavity at Brewster angle causes a beam translation. Moreover, due to the optical activity of  $\text{LiIO}_3$ , the polarisation of the fundamental radiation rotates strongly and this forces the laser to jump to another wavelength, owing to the polarisation sensitivity of the birefringent filter used for the ring laser tuning. However, in the case of crystals with thickness less than one millimetre, the beam walk-off and the effects due to the optical activity are small and can be compensated by adjusting the laser cavity. The optimum thickness for the crystal thus becomes a compromise between the SHG efficiency and ease and stability of operation.

Figure 5.01 shows the details of the crystal cut and orientation of the crystallographic coordinates. The crystallographic coordinates  $x$ ,  $y$  and  $z$  are tilted with respect to the  $r$ ,  $s$ ,  $t$  coordinates. The polished crystal faces are parallel to the  $s$ - $t$  plane. The incident, refracted and transmitted beam propagate parallel to the  $r$ - $t$  plane with the electric field vector  $E$  inside the crystal perpendicular to the optic axis  $z$ .

The SHG efficiency of  $\text{LiIO}_3$  crystals is independent of the angle  $\phi$  [3]. At  $\nu_{\text{opt}}$ , the frequency for which the crystal is cut, angle of incidence  $\alpha$  is the Brewster angle and the angle  $\theta$  is the phase matching angle  $\theta_m$ . At the other laser frequencies, different phase matching angles can be obtained by rotation around the normal to the crystal surface, after changing the angle of incidence. In the present investigations, both Brewster-cut ( i.e.,  $\phi = 45^\circ$  when  $\alpha = \text{Brewster angle}$  ) and perpendicular-cut ( i.e.,  $\phi = 45^\circ$  when  $\alpha = 90^\circ$  ) crystals were used. These were of size  $10 \times 10 \times 0.7$  mm and were supplied by Gsänger Optische Komponenten GmbH, Germany, bonded onto aluminium rings to facilitate mounting. The crystal surfaces were plane parallel within 10 arc seconds for maintaining cavity alignment and organised tuning of the laser. Both the crystals were cut for a wavelength of 616 nm.

## 5.02 Experimental details :

Spectra-Physics model 380 A ring dye laser, pumped by model

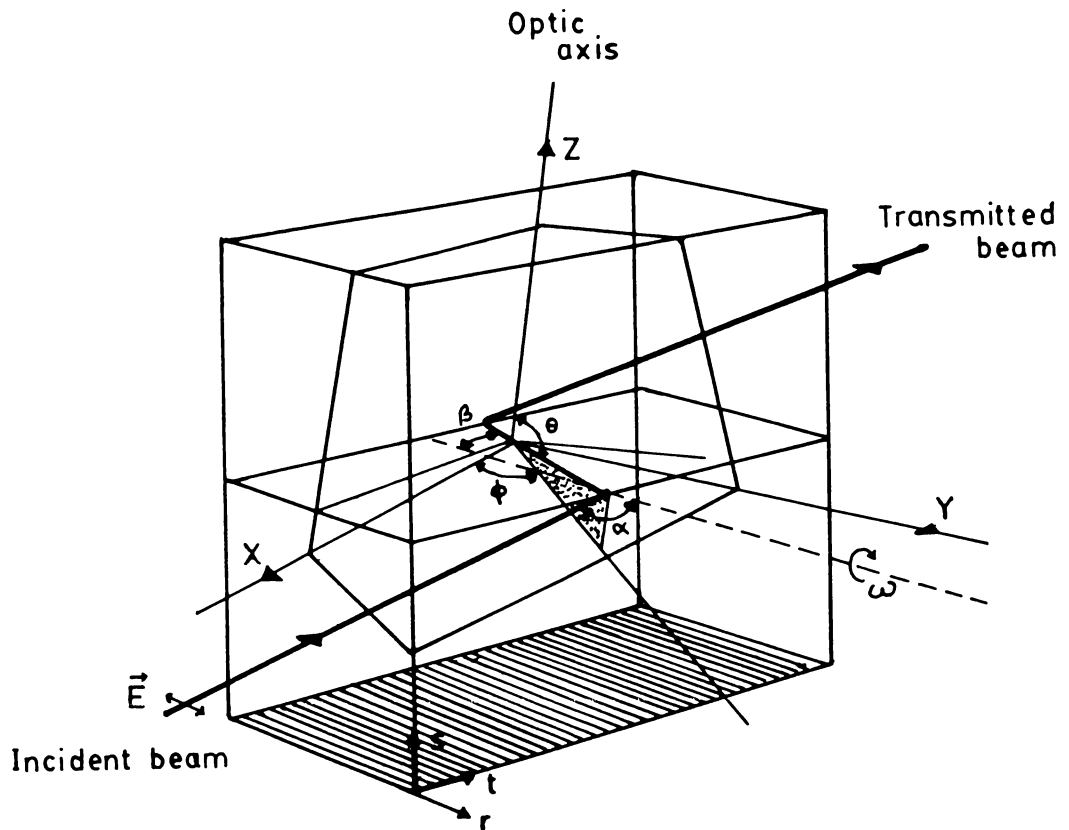


Figure 5.01 The crystal cut. The crystallographic coordinates are rotated and tilted versus the  $r, s, t$  coordinates. The polished faces are parallel to the  $s-t$  plane. The incident, refracted and transmitted beams are parallel to the  $r-t$  plane. For  $\nu_{opt}$  the angle  $\alpha$  is exactly the Brewster angle and the vector  $E$  inside the crystal is perpendicular to the optic axis  $Z$ . The angle  $\theta$  (between refracted beam and the optic axis) in this case is a phase matching angle  $\theta_m$  for  $\nu_{opt}$ . For the other laser frequencies  $\nu_1$ , the different angles  $\theta_m$  can be obtained by crystal rotation  $\omega$  around the normal and appropriate change of incidence angle  $\alpha$ . At every laser frequency (except  $\nu_{opt}$ ) phase matching is achieved for angles slightly different from the Brewster angle. (After ref. [7]).

171 Argon ion laser is used for the experiments. Figure 5.02 shows the cavity configuration of the ring laser, with the  $\text{LiIO}_3$  crystal inserted at the intracavity beam waist between the mirrors  $M_2$  and  $M_3$ . The standard ring laser mirrors  $M_3$  and  $M_4$  were replaced by the Spectra-Physics Rhodamine 6G Optics [8], consisting of a UV transmitting mirror  $M_3$  and a 0.25 % output coupler  $M_4$ . The crystals were fitted in a miniature mount capable of X and Y movements and rotation around an axis passing through the centre of the crystal. The crystal surfaces were flushed with nitrogen gas, flown through the gas manifold fitted on the crystal holder. This reduce the crystal degradation by making the atmosphere dry.

### 5.03 Results and discussions :

The ring laser is operated at the desired fundamental wavelength by tuning the birefringent filter. On introducing the crystal into the cavity, lasing was lost; but could be easily regained by positioning the crystal at Brewster angle (about  $62^\circ$ ) and slightly adjusting  $M_2$  to compensate for the small beam walk-off. The fundamental frequency transmitted through  $M_4$  was monitored on a Burliegh model WA 20 wavemeter during the whole process of crystal alignment. After inserting the crystal and setting  $\alpha$  at Brewster angle, the crystal is rotated slowly around its normal (we call this  $\omega$  rotation). If rotation around the normal does not yield laser action, the whole process is repeated with  $\alpha$  slightly increased or decreased from Brewster angle. The UV radiation coming out through  $M_3$  can now be observed on a Zinc

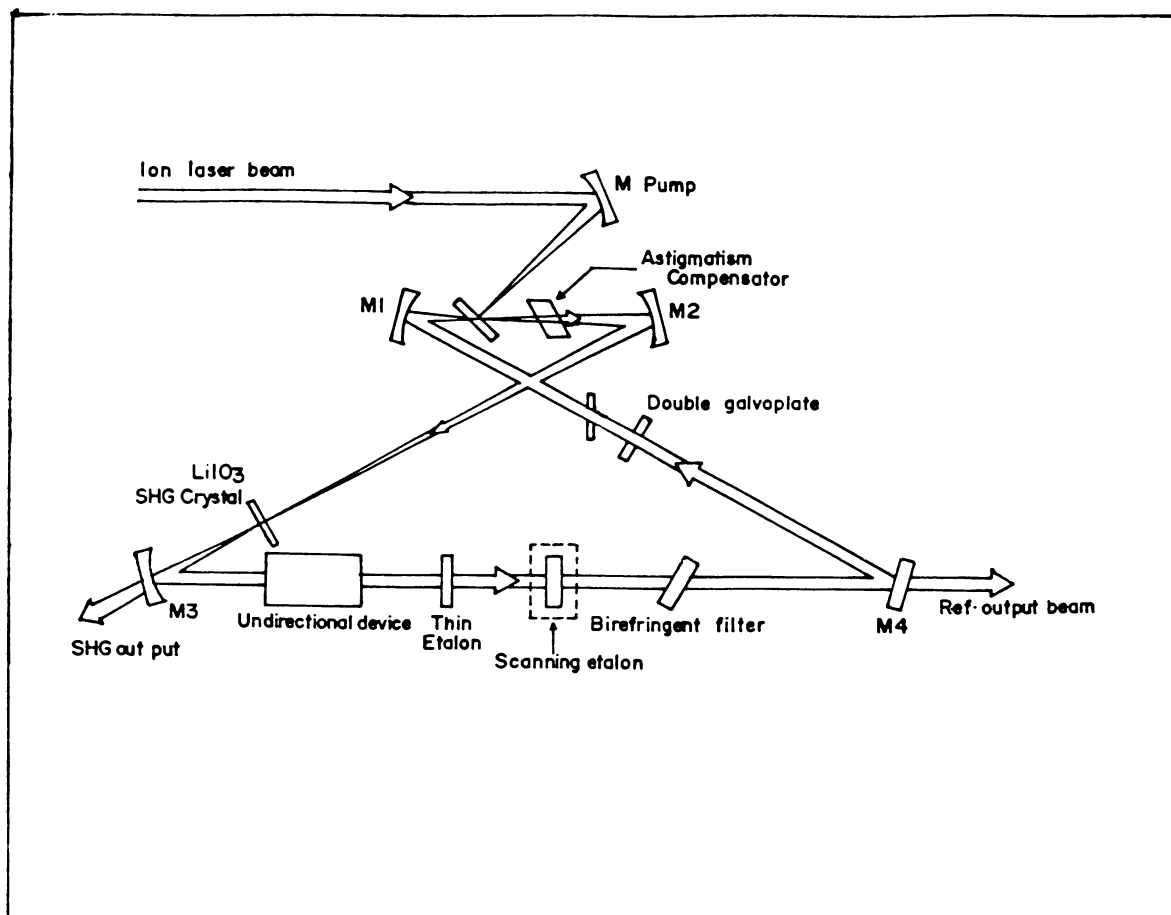


Figure 5.02 Cavity of the ring dye laser, showing the beam waist at which the  $\text{LiIO}_3$  crystal is introduced.

Sulphide screen or even on a business card.

Fine tuning of  $\alpha$  and  $\omega$  for optimisation of UV power is done with the help of a Hamamatsu R 212 photomultiplier tube and an analogue read-out. UV filters of known transmission were used to avoid saturation of the PMT. The SHG power at different wavelengths in the tuning range of the ring dye laser were determined from the anode sensitivity of the PMT. Figure 5.03 shows the variation of SHG power with wavelengths for Brewster and Perpendicular cut crystals for an argon ion laser pump power of 9 watts in the multiline mode of operation. The maximum SHG power of 1.85 mW was obtained at 302.5 nm for this pump power while using the perpendicular cut crystal. Increasing pump laser power enhances the SHG power and also extends the tuning range beyond the 292.5 - 308 nm limits shown in figure 5.03.

In the case of the intracavity phase matching by angle tuning, high conversion efficiency is achieved by setting the crystal for maximum fundamental power unlike the requirement of optimal phase conditions for extracavity SHG. Since the etalons were not used inside the ring laser cavity during measurements the laser linewidth was about 3 GHz. Although the SHG power obtained using angle tuned thin  $\text{LiIO}_3$  crystals is lower than that obtained by using temperature tuned ADA crystals, the advantages of broad tuning range, ease of operation and low-cost make this technique more attractive for UV laser spectroscopy using ring dye lasers. It is also possible to extend the SHG tuning range also to improve the SHG efficiency at any particular wavelength by using crystals cut for that particular wavelength. In what

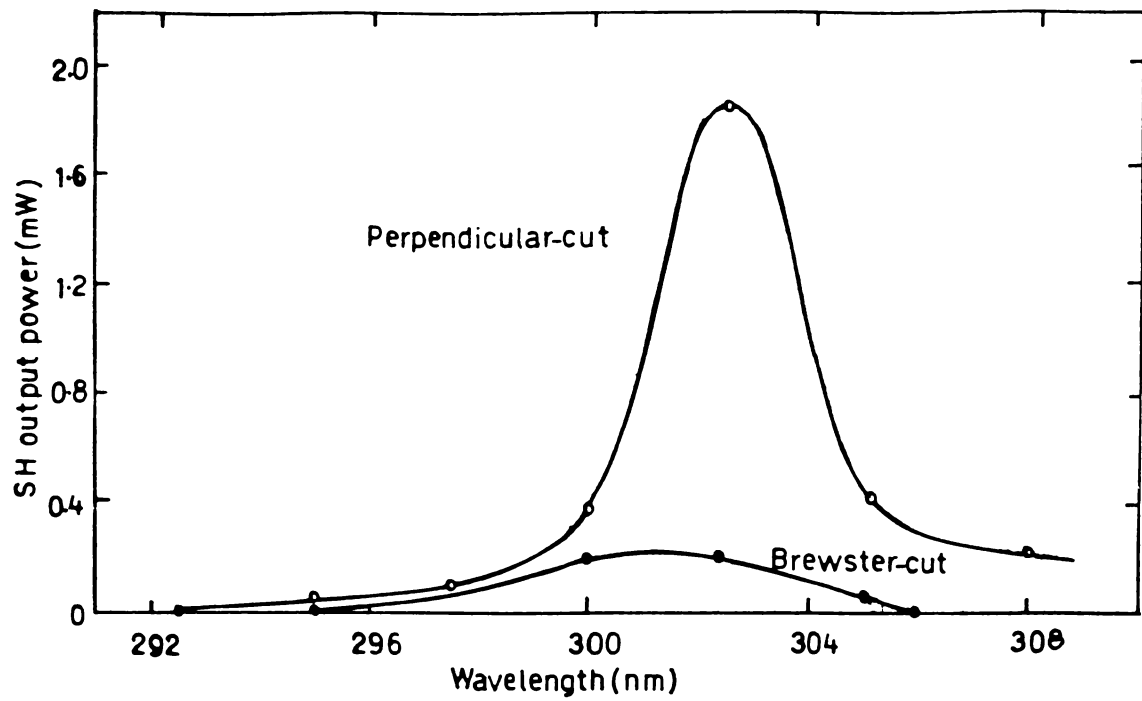


Figure 5.03 Tuning curves for the two crystals.

follows an experiment which demonstrates the potential of the UV radiation thus generated from the ring laser, is explained.

#### 5.04 An experiment using the second harmonic radiation - detection of hydroxyl radicals :

Detection and measurement of trace species in gases is an important area in which lasers are found useful . In laser absorption spectroscopic methods, the strength of the signal depends on the number of molecules available on the path of the laser beam. Use of samples in pressurised cells prevent the acquisition of any high resolution data. Therefore a multipass cell is used in such investigations [9]. In the following experiment for detection and measurement of hydroxyl (OH) radical concentration using the second harmonic radiation generated in a ring laser, we also have made use of multipass cell [10].

The experimental set-up is as shown in figure 5.04. Second harmonic was generated from a ring dye laser as mentioned above. This is tuned to 308 nm, which is close to the  $Q_1(2)$  line of the  $^2\Pi(v''=0) \rightarrow ^2\Sigma^+(v'=0)$  transition of the OH radical, which has a large absorption cross-section. The fundamental wavelength is monitored using a wavemeter (Burliegh WA 20). The UV beam is allowed to enter the multipass cell and exit through the outlet after a numbr of to-and-fro passages in the cell. The output is then detected using a PMT and lock-in amplifier. The input beam is chopped at about 150 KHz as a reference to the lock-in amplifier. The output of the lock-in

amplifier is fed to a ratiometer along with that of another PMT which monitors the SHG power. The reading in the ratiometer gives a relative measure of the absorption of the UV radiation inside the multipass cell.

The multipass cell is pumped to pressure of about  $10^{-4}$  Torr and the ratiometer reading is noted for different pathlengths, which can be read-out from the calibration on the multipass cell. OH radicals is then introduced into the cell, by keeping an electrical discharge in a glass chamber containing water vapour. The pressure is adjusted as the above and the ratiometer readings are again noted for the same pathlengths. The concentration of the OH radicals inside the multipass cell is then determined using the relation [11,12],

$$I_{\nu} = I_0 \exp \left( -n \left\langle \frac{\Delta n}{n} \right\rangle \sigma_0 L \right) \quad 5.01$$

where  $I_{\nu}$  is the normalised intensity of light transmitted in the presense of OH radicals,  $I_0$  is the normalised intensity transmitted in the absense of OH radicals,  $n$  is the concentration of the absorbing species (OH),  $\left\langle \frac{\Delta n}{n} \right\rangle$  is the fraction of population residing in the rotational level from which absorption transition originates,  $\sigma_0$  is the total absorption cross-section and  $L$  is the pathlength.

Making use of the literature values for  $\left\langle \frac{\Delta n}{n} \right\rangle$  and  $\sigma_0$  [11], we have calculated the concentration of the OH radicals in the multipass cell at various vapour pressures. This is shown in

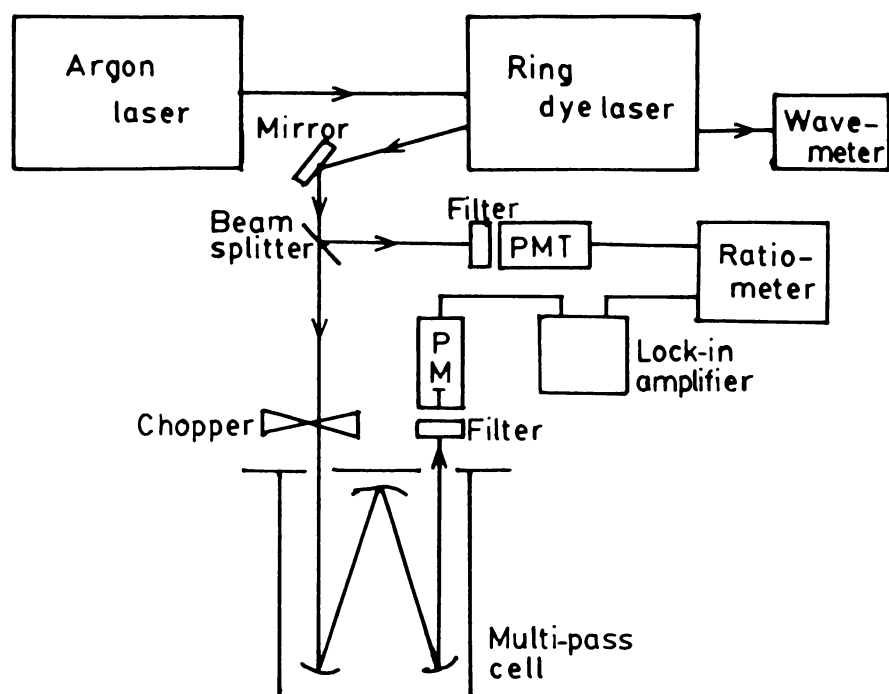


Figure 5.04 Set-up for the detection of hydroxyl radicals. (Arrangements for the production of the hydroxyl radicals are not shown)

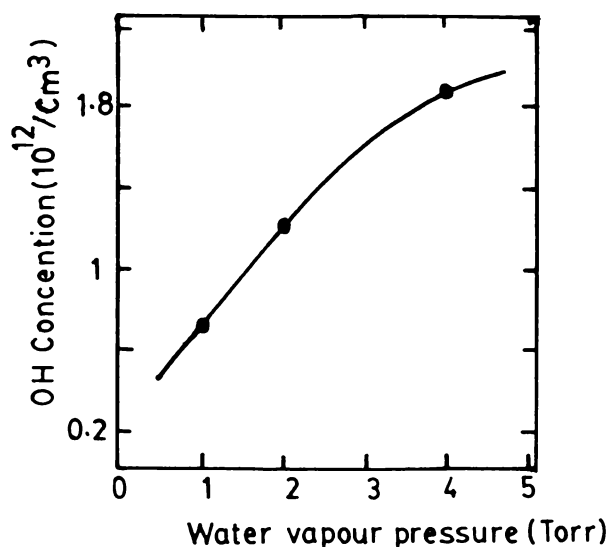


Figure 5.05 Hydroxyl radical concentration vs. water vapour pressure in the cell. Points represent averages of measurements made with different path-lengths.

the figure 5.05. The different points corresponding to the same pressures are the values obtained with measurements repeated with different pathlengths. These points indicate that there is a saturation in OH radical concentration as the vapour pressure increases. The maximum concentration detected is about  $2.2 \times 10^{12}$  OH/cm<sup>2</sup> at a discharge pressure of 4 Torr.

## REFERENCES

- [1] R S Adhav and M Orszag, "Frequency doubling crystals - unscrambling the acronyms", *Electro-Optical Systems Design*, December 1974.; R S Adhav, "Materials for Optical Harmonic Generation", *Laser Focus*, June 1983
- [2] "Second Harmonic Generation - Method of phase matching by angular tuning in tetragonal phosphates and arsenates", Data sheet No. 706 ( January, 1973) and "Second Harmonic Generation - 90° phase matching by temperature tuning in tetragonal phosphates and arsenates", Data sheet No. 707 (January 1974), Quantum Technology Ltd., Canada.
- [3] F Zernike and J E Midwinter, "Applied Nonlinear Optics" (John Wiley, 1973)
- [4] S K Kurtz, in "Laser Handbook", Vol 1, ed. F T Arecchi and E O Schulz-Dubois (North Holland, 1972); "Choosing a frequency doubler for a Nd:YAG and a ruby laser", Data sheet No.716 (May 1983), Quantum Technology Ltd., Canada.
- [5] e.g., D S Chemla, *Rep. Prog. Phys.*, **43**, 1190 (1980)

- [6] A I Ferguson and M H Dunn, *Opt. Commun.*, 23, 177 (1977); J J ter Meulen, G W M van Mierlo and A Dymanus, *Phy. Rev. Lett.*, 43, 29 (1979); E R Eliel, W Hogervorst, K A H van Leeuwen and B H Post, *Opt. Commun.*, 39, 41 (1981)
- [7] W A Majewski, *Opt. Commun.*, 45, 201 (1983)
- [8] Product literature of spectra Physics Ring Dye Laser.
- [9] J U White, *J. Opt. Soc. Am.*, 32, 285 (1942); T H Edwards, *J. Opt. Soc. Am.*, 51, 98 (1961); G J Rayl, *Appl. Opt.*, 15, 921 (1976)
- [10] N Subhash, M K Satheeshkumar, T M Abdul Rasheed, K P B Moosad, and K.Sathianandan, *J. Opt.*, 16, 51 (1987)
- [11] M Bakalyar, J U James and C C Wang, *Appl. Opt.*, 21, 2901 (1982)
- [12] N Subhash, in "*Laser Absorption Spectroscopic Measurement of OH Radicals*", Technical Report No. 48-1987, Centre for Earth Science Studies, Trivandrum, India. p.13

## CHAPTER 6

### CONCLUSIONS

Nature manifests itself in very many wonderful forms through the windows of nonlinearity. This was known to man for quite some time. In early sixties of this century, Nicolaas Bloembergen suggested that optics is no exception to this. A new branch of physics was thus born. Soon after, by the advent of lasers, it was possible for the mankind to open the windows of nonlinearity in optics. Today, the various phenomena in nonlinear optics encountered by scientists all over the world comes out in a number of imaginative acronyms - SRS, SBS, SRL, SERS, SHRS, CARS, DFWM, OPC, CSRS, TRIKE, RIKES, HORAS, HORSES etc. [1]

Though there is hectic activity in experimentally exploring nonlinear optical phenomena all over the world, there have not been much attempts in this field in our country. Reports on nonlinear optical experiments are limited to a few [2]. This is mainly because of the lack of enough laboratory and other infrastructural facilities. The present thesis is a report of an attempt made in this direction. The phenomena explored in this work are mainly two - (i) Optical Phase Conjugation (OPC) in some saturable absorber samples and (ii) Continuous Wave (CW) Second Harmonic Generation (SHG) in a ring dye laser.

OPC is a frontline area of research. A few groups in our

country are known to have made attempts on this, but have not been very successful. There are a couple of reports in literature [3-5]. As often happens in frontline areas of research, authors fail to furnish all the vital information regarding the experiments while reporting the achievements. This may be one of the reasons why there are not many reports on OPC experiments from our country. In our case, a few experts from abroad have been kind enough to share their expertise. This include (i) G Indebetouw, Physics Department, Virginia Polytechnic Institute and State University, USA, [6] (ii) L M Bernardo, Physics Laboratory, University of Porto, Portugal [7] (iii) H Fujiwara, Muroran Institute of Technology, Japan [8] and (iv) P Günter, Solid State Physics Laboratory, Swiss Federal Institute of Technology, Switzerland [9]. Whatever OPC signals which we have recorded and reported in this thesis are the results of long and persistent endeavours made through a few years.

Results on three saturable absorber dyes, viz. eosin, erythrosin B and Rose Bengal have been presented in the thesis. Of these, some results on eosin and erythrosin have been reported previously by other authors. But in contrast to their results, in the present investigations erythrosin B is shown to be more efficient of the two. First report of the use of Rose Bengal for OPC appeared in literature from the present investigations. Similarly, the use of polyvinyl alcohol (PVA) as a matrix also has been reported for the first time. The fact that PVA matrix is more efficient than the previously reported gelatin matrix

also has been brought to light as a result of the present studies. The material presented as the characterisation of the samples is expected to develop into a clear-cut procedure for the search for better materials of this class for OPC applications. Novel ideas like observing the fluorescence emission for confirming the saturable absorption have been introduced.

As often happens in scientific investigations, the present studies have generated more questions than answers. Although erythrosin B shows the best efficiency compared to the other two dyes, at present one cannot say why it is so. In all physical properties the position of erythrosin B is in between that of the other two and therefore one would tend to presume the same behaviour in OPC efficiency also. Actually it was with this idea that Rose Bengal was selected for investigations - it was expected to show much more efficiency than erythrosin B. But erythrosin B always showed the best efficiency. Competing mechanisms like photo-bleaching may be contributing to this. A more detailed investigation of the various parameters involved would, therefore, be of much interest. Of the three dyes erythrosin B showed an exclusive behaviour in the luminescence spectra - a double peaked structure. More studies in this direction also is expected to provide fruitful results.

Similarly, there is a question on the temporal characteristics of the OPC signal. Earlier studies have shown that there exists an initial peak in the OPC signals from these systems. Some authors have experimentally demonstrated this

also. But these experiments have ignored many aspects such as the vibration sensitivity of the interaction. While attempting to record the temporal profiles of the OPC signals we have realised that these are extremely sensitive to vibration pick-ups and if one is not extremely careful, there are possibilities of detecting the wrong signals [10]. Laboratory constraints did not allow us to probe this much further. Recently, Ravindrakumar [11] have carried out careful studies of such samples which have shown that there are some inherent fluctuations for the OPC signals, irrespective of initial peaks of vibration pick-ups. Joby Joseph [12], working on BSO crystals, has observed that even acoustic vibrations (from a motor or an air-conditioner working in the room) can cause fluctuations to the OPC signals. In summary, there are much more things to be studied about the time development of the OPC signals from these systems.

Although theoretical considerations would tell us that for OPC a monochromatic radiation is almost essential, there are a few reports in literature, where scientists have obtained phase conjugate beams using wideband radiations [13-16]. Broadband effects in DFWM have been theoretically studied in two contexts viz., (i) where an incoherent probe beam interacts with the medium alongwith monochromatic pump beams [17] and (ii) where coherent chaotic fields are involved [18]. It was interesting therefore to look for a phase conjugate beam of a wideband laser as the Nd:glass. Literature does not show any reports of the use of a Nd:glass laser and an absorbing dye in the DFWM scheme for OPC investigations. In the present studies these were

employed. There were lots of problems due to noise, but at the end of a number of attempts we could detect some OPC signals. This has been reported by us [19] and this contributes to the list of lasers and nonlinear media successfully employed for OPC.

One would presume that progress in science would invariably increase the speed at which the new sciences born in the research laboratories are brought to the class-rooms. In OPC, however, increasing sophistication of the experimentation has made it inaccessible at the level of class-room physics. One or two attempts in this direction have been reported in pedagogical journals [20,21]. The present investigations cover a contribution in this also [22].

SHG is one of the early detected nonlinear optical phenomena. Because of device possibilities, research in this area easily picked up pace and various interesting results have been reported. A number of new materials for SHG applications have been discovered. But almost all of these had to be used with pulsed lasers. CW SHG is an obvious way of getting narrow linewidth, tunable UV radiation for a number of spectroscopic investigations, but attempts in this directions have not been very successful. Thin crystals of Lithium Iodate have been employed by a previous author in the case of a stabilised ring dye laser. In the present investigations the use of these crystals have been successfully extended in the case of a much less sophisticated laser. The method proves to be less expensive and easier to handle, so that an average laser user

employed. There were lots of problems due to noise, but at the end of a number of attempts we could detect some OPC signals. This has been reported by us [19] and this contributes to the list of lasers and nonlinear media successfully employed for OPC.

One would presume that progress in science would invariably increase the speed at which the new sciences born in the research laboratories are brought to the class-rooms. In OPC, however, increasing sophistication of the experimentation has made it inaccessible at the level of class-room physics. One or two attempts in this direction have been reported in pedagogical journals [20,21]. The present investigations cover a contribution in this also [22].

SHG is one of the early detected nonlinear optical phenomena. Because of device possibilities, research in this area easily picked up pace and various interesting results have been reported. A number of new materials for SHG applications have been discovered. But almost all of these had to be used with pulsed lasers. CW SHG is an obvious way of getting narrow linewidth, tunable UV radiation for a number of spectroscopic investigations, but attempts in this directions have not been very successful. Thin crystals of Lithium Iodate have been employed by a previous author in the case of a stabilised ring dye laser. In the present investigations the use of these crystals have been successfully extended in the case of a much less sophisticated laser. The method proves to be less expensive and easier to handle, so that an average laser user

rather than a laser technologist can afford it.

## REFERENCES

- [1] M D Levenson, in "Introduction to Nonlinear Spectroscopy" (Academic Press, 1982)
- [2] K C Rustogi, S C Mehendale and P K Gupta, *Appl. Phys. Lett.*, **43**, 811 (1983) ; S C Mehendale, P K Gupta and K C Rustogi, *Appl. Phys B*, **32**, 217 (1983)
- [3] Y V G S Murty, R Vijaya and K R Murali, *J. Optics (India)*, **16**, 85 (1987), # B 3.1
- [4] G Ravindrakumar, S N Saha and K K Sharma, Proceedings of the First National Symposium on Lasers and Applications, IIT Kanpur, 02-05 Dec 1987, p.40
- [5] B R Prasad, R K Mohan, P S Narayanan, C K Subramanian and P Chandra Sekhar, *Current Science*, **57**, 648 (1988)
- [6] G Indebetouw, Private communication.
- [7] L M Bernardo, Private communication.
- [8] H Fujiwara, Private communication.
- [9] P Günter, Private communication.
- [10] K P B Moosad, to be published.
- [11] G Ravindrakumar, Private communication.
- [12] Joby Joseph, Private communication.
- [13] I G Zubarev and S I Mikhailov, *Sov. J. Quantum Electron.*, **4**, 683 (1974)
- [14] V I Popovichev, V V Ragul'skii and F S Faizullov, *JETP Lett.*, **19**, 196 (1974)
- [15] M V Vasil'ev, A L Gyulamiryan, V V Ragul'skii, P M Semenov

- and V G Sidorovich, *Sov. Tech. Phys. Lett.*, 7, 490 (1981)
- [16] P I Bal'kyavichyus, A S Dement'ev, E K Kosenko, I P Lukoshyus, E K Maldutis and V P Tarulis, *Sov. Tech. Phys. Lett.*, 7, 163 (1981)
- [17] G Alber, J Cooper and P Ewart, *Phy. Rev. A*, 31, 2344 (1985)
- [18] R Saxena and G S Agarwal, *Opt. Lett.*, 8, 566 (1983)
- [19] K P B Moosad, N Subhash, V P N Nampoori and K Sathianandan, Communicated to *J. Phys. D : Appl. Phys.*
- [20] I S Ruddock and G Scott, *Eur. J. Phys.*, 4, 45 (1983)
- [21] G Indebetouw and T J Zukowski, *Eur. J. Phys.*, 5, 129 (1984)
- [22] K P B Moosad, *Eur. J. Phys.* (in press)

## APPENDIX I

### LUMINESCENCE SPECTRA OF THE DYES EOSIN, ERYTHROSIN B AND ROSE BENGAL DOPED IN DIFFERENT HOST MATRICES.

#### I.01. Introduction :

Luminescence properties of dyes are generally studied with the aim of utilising the emission for various purposes, including laser action. As described in chapter 3, interest in organic dyes of low fluorescence efficiency has been generated recently, due to their capability in OPC. The dyes eosin, erythrosin B and Rose Bengal are of low fluorescence quantum efficiency, as compared to their nearest relative in the Xanthene family, viz., fluorescein. Of these dyes, fluorescence spectra of eosin is fairly well-known. Fluorescence and delayed fluorescence of eosin have been exhaustively studied in the past [1-3]. Fluorescence quantum yield of eosin is much more compared to that of the other two. Lasing has been observed in eosin and therefore it has been recently listed as a laser dye [4]. Much less work have been done on the fluorescence characteristics of erythrosin B and Rose Bengal.

In most of the investigations carried out on eosin dye, either a liquid solution is used [1-3] or the dye is incorporated in a rigid, glassy matrix [5]. Only few reports have appeared on investigations of the fluorescence characteristics of eosin and the other dyes doped in polymer matrices. Buettner [6] has measured the triplet lifetimes of

these dyes, doped in gelatin and other polymers, by flash photolysis method. Interest in spectroscopic studies of the optical properties of dyes incorporated in solid matrices had been mainly due to the possibilities of availing information on the orientational details of the dye molecules in the host matrix. A new interest in such materials has been developed as possible media for laser based devices [7]. Matsuoka et al. [8] have reported the studies on the absorption spectra of acridine orange and some of its derivatives doped in polyvinyl alcohol matrix. Their interest was mainly on the orientational aspects. Paschenko et al. [7] have reported studies on the fluorescence characteristics of acridine orange and neutral red dye incorporated in polyvinyl alcohol films. They have studied the quantum yield, lifetimes and anisotropy of fluorescence as functions of concentration.

Studies on the fluorescence characteristics of the dyes used for OPC are important in understanding the underlying mechanisms of the production of the PC beams. In certain cases it has been observed that the fluorescence efficiency and OPC efficiency bear an inverse relationship [9]. Since much data on the above dyes are not available in literature, a few studies have been carried out on the luminescence spectra of these dyes, doped in matrices of gelatin, polyvinyl alcohol (PVA) and boric acid glass (BAG). These are presented below.

#### I.02. Experimental details :

Samples were prepared in the same way as described in

chapter 3. The set-up for recording the spectra are shown in figure I.01. Excitation is done by a suitable line of the argon ion laser. Luminescence emission is collected in a direction perpendicular to the exciting beam, condensed using a converging lens, and allowed to fall on the entrance slit of a monochromator (Jarrell-Ash 0.5 meter) attached with a PMT (EMI 9683 KQB, having a S20 cathode). Signals from the PMT is charted out using a chart-recorder.

### I.03. Results and discussions :

In figures I.02 (a) to (c), the luminescence spectra of the three dyes in different host matrices are shown. Films prepared from solutions of equal molar concentrations are used in the case of gelatin and PVA samples (4.3 mg of eosin, 6.1 mg of erythrosin B and 7 mg of Rose Bengal, dissolved in 20 ml of distilled water). For BAG samples, the same masses of the dyes are mixed with two grams of boric acid. For comparison, spectra from dilute aqueous solutions are also recorded. In the case of the BAG samples, since they do not show much absorption at the 514.5 nm, (as is discussed in chapter 3) excitation is achieved by the 476.6 nm line of the argon ion laser. In all the other cases, excitation is achieved by the 514.5 nm line.

In all the cases, luminescence emission peak shifts towards the red as the rigidity of the host matrix increases. For erythrosin B in gelatin and PVA, emission is double-peaked. The second peak may be due to the large phosphorescence emission. Of all the three dyes, erythrosin B always showed the best

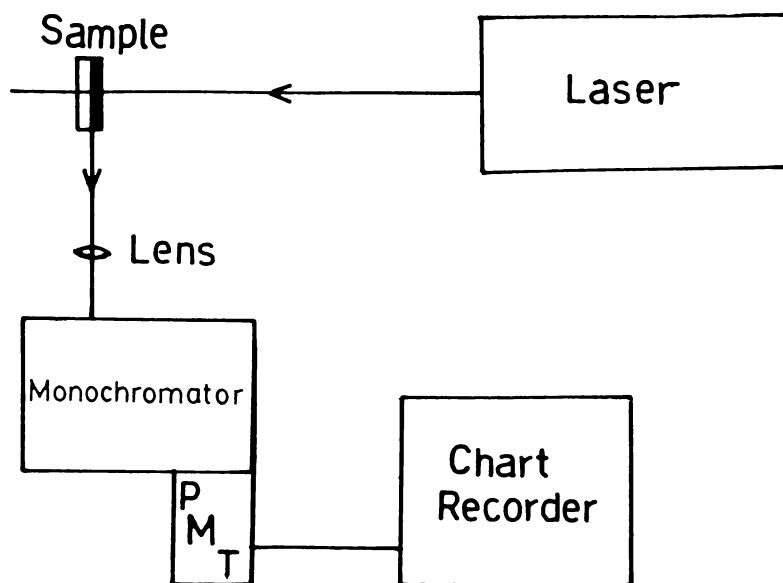


Figure I.01 Set-up for recording the luminescence spectra from dyes doped in solid matrices.

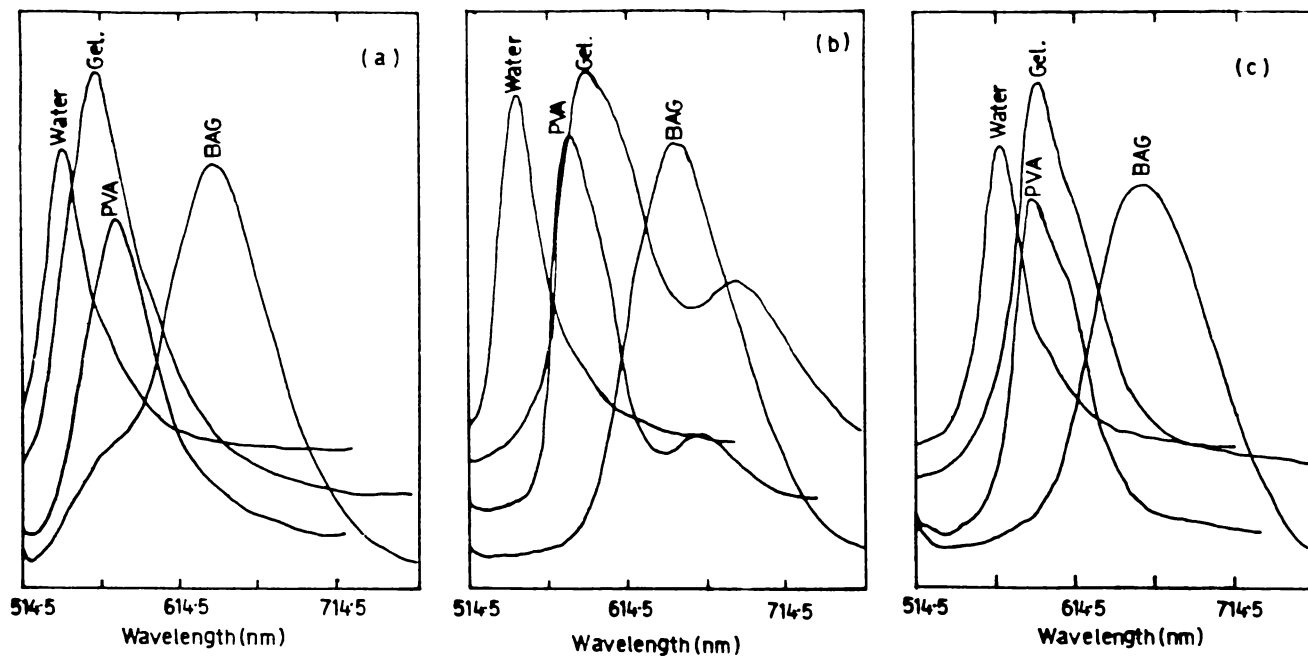


Figure I.02 Luminescence spectra of three dyes in various solid matrices, as compared to the corresponding spectra in dilute water solutions. (a) eosin, (b) erythrosin B and (c) Rose Bengal. Scales are different on the vertical axes.

efficiency for OPC (as described in chapter 4). The absorption spectra of these dyes are similar in character (presented in chapter 3). Molecular weight of erythrosin B is in between that of eosin and Rose Bengal. Since the distinction of erythrosin B is manifested clearly in the luminescence spectra also, it is speculated that probing further into this would be much interesting and would provide useful information regarding the mechanism of formation of the PC beam.

The concentration dependences of the double-peaked nature of the spectra have been recorded and are presented in the figures I.03 (a) and (b).  $C$  denotes relative concentration.  $C$  mg of the dye is dissolved together with 2 gms of gelatin or PVA in 40 ml of distilled water. As concentration increases the second peak becomes increasingly prominent, in both the cases. A dilute aqueous solution of the dye do not show much concentration dependence, as shown in the figure I.04.  $C$  denotes the relative concentrations. For  $C = 1$ , 43.2 mg of the dye is dissolved in 1600 ml of distilled water.

In the figure I.05, the concentration dependence of the luminescence spectra of eosin in gelatin films is shown. In these cases,  $C$  mg of the dye is dissolved in 20 ml of distilled water, together with 2 gms of gelatin. A slight red-shift with the concentration is the only noticeable feature in these spectra.

In summary, the luminescence spectra of the three dyes, viz. eosin, erythrosin B and Rose Bengal, in matrices of gelatin, PVA and BAG are recorded. Erythrosin B shows double-peaked spectra

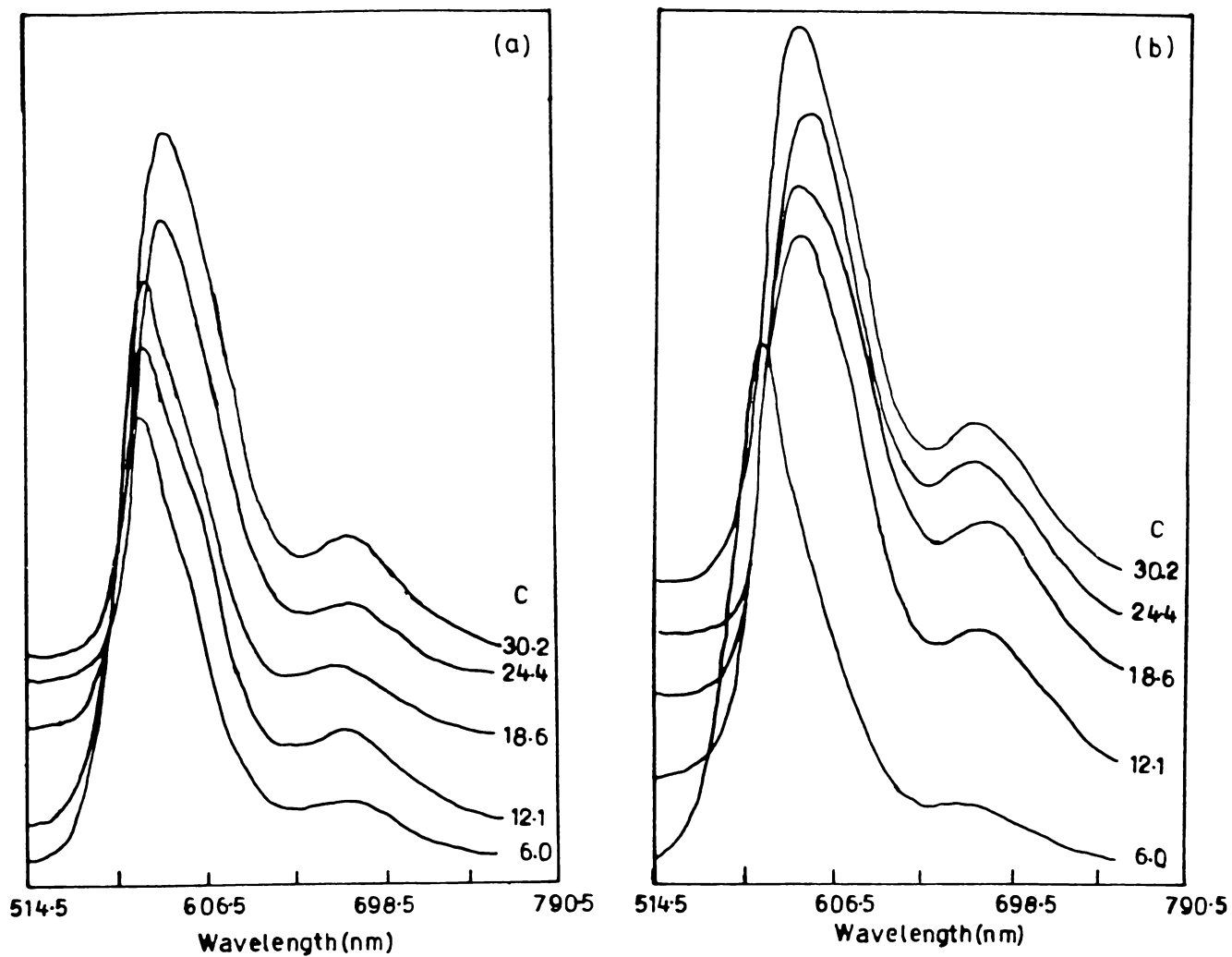


Figure I.03 Concentration dependence of the spectra of erythrosin B in (a) gelatin matrix and (b) PVA matrix. C denote relative concentrations as described in the text. Scales are different on the vertical axes.

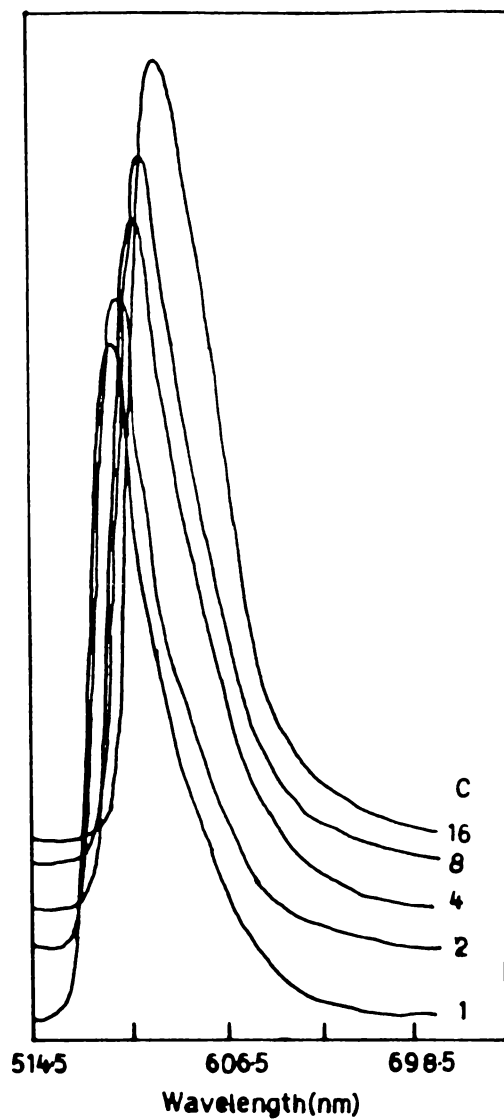


Figure I.04 Concentration dependence of the luminescence spectra of erythrosin B in dilute water solutions. C denote relative concentrations as described in the text. Scales are different on the vertical axis.

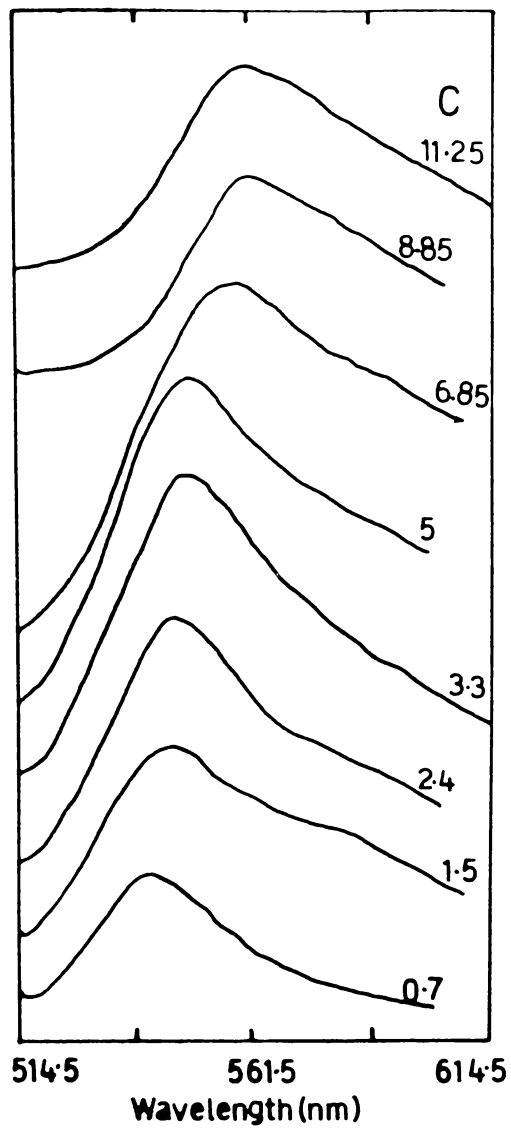


Figure I.05 Concentration dependence of the luminescence spectra of eosin in gelatin matrix. C denote relative concentrations as described in the text. Scales are different on the vertical axis.

in the cases of gelatin and PVA samples. It is suggested that more studies in this direction can shed light on the details of the formation of the PC beam in a four wave interaction in these samples.

#### REFERENCES

- [1] C A Parker, in "The Triplet State", ed. A B Zahlan (Cambridge University, 1967), p.360
- [2] S P McGlynn, T Azumi and M Kinoshita, "Molecular Spectroscopy of the Triplet State" (Printice-Hall, 1969)
- [3] C A Parker, in "Advances in Photochemistry" ed. W A Noyes Jr., G S Hammond and J N Pitts Jr. (Wiley Interscience, 1964)
- [4] Mitsuo Maeda, in "Laser Dyes" (Academic, 1984), p.101
- [5] L S Forster and D D Dudley, *J. Phys. Chem.*, 66, 838 (1962)
- [6] A V Buettner, *J. Phys. Chem.*, 11, 3253 (1964)
- [7] V Z Paschenko, A N Ponomaryev and V I Yuzhakov, *J. Lumines.*, 36, 57 (1986)
- [8] Y Matsuoka and B Norden, *Chem. Phys. Lett.*, 85, 302 (1982)
- [9] H J Hoffman and P E Perkins, *IEEE J. Quantum Electron.*, QE22, 563 (1986)

## APPENDIX II

### OPTICAL PHASE CONJUGATION AS LABORATORY EXPERIMENTS AT THE POSTGRADUATE LEVEL

#### II.01. Introduction :

OPC via DFWM, being a very efficient technique for precisely reversing both the direction of propagation and the overall phase factor of a light beam for various applications, has acquired great scientific importance. It is a fast-growing area of research and several publications are coming out everyday. Exhaustive reviews have appeared on this topic [1-3] in the past few years. It is high time that OPC is included in the laboratory courses of postgraduate level students undergoing a course in laser applications. But, being a fast developing area, experimentation in OPC is increasingly becoming sophisticated and expensive. There have been few attempts to simplify the experimentation to the level of routine laboratory experiments in the postgraduate laboratory courses.

Ruddock and Scott [4] have described a relatively simple method for observing OPC using a free-running pulsed solid-state laser. They have used thin films of a saturable dye solution as the nonlinear media. A counter-propagating beam was formed by retro-reflecting the laser beam on a mirror. Sample was kept in contact with the mirror and a probe beam was obliquely incident on it. The crux of the method lies in the use of two storage

oscilloscopes simultaneously for detection, which renders the method rather expensive. These storage oscilloscopes are used, one for detecting the signal and the other for monitoring the pump beam (more details of this method is given in the section II of the chapter 4). The signal level is always very low. Because of the pulsed nature of the source used, it is not possible to demonstrate the most exciting property of OPC, viz. the aberration-correction.

A second attempt in this direction has been reported by Indebetouw and Zukowski [5]. They have achieved OPC using a CW laser (argon ion laser), working at power levels of 100-700 mW. The nonlinear medium used by them was again an absorbing dye solution, sandwiched in the form of a thin film, between two glass plates separated by thin mylar sheets. They have demonstrated OPC and some other nonlinear optical effects using this medium. But here also the signal levels are very poor. Series of apertures were used along the beam paths to isolate the signal from the scattered noise. Keeping thin mylar sheets pressed between glass plates and filling them with dye solutions itself appear to be a tricky job. Moreover, for taking some measurements, they had to resort to sophisticated techniques like heterodyne detection [6].

The relatively high efficiencies of low power saturable absorbers as described in the chapter 3, makes them attractive candidates for the purpose of postgraduate laboratories. One does not have to look for solid matrices like gelatin or polyvinyl alcohol. A typical example is described below [7].

## II.02. Nonlinear medium :

Erythrosin B dye, which is available in any clinical laboratory, is used as the saturable dye. For a solid matrix, a popular brand of synthetic gum ( CAMEL Adhelin synthetic multipurpose office glue ) is used. The dye readily dissolves in the gum and the red-coloured viscous solution thus obtained was painted over glass slides. On drying, these formed the necessary films, which are found to be excellent nonlinear media for demonstrating OPC using an argon ion laser working at 514.5 nm wavelength, with a few tens of milliwatts output power.

## II.03. Experimental set-up :

The set-up for the experiments is the usual counter-propagating geometry, sketched in figure II.01. All the optical components are home-made ones. Silver or Aluminum coated glass plates are used as mirrors and partially coated or uncoated glass plates as beam splitters. The only expensive item in the set-up is the argon ion laser itself. In contrast to the experiment of Indebetouw and Zukowski [5], less number of apertures are necessary to isolate the signal from scattered light. The PC beam spot is very clearly visible on a screen kept in the retro-direction of the probe beam. The following tests confirm that this beam originates from a four-wave interaction in the sample.

- i. When any one of the beams are interrupted, the signal vanishes.

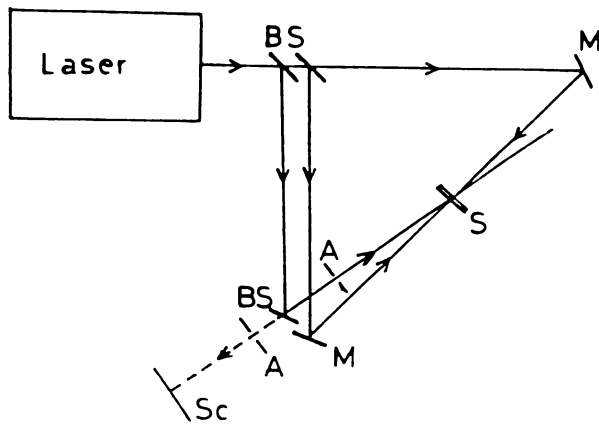


Figure II.01 Set-up for observation of OPC in dyes held in glue films. M - Mirrors, BS - Beam splitters, S - Sample, Sc - Screen, A - Apertures.

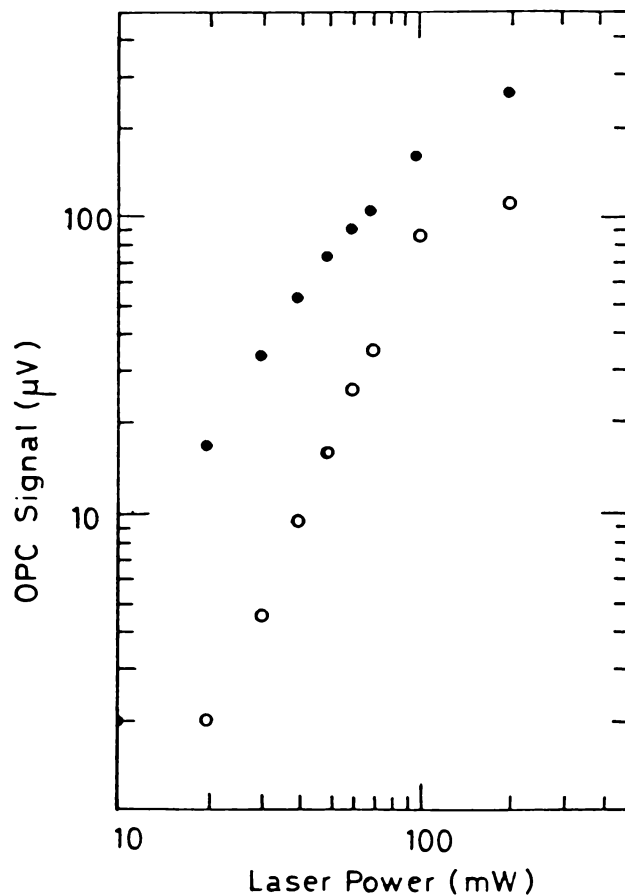


Figure II.02 Signals recorded using the above set-up, for (●) erythrosin B and (○) Rose Bengal held in CAMEL (Adhelin) glue films. In place of the screen Sc, a monochromator-PMT-Lock-in amplifier combination was used for detection.

- ii. There is no signal at all, when the sample is replaced by a similarly-prepared film using Rhodamine 6G dye.

Since the signal beam is bright enough, detection can be made using a simple photodiode and a voltmeter. A coloured-glass filter can be used in front of the photodiode to cut-off the contribution from the fluorescence of the sample (this is not essential, since this contribution is very small for erythrosin dye) and to limit the intensity to the saturation limit of the detector.

#### II.04. Results and discussions :

Since the signal beam-spot is clearly visible on the screen, the standard aberration-correction properties [1] can be demonstrated. This can be done by introducing a cylindrical lens on the path of the probe beam to focus the probe beam in a line at the interaction region and observing that there is no corresponding change of shape in the PC beam imaged on the screen.

Figure II.02 shows the signal strengths recorded using the above set-up. Instead of a coloured-glass filter and photodiode, a monochromator-photomultiplier tube combination, tuned to 514.5 nm was used for detection. The same measurements can be done using a photodiode-voltmeter combination.

The dye has fairly good absorption at the other wavelengths of the argon ion laser. Therefore, it is possible to observe OPC

in these samples, using those wavelengths also. As one would expect, the signal strength roughly follows the absorption spectrum of the dye in the glue matrix. Figure II.03 shows the relative signal strengths from the above sample at the different wavelengths of argon ion laser. In the background the absorption spectrum of the dye, held in the glue matrix, is shown for comparison.

As mentioned in chapter 4, the effects of wash-out due to vibration pick-ups and photobleaching are to be taken care of while introducing this in laboratories. To avoid the flickering of the signal due to vibration pick-ups, some kind of averaging may be used in measurements. The measurements shown in figure II.02 this is done by a lock-in detection. But for actual laboratory experiments a capacitance averaging will be sufficient. Continuous exposure to the laser beams cause photo-bleaching of the dye, especially when the power levels are high. This can be observed on the films as small spots of colour-change. For the purpose of laboratory-training experiments, this is not a serious problem, since one can always choose a good portion of the film or even prepare a new film.

To conclude, dyes held in solid matrices form a very inexpensive, easy-to-prepare and efficient medium for OPC experiments at the level of postgraduate laboratory courses. High signal-to-noise ratio can be obtained and therefore it is possible to demonstrate the aberration-correction properties of the PC beam.

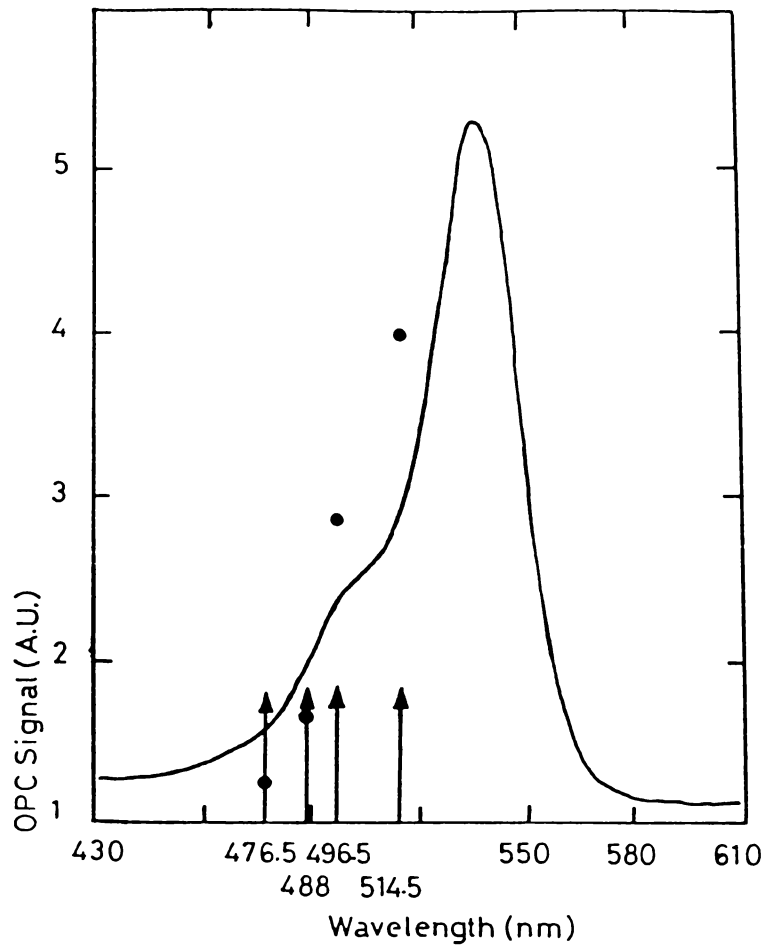


Figure II.03 Relative OPC signal strengths at the different argon ion laser wavelengths, for erythrosin B held in CAMEL (Adhelin) glue films, plotted alongwith a suitably scaled absorption spectrum.

## REFERENCES

- [1] D M Pepper, *Opt. Engg.*, **21**, 156 (1982)
- [2] R Fisher (ed.), "*Optical Phase Conjugation*" (Academic, 1983)
- [3] B Ya Zeldovich, N F Pilipetsky and V V Shukunov, "*Principles of Phase Conjugation*" (Springer-Verlag, 1985)
- [4] I S Ruddock and G S Scott, *Eur. J. Phy.*, **4**, 45 (1983)
- [5] G Indebetouw and T J Zukowski, *Eur. J. Phy.*, **5**, 129 (1984)
- [6] G Indebetouw, Private communication.
- [7] K P B Moosad, *Eur. J. Phys.* (in press)

